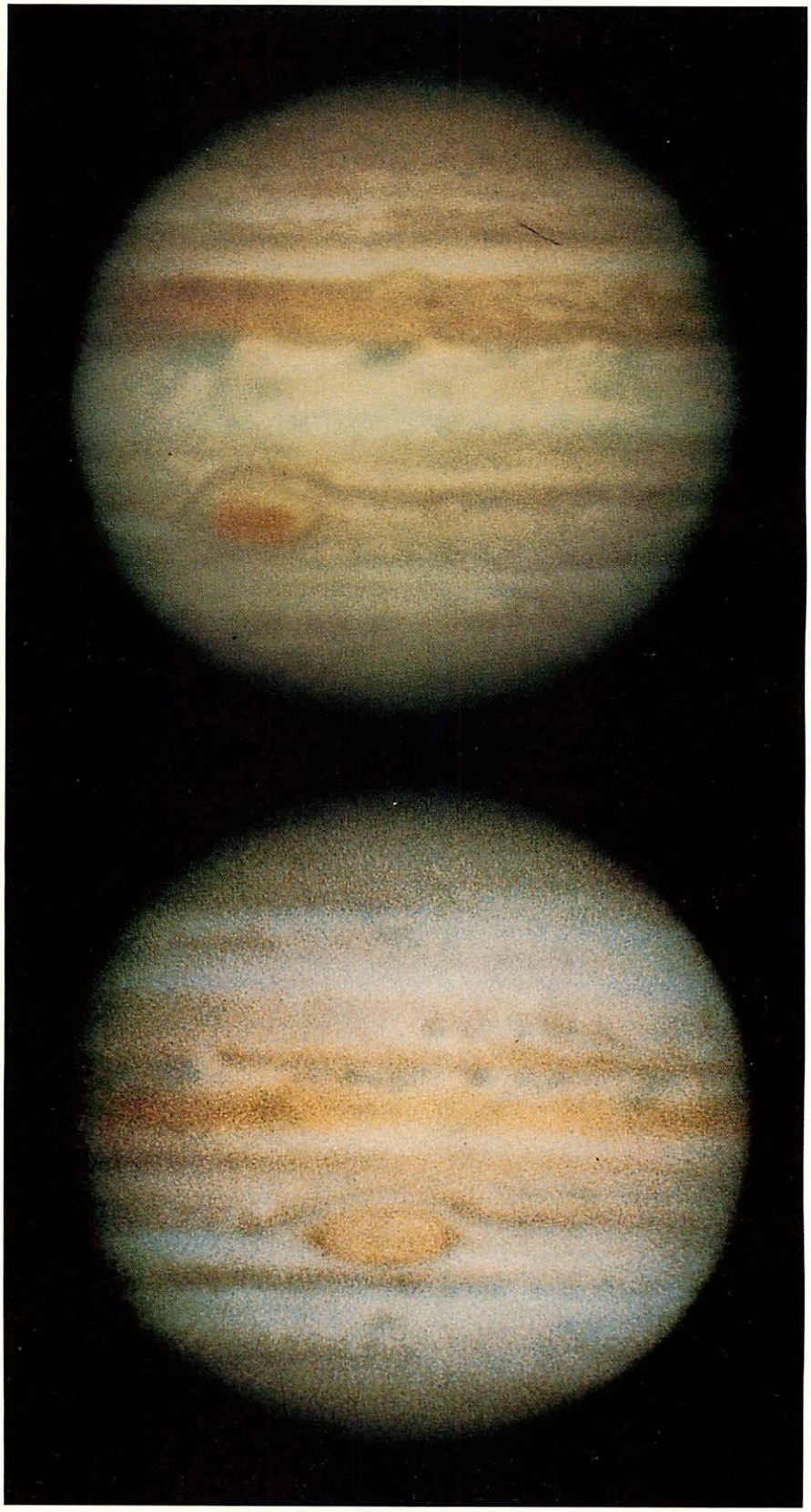

Dec 23, 1966 08:42:35 UT
May 18, 1968 03:03:00 UT

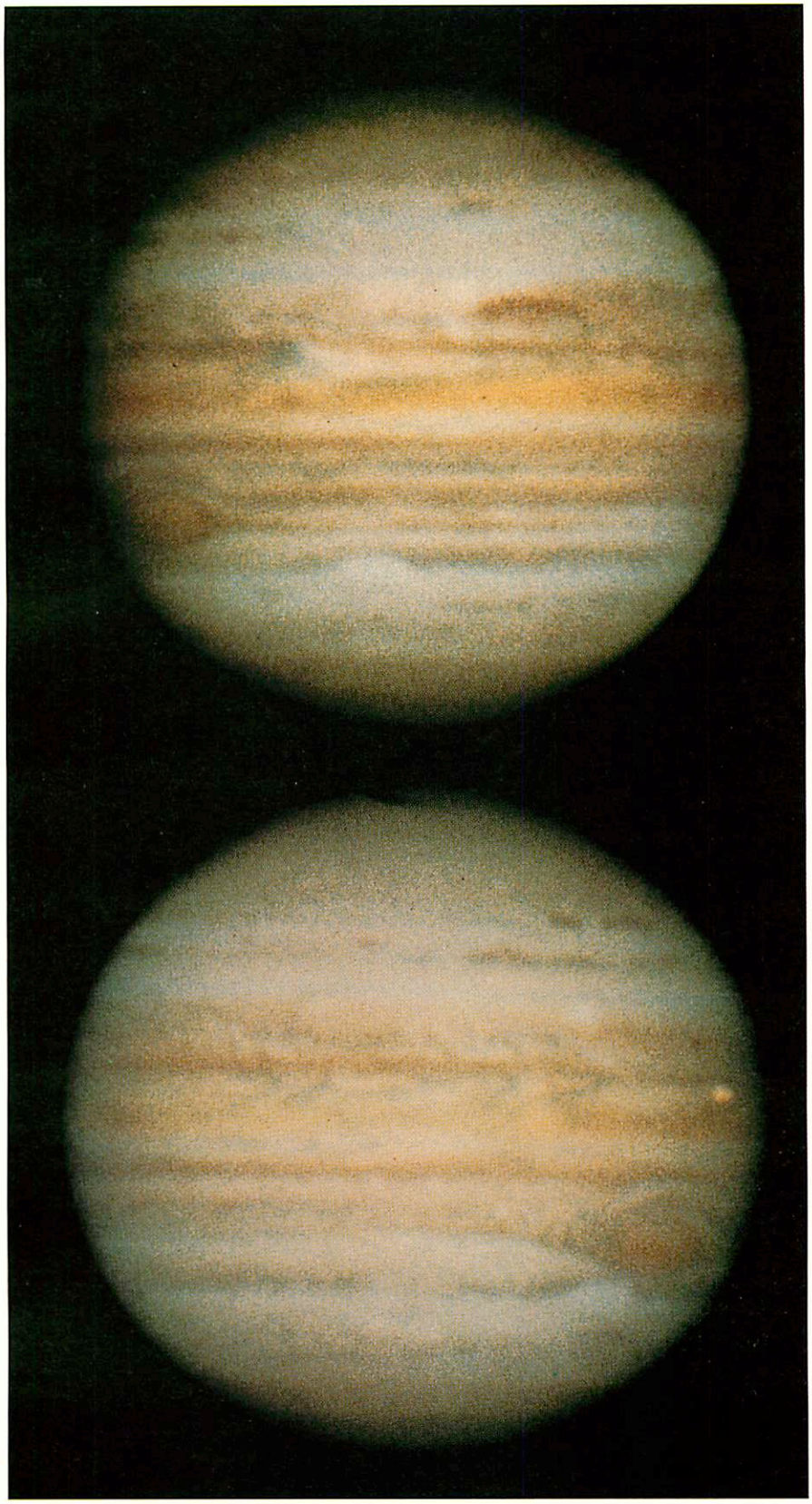

Apr 9, 1968 04:20:21 UT
Jan 25, 1968 10:13:40 UT

NO. 173 INTERPRETATION OF THE JUPITER RED SPOT, I.*

by Gerard P. Kuiper

ABSTRACT

Sec. 2 briefly reviews the LPL research programs on Jupiter. They include continuing photographic coverage of the planet in color and in several wavelength bands; IR image scans especially around 5μ; medium and high-resolution spectral studies in the photographic and the lead-sulfide regions, with laboratory comparisons; photometric and polarimetric studies; far-IR measurements at high altitudes; chemical studies designed to match formation of Jovian cloud particles; and participation in the NASA Pioneer missions. They are followed in Sec. 3 with some preliminary interpretative remarks, in part suggested by the remarkable IR spectra and IR images of the Earth and Mars obtained at NASA-Goddard (Figs. 5 and 6). This leads to a discussion of the Red Spot and the White Ovals in Sec. 4.

---

* This investigation was initiated by an invitation by *Sky and Telescope*, in Sept. 1971, to summarize the large collection of LPL data on Jupiter which I had examined during the summer months of 1971. The resulting new interpretation of the Red Spot and the related data on the Jupiter clouds were published in *Sky and Telescope*, Jan-Feb. 1972. The present text on the Red Spot (Secs. 4 and 5) was completed as here presented Dec. 1971. Some data about the Earth and Mars were later added in Secs. 2 and 3.

With the aid of λ8900 CH_4 filter photographs it is shown that the Red Spot is normally the highest cloud feature in the Jovian atmosphere, located squarely on the South Tropical Zone at 22°S, itself high and prominent (Fig. 1). This Zone and its Spot are compared with the highest (and most regular) cloud zone on Earth, the North Tropical Convergence (Figs. 7-8), containing several moving centers (Fig.10). A definite analogy is found to exist. The Red Spot is a rising column, obviously having its own energy source; it spreads outward at the top level, in anti-cyclonic rotation. The cyclones of the terrestrial Tropical Convergence behave likewise, the energy source being the latent heat of condensation. It is concluded that the large and persistent Jovian cloud masses, of which the Red Spot is the largest, are major organized storm arrays embedded in a near-stagnant atmosphere, each probably possessing numerous short-lived rising "hot" columns driven by released latent heat; and covered by a horizontally-expanding gigantic cirrus cloud system, in anti-cyclonic rotation. The meteorological theory of Organized Cumulus Convection is applied to the Red Spot and the White Ovals. The theory allows for their dimensions. Evidence exists that the array of hot towers under the Red Spot is eccentric (Fig. 14). The 90-day and the occasional 5-8 year fluctuations in the motion of the Red Spot may be due to processes analogous to those found in the Earth's Tropical Convergence. The 90-day oscillation, discovered by Solberg in 1965, has been observed for 8 years now (cf. Fig. 16); its trochoidal-type motion is typical for translating vortices (Fig. 17).

The meteorology of the Jupiter atmosphere may lead to cyclic outbreaks due to the restoration of the adiabatic gradient by the planetary heat flux after a previous major "discharge"; the process resembles that attending terrestrial cumulus formation. This cyclic process could contribute to the propagation of the Red Spot through the STropZ with a period averaging about 5 years, corresponding to an average daily rotation period of $9^h55^m38^s$. On this model the Red Spot could indeed be unique in its Zone and of indefinite life. The long-term trends in the Red Spot period, varying every 20-30 years (Sec. 4*b*), could be due also to meteorological processes within the STropZ.

A recent rediscussion of the SEB outbreaks by Reese (1972) indicates that three sources are responsible, which define a common and constant period of rotation, in close agreement with that defined by the decametric radio observations. This constant rotation period suggests that the Jupiter subsurface is solid and strengthens the earlier discussion of the rotation of the surface layers of Jupiter based on Figure 12. The gas eruptions probably interact with the incipient atmospheric instability having its own relaxation time of roughly 5-10 years. All three SEB sources are located 14° S and are reviewed in the context of other NS asymmetries shown by the planet.

Plate I reproduces four LPL color records of Jupiter showing various appearances of the Red Spot, the White Ovals, the blue festoons, and other clouds. Fuller discussions of these and of the intricate cloud belts will be published separately. Appendix I gives comments on earlier views of the planetary heat flux, the contraction time scale, and models of the Red Spot; Appendix II by S. M. Larson gives a fuller interpretation of Figure 1.

1. Introduction

This paper is the first of a series summarizing the Laboratory's studies of the planet Jupiter directed toward a physico-chemical and meteorological understanding of its atmosphere and clouds. Such a program draws on numerous data sources - often very inadequate. The complexity of the visible phenomena, and the explosive growth of terrestrial global meteorology, point to the necessity of considering all Jupiter observations in context, with the development of novel methods of observation always at a premium. The relative merits and costs of planetary research from a mountain observatory, an aircraft, a balloon, a satellite, and a deep-space probe, are important factors in reviewing the past decade and plans for the 1970's.

The planet Jupiter is somewhere intermediate between the Earth and the Sun. Therefore, even atmospheric studies must make some reference to the planet's interior. Hubbard's (1970, p. 693) models J8 and J9 make the hydrogen weight fractions 0.66 and 0.59, the central temperatures 7300° and 7500°K, the Helmholtz-Kelvin contraction time scale 4×10^9 years. "Thus the present model of Jupiter and the most recent determination of the net Jovian energy flux are consistent, but only marginally so" (*op. cit.* p. 696). The computed contraction of the surface is only 0.7 mm/year. The planet is assumed to be in convective equilibrium and to rotate as a solid body. This newly-derived hydrogen weight fraction, around 0.6, is more consistent with recent ideas on the origin of the solar system (via the formation of protoplanets that suffered subsequent mass losses) than the earlier fraction of 0.8 (de Marcus,1958) which nearly equalled that of the Sun. On the other hand, for the Jupiter atmosphere the He, C, and N ratios to H appear almost identical to those in the Sun (Owen, 1970, Table 1).

Smoluchowski (1971) adopts Hubbard's model and interprets his radial variation of temperature to imply that the planet is solid, at least from 0.55-0.8 R_J, where helium is immiscible with hydrogen (and might form small liquid inclusions in the metallic hydrogen). *Above 0.8 R_J solid molecular hydrogen is expected* and below about 0.45 R_J to the core, a liquid hydrogen-helium alloy containing also any heavier elements. The liquid part would be in convective equilibrium and produce the magnetic field. The derived pressure and temperature at the 0.8 R_J interface are 2.10^6 atm and 3600°K (Hubbard, *op. cit.*). A thin layer of liquid molecular hydrogen is assumed to exist "somewhere near 0.9 R_J and much less than 0.1 R_J thick", with $p \sim 10^5$ atm, $T \sim 2000$°K. This layer would be essentially an insulator if pure hydrogen; it cannot then generate a magnetic field of its own, and *cannot be responsible for the Red Spot by a magnetic process* (Smoluchowski, *op. cit.*).

The structure of the upper 1-2 percent of the planet (700-1400 km depth) is not well defined by the theoretical model studies and *will require improved empirical definition.* This type of information is likely to come from improved knowledge of the $120° < T < 320$°K region, the deepest parts accessible through holes in the clouds with observations made around 5μ; from the radio wave emission at different wavelengths and its distribution over the disk; and radar echoes to probe for density discontinuities at depth. Opacity studies of the uppermost layers have been made by Trafton (1967). No reference is made here to radio observations or to the Jovian magnetosphere, since they do not appear to relate directly to the Jovian cloud layers. A review by Newburn and Gulkis (1971) considers all recent observations and theoretical deductions.

2. LPL Research Programs on Jupiter

a. Photographic Studies and Image Scans - Photography of the planet in color and through filters (0.3-1.0μ) has been carried out with the 61-inch telescope since its first night of operation, October 8, 1965. The optics were produced by Mr. Robert Waland. The primary is F/4, made good to λ/40. Two secondaries are provided, F/13.5 and F/45, giving 10 and 3 arc sec/mm, respectively. Enlarging cameras can produce images up to F/75 or larger, as desired. In recent years we have added zero-deviation double prisms that *compensate for atmospheric dispersion* (they can be moved and turned along the optical axis in front of the focal plane, adjusted by visual inspection). Planetary resolutions down to 0.15 arc sec have been obtained. About one quarter of the telescope time has been assigned to this program. This planetary photography program has been very demanding, requiring constant attention to detail: the nature of the dome construction, dome paint, exhaust fans, their location and speeds, small exhausts on rim of mirror, optimum use of wind screens and the dome's slit width; scale of planetary images depending on brightness of sources; in-house color processing to cut exposure times to 1/4; methods of compositing, etc. For the first year this work was done by Messrs. D. Milon, A. Herring, and E. Whitaker, partly with my participation; thereafter mostly by J. W. Fountain, S. M. Larson, R. B. Minton, and J. Barrett. Messrs. J. Fountain and S. Larson describe in *LPL Communication No. 174* the photographic techniques developed. One complex but thoroughly promising technique has not yet been used except experimentally: image reconstruction for the instrumental and atmospheric blurring functions. This subject will be treated in this Series.

Because of the planet's recent southerly declination, we have supplemented our Jupiter photography at telescopes in the Southern Hemisphere: the 60-inch reflector of the Cerro Tololo InterAmerican Observatory in February and May, 1969 (incidental to the Mars observations that year); and especially the 24-inch refractor of the Bosscha Observatory, Lembang, Java, during May, July, August, September, 1971. Mr. Steve Larson undertook the May 1971 run in Java; Mr. John Fountain, all the others. We are much indebted especially to Dr. Bambang Hidajat for his hospitality.

During the summer of 1971 I examined the entire LPL Jupiter collection, then over 12,000 frames in color and 30,000 filter frames (UV to IR). The impact was unforgettable and left me convinced that increased effort on this planet was justified. Clearly, the use of color film and high image resoluton were indispensable. After my examination I invited Mr. W. E. Fox, Director of the Jupiter section of the Brit. Astr. Assoc., as a consultant for two months. His remarkable visual memory of the everchanging details of the Jupiter cloud patterns, much of it recorded in the *Journal* of the B. A. A., was a source of much stimulation as we jointly re-examined the LPL collection. I had made a provisional quality classification of the entire Jupiter collection in my earlier examinations which was later refined by Mr. R. B. Minton and made the basis for a log of the LPL data to be published later. The planet was found to be in constant turmoil during the years 1965-71, especially in 1971, with everchanging larger and smaller cloud masses seen in six main colors: orange, brown, dark brown, yellow, cream, and light blue.

The study of Jupiter's zonal motions and of the clouds in each zone has been pursued for nearly a century, with Peek (1958) summarizing the results known up to that date. The first extensive photographic measures were made at the New Mexico State University by B. Smith and C. Tombaugh who in 1963 published a paper "Observations of the Red Spot On Jupiter". Chapman and Reese (1968) published another important study on Jupiter and included references to parallel investigations. Gordon Solberg, at LPL in 1971, had discovered at New Mexico a somewhat irregular 90-day oscillation in longitude of 0°.8 average semi-amplitude that he traced back to at least 1964. A major irregular drift with some 1200° total amplitude between 1831 and 1970 has long been known and been the source of much speculation (Peek, 1958). The September 1974 and especially the October 1975 oppositions of Jupiter will be the most favorable in the next decade (planet near the equator and at perihelion). A maximum ground-based effort will be called for. In addition, two independent methods of image processing are being pursued on selected images of the entire LPL collection since 1965, promising resolution gains of 1.5-2.0.

In addition to the Jupiter photography in color and through filters, we have since 1968 taken photographs in the strong methane band at 8900Å, to show only the *uppermost cloud layers*. Figure 1 reproduces representative methane pictures for 1968-71. They are printed in two degrees of contrast to bring out their full range of intensities. The filter is 200Å wide, the methane band deep, and thus the exposures are roughly 100 times longer than normal near-infrared exposures. Either high-speed infrared film is used or an S1 image tube, with results comparable in quality. Figure 2 shows the alignment of Figure 1*c* with a red photograph taken nearly simultaneously. Fuller accounts of these studies are found in the *Communications* immediately following the current issue.

The proof that Figure 1 shows *real elevation differences* in the cloud cover and *not merely albedo differences* is given by Mr. S. Larson in Appendix II. Later an improved methane filter became available which transmitted less radiation from one of the wings of the broad CH_4 bands.

Whereas the methane records of Figure 1 show the *highest* cloud layers, the *deepest* penetration into the Jupiter atmosphere (at least for $\lambda<35\mu$) is achieved between 4.5 and 5.5μ, where both methane and ammonia are very transparent. The penetration into the Jupiter atmosphere as a function of λ is the most powerful tool to explore empirically the vertical structure of the atmosphere, including the various cloud layers. This matter is reviewed more systematically in Sec. 3*a*, below, on the basis of both the Jupiter emission spectrum and the known CH_4 and NH_3 absorptions.

b. Jupiter's Spectral-energy Curve - This curve consists of the reflected and scattered sunlight, from 0.2-3μ±; and the thermal emission beyond, with some overlap, 3-4μ.

The interests of the spectral-energy curve are manifold. The shortwave (solar) part contains numerous CH_4 and NH_3 bands of a great variety of strength - affording the opportunity to view the planetary atmosphere and its clouds from *a range of different depths* - the strongest bands merely showing the uppermost layers, etc. The study of vibrational and especially rotational temperatures (requiring high spectral resolution) adds specific *temperature data* to the different atmospheric layers so investigated. These data in turn must correlate with the local presence or absence of a *cloud layer*, the colors and composition of these clouds, etc., topics reviewed below.

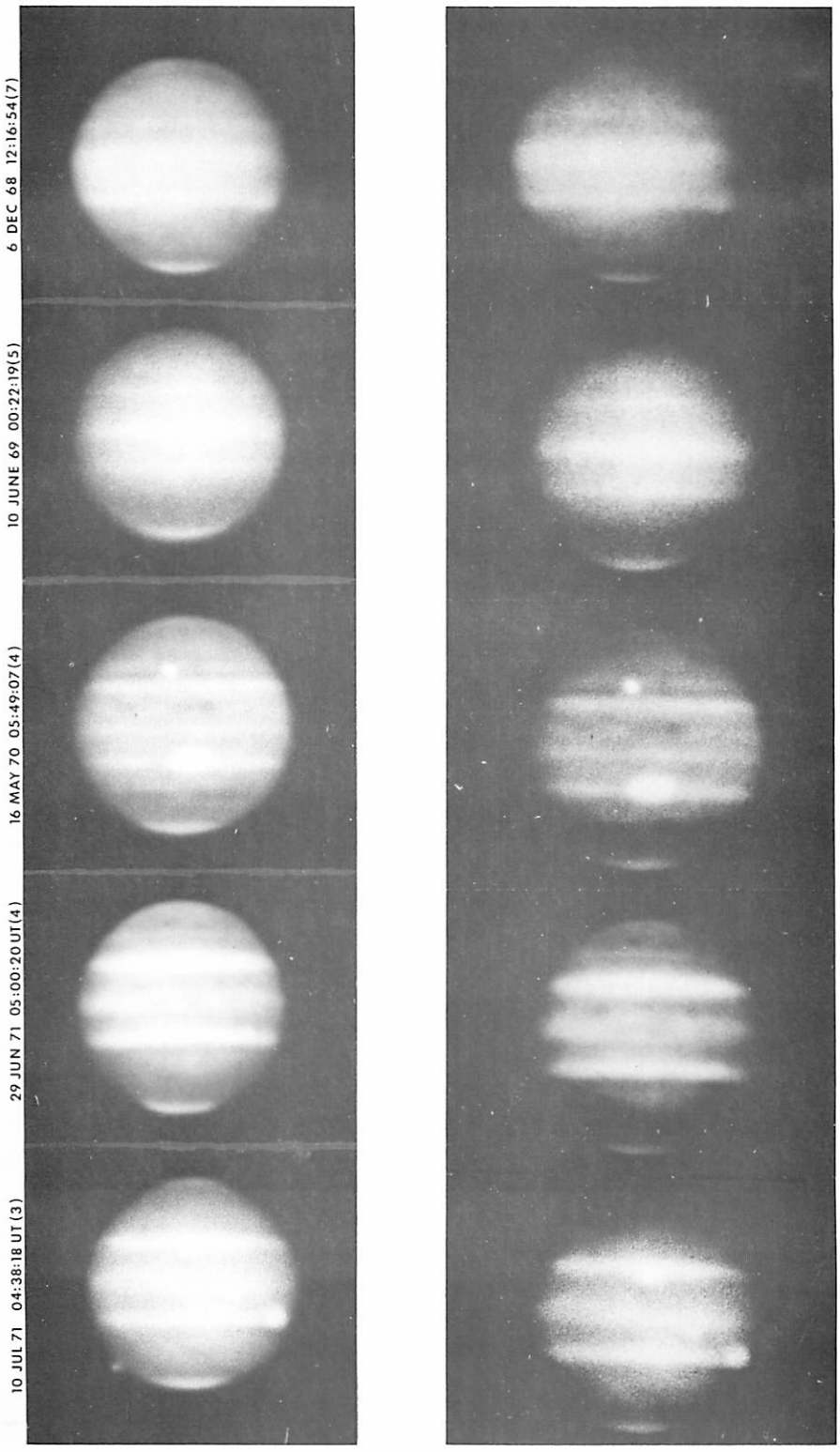

Fig. 1 61-inch photographs of Jupiter in the 8900Å methane band, 1968-1971. Composites, with times and numbers of frames shown in margin. Lower photograph shows two satellites and Red Spot as well as SEB disturbance. Middle photograph shows Red Spot and Io

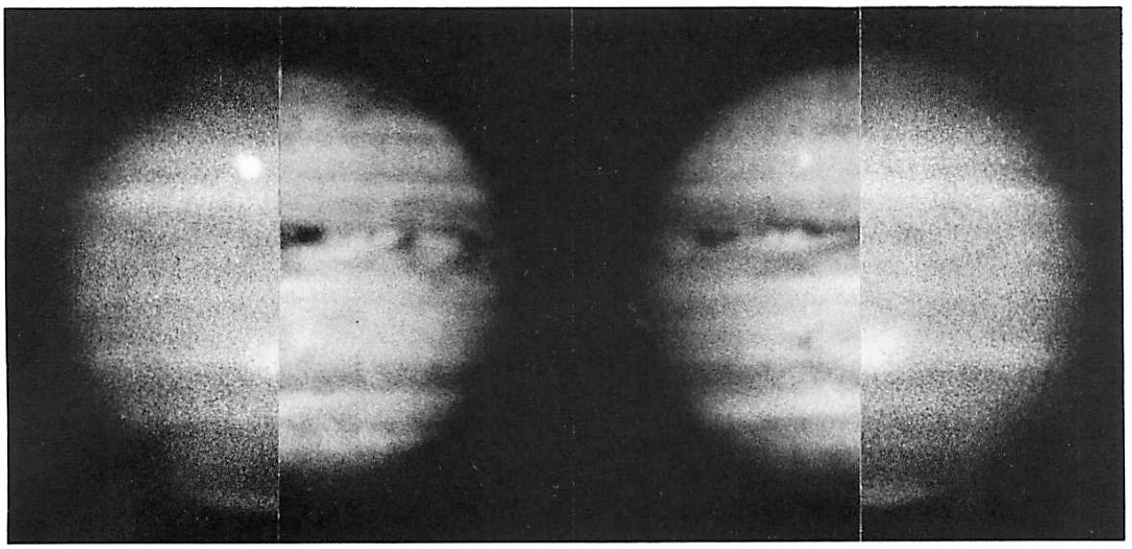

Fig. 2 Alignment of Fig. 1c with red photograph taken nearly simultaneously

The thermal-emission part supplies analogous data for the longer wavelengths. We are here dealing with some extremely strong fundamental vibrations; new effects due to H_2 and possibly other constituents, and H_2O at the deepest penetrations. The *radiation balance* of the planet is involved and all the complexities of a multi-layered atmosphere with an active meteorology, internally driven, unlike the Earth whose atmosphere is largely solar-driven.

A brief summary of the empirical data on the planet and on laboratory spectra must precede further comments.

The solar part of the reflection curve of Jupiter is shown, in outline, in Fig. 3*a*. It consists of a rather featureless blue and violet section, depressed toward the ultraviolet by the general color of the planet and attributed to scattering of sunlight by particles that are on the average somewhat yellowish. Rayleigh scattering by the overlying gas is not a major contribution though definitely present at the ultraviolet end, particularly for the poles of the planet, as was shown by Dr. Gehrels *et al.* (Fig. 4, below). The part $\lambda > 0.6\mu$ is cut up by absorption bands, generally increasing in strength toward longer wavelengths. The identifications are marked in the diagram. These identifications are based on laboratory comparisons, often made one at a time, ever since R. Wildt identified NH_3 in 1931 and in 1932 suspected some other photographically recorded bands were due to CH_4. T. Dunham pursued the matter with the much greater powers of the 100-inch Coudé spectrograph after 1932(cf. Dunham, Chapter XI, 1952). He confirmed the identification of NH_3 (approx. 5-10 meter atm.; *op. cit.* p. 303), though not all observed near-IR bands were yet matched by laboratory spectra.

Kuiper (1952) repeated the medium-resolution photographic spectral studies, 0.4-1μ, and obtained laboratory matching spectra throughout; and extended the spectral range with the newly developed PbS cell to about 2μ (*op. cit.* p. 364). Greatly improved spectra from 0.90-1.63μ, with sets of matching laboratory spectra of NH_3 and CH_4, were published later (Kuiper, 1963).

Systematic laboratory tests of numerous possible constituents in planetary atmospheres were published by Kuiper and Cruikshank in 1964 and 1967 (*LPL Comm. Nos. 34* and *79*). The gases examined were CH_4, NH_3, N_2O, CO, COS, C_2H_2, C_2H_4, C_2H_6, CH_3SH, CH_3NH_2, H_2S. A new study of the Jupiter spectrum for the region 0.95-1.62μ with 1.5 times the resolution of my 1963 study, also having detailed new laboratory comparisons, was published in 1968 by Cruikshank and Binder (*LPL Comm. No. 103*). They also derived new upper limits for C_2H_2, H_2S and HCN, and derived with great care composite spectra of CH_4 and NH_3 to match Jupiter. Important higher-resolution studies in the photographic infrared were made by Owen (1965) covering the region 0.77-1.12μ which led to upper limits of the abundances of 8 interesting compounds (C_2H_2, C_2H_4, C_2H_6, CH_3NH_2, CH_3D, HCN, SiH_4, HD). He clarified the identifications in the region of the 7900Å ammonia band which is indeed present in Jupiter, but not in Saturn; he found that the previous attribution of the Saturn absorptions to ammonia was mistaken; they were instead due to methane. Owen (1965) also reviewed the *temperatures* derived from different bands of NH_3 and H_2 (i.e., different levels in the atmosphere), finding a range from 128-200°K, indicating very considerable vertical thermal structure in the layers visible between 0.8μ and 3.75 cm, in accordance with temperature measurements quoted below. Moroz and Cruikshank (1969) studied from IR spectra, 1.3-1.6μ, the surface distribution of NH_3 and CH_4. They found a strong latitude effect on NH_3 as well as frequent time variations and a marked E-W inequality, all interpreted in terms of the effective cloud level.

IR spectroscopic investigations of much higher resolution were made by Connes *et al.* (1969) with the first Connes interferometer at the 1.8 meter Hautes Provence telescope; and later with the same interferometer at the 90-inch Steward Observatory telescope, by H. Larson and U. Fink. These results extend beyond this exploratory review of the solar part of the reflection curve of Jupiter.

The *thermal part* of the Jupiter energy curve, 3-1000μ, is known largely through the persistent research efforts, extending over several years, by Dr. Frank Low and associates. We shall refer to these investigations in order of increasing wavelength. The paper by Gillett, Low, and Stein (1969), based on 1967 observations with the 28-inch and 60-inch telescopes, deals with the Jupiter spectrum between 2.8 and 14μ. Because of its importance, we reproduce in Fig. 3*b* the plot of measures. The blackbody temperature from 9-14μ corresponds roughly to 125°K, in agreement with both earlier and later measures in that region (averaging about 128°K). This comparatively low temperature (in terms of the expected value for NH_3 cloud formation) had been interpreted by Kuiper (1952, p. 380) as due to the very strong double ammonia band covering the entire interval 9-14μ. This interpretation was confirmed by Gillett *et al.* who published the absorption spectrum of NH_3 for 10 cm path-length, 1 atm pressure, reproduced in Fig. 3*c*. The extraordinary new feature of the Gillett *et al.* contribution was the intensive emission between 4.4 and 5.5μ, equivalent to a blackbody temperature just under 230°K. These and subsequent studies *have shown this region to be the most extraordinary spectral band of the planet, allowing deep penetration into the Jupiter atmosphere* and an entirely novel set of investigations of the Jupiter clouds.

In April and May 1969 Westphal (1969) discovered *localized* thermal emission from Jupiter at 5μ, with peak brightness temperatures of at least 310°K, in narrow elongated regions between 5° and 20°N latitude. Low and Armstrong, independently, using the 61-inch telescope in June 1969, with 7 arc-sec resolution, found the North Equatorial Belt to have a higher temperature than the remainder of the disk. This work was later continued with higher resolution, with samples quoted on p. 221 of *LPL Communication No. 172*. These remarkably high temperatures prove that the Jupiter atmosphere is far from isothermal as had been assumed in some earlier model and opacity studies. Dr. Low's image scanner may be used also in the other atmospheric windows.

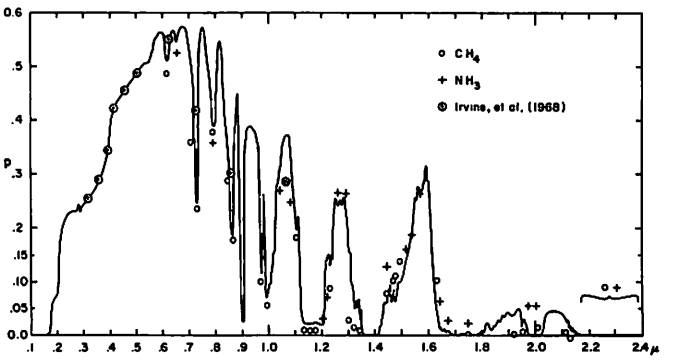

Fig. 3*a* Jupiter reflection curve (geometric albedo), 0.15-2.4μ. Sources: Anderson *et al.* (1969), Irvine *et al.* (1968), LPL spectral data and Johnson (1970). CH_4 circles, NH_3 crosses. (Ordinates 1-2μ somewhat uncertain)

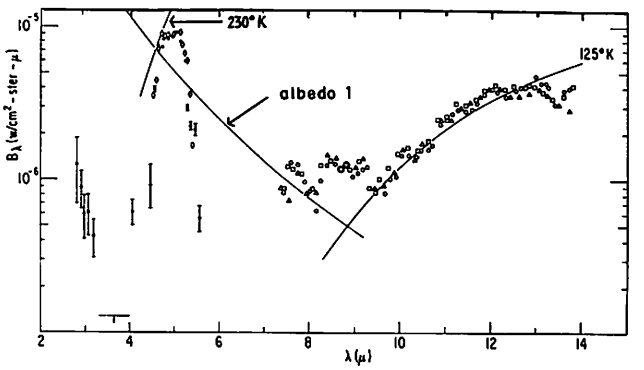

Fig. 3*b* Monochromatic surface brightness of Jupiter, 2.7-14μ (Gillett *et al.* 1969, Fig. 1). Arc at left, solar reflection if albedo is 1

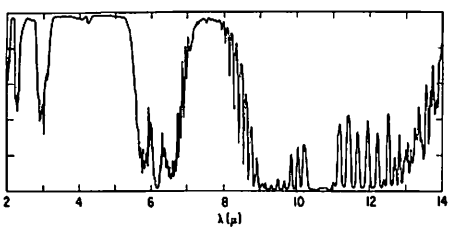

Fig. 3*c* NH_3 absorption spectrum of 10 cm at 1 atm, 2-14μ. (Gillett *et al.* 1969)

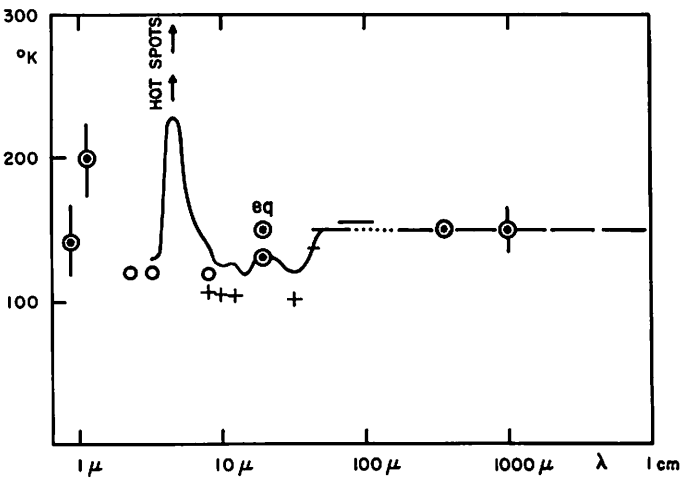

Fig. 3*d* Jupiter emission vs. wavelength, 3μ-1 cm, expressed as radiation temperature. Symbols as in 3*a*. Sources in text except values near 1μ based on H_2(.64, .82μ) and CH_4(1.1μ) (Owen 1965)

More extensive exploration of the Jupiter disk in the 5μ window was described in "High Resolution Measures of Jupiter at 5 Microns" by Keay, Low, Rieke and Minton (*Ap. J.* in press). The observations were made with the 61-inch telescope, mostly in May 1972.

The region around 20μ (approx. 17-24μ) was investigated (F. Low, 1966) at the Catalina Observatory. Low found an equatorial hot band on Jupiter, from approximately -10° to +10°, with a temperature of 150±5°K, with the rest of the planet at about 130°K.

Very recently Low, Rieke, and Armstrong succeeded in measuring the planet for the first time from Mt. Lemmon in the 28-40μ atmospheric window (*Ap. J. Letters*, in press). The wavelength band centered at 34μ is accessible only on very dry nights. The Jupiter temperature found was around 120°K.

Armstrong, Harper, and Low (1972) published results of the far-infrared brightness temperatures of Jupiter, measured in several bands from 30-300μ. The results are 136±1° for 30-45μ; 150±5° for 45-80μ; 153±7° for 65-110μ; and values close to 150°K for the intervals 125-300μ and around 350μ. The last result (350μ) was in fact obtained from the Mt. Lemmon IR Observatory where observations at that wavelength are possible under dry atmospheric conditions, with the results fully published by Harper, Low, Rieke, and Armstrong (1972). Currently the same authors are making further measures in the 1-1.4 mm range.

Low and Davidson (1965) measured the brightness temperature at 1 mm to be 155 ± 15°K. This level is maintained to about 3 cm beyond which the radiation temperature rises owing to increased penetration (Gulkis, personal communication). The entire set of data is summarized in Figure 3*d*. A portion of this energy curve (responsible for about 1/3 of the total planetary emission) lies between 20 and 35μ, an area specially studied by Owen and Walsh (1965).

c. Medium and High Resolution Spectroscopy - A new Laboratory effort in planetary spectroscopy began by using medium-resolution *interferometers*, with the initiation of the NASA Convair-990 flights out of NASA-Ames in April 1967. This program has been described in the *LPL Communications*, starting with *Nos. 93* and *94*, "Program of Astronomical Spectroscopy from Aircraft" and "Solar Comparison Spectra 1.0-2.5μ from Altitudes 1.5-12.5 km". Papers on the Venus spectrum followed, describing the discovery of H_2O on that planet (previous announcements of 50-100 times the real amount were thereby superseded), based on the CV-990 observations with a Block interferometer with resolution 8 (and later 5) wave-numbers; or resolution 1000 at 1.25μ and 500 at 2.5μ. Jupiter was also observed, both at the Catalina Observatory and on the CV-990, but no results were obtained distinctly better than with the grating (A) spectrometer. This was due to the smallness of the 12-inch telescope used on the CV-990, the low IR intensity of Jupiter, and to Jupiter's absorptions mostly coinciding with the water-vapor bands so that little was gained from high altitude at 1-3μ. Dr. H. L. Johnson (1970) investigated the spectrum of Jupiter from 1.2-4.2μ, with resolution 8 cm^{-1}, and derived ratio spectra in terms of the Moon.

Excellent results were obtained with the much higher-resolution original *Connes interferometer*, on indefinite loan from Dr. Pierre Connes of Paris, France, and placed at the Coudé focus of the 90-inch Steward Observatory telescope on Kitt Peak. Drs. Harold Larson, Uwe Fink, and Guy Michel (of Paris) have succeeded in

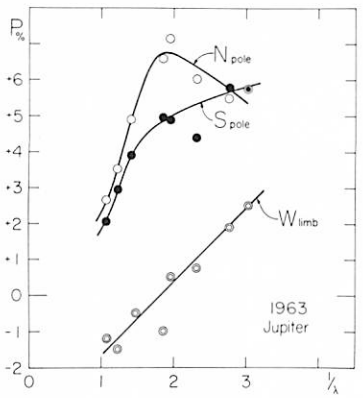

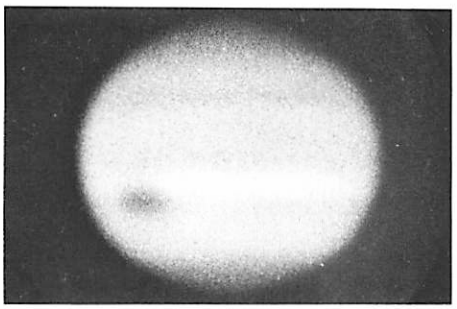

Fig. 4*a* Asymmetry between two hemispheres of Jupiter derived from polarization measurements (Gehrels *et al.*, 1969); *b*. Jupiter at λ3000Å, 1971, April 8, 10:26:40 UT. (J. Fountain)

solving the numerous problems with the mounting and operation of this instrument. The interferometer is capable of a resolution of 180,000. Eight interferograms of Jupiter have been obtained so far, representing about 30 hours of net observing time. Five interferograms were obtained with resolution of 55,000; they have been Fourier-transformed and are being averaged and analyzed. These new spectra should give improved abundances, new isotope ratios, gas temperatures, and hopefully, new trace constituents.

A 500-channel spectrometer for the 0.35-1.0μ region using a cooled silicon-diode detector is being assembled for spectroscopy of small portions of the planetary disks, satellites, standard stars, and laboratory comparison sources. A later paper on the results will be issued.

d. Photometric and Polarimetric Studies - Dr. Tom Gehrels and his group have developed the measurement of polarization over a wide range of wavelengths, reaching a precision in the orthogonal ratios down to a few ten-thousandths. They found a systematic difference between the South and North Polar caps as well as the planet's limb (Gehrels *et al.*, 1969), as shown in Figure 4*a*. They interpreted the results as due to scattering by molecules plus aerosols; the North Pole shows a molecular optical depth in visible light of 0.6, the South Pole of 0.4, the equator of 0.05; the amounts of hydrogen deduced were 240, 160, 20 km atm., respectively. More recently, Mr. Lyn Doose (Ph. D. dissertation) systematically scanned the entire Jupiter disk with the 61-inch both *photometrically* for about 20 wavelength bands; and *polarimetrically* in 7 bands. The photometric scans included the 8890Å CH_4 band and a comparison band at 9200Å. They were used especially in the study of the Red Spot, both cloud level and scattering properties. Mr. Doose found the Red Spot to be about 5 km elevated above the surrounding cloud deck. It should be noted that the spectroscopically-determined H_2 content is about 4 times larger, 85 ± 15 km atm (Owen, 1969, p. 356). This difference can only partly be attributed to the wavelength difference of the two determinations 0.55 and 0.70μ.

What are the Jupiter *cloud colors*? LPL started a 40 narrow-band filter photometric program of the Jovian planets and satellites a year ago, covering 0.3 to 1.1μ, with spectral resolution $\lambda/\Delta\lambda$ about 30. The program was carried out by Mr. W.

Wamsteker. Data for the four Jovian satellites were published in *LPL Communication No. 167*; the four Jovian planets, the Saturn Ring, and Rhea of Saturn are still under observation. The results on the solid bodies (no atmospheres) have been less informative than hoped for. The region 1-4μ is much more informative (Kuiper, 1957; Fink *et al.*, 1973).

e. Far-IR Measures at High Altitude - Low, Aumann, and Gillespie (1969) measured the total IR emission of both Jupiter and Saturn (5-100μ) on high-altitude flights with the NASA Lear Jet. They found the infrared emissions of the two planets 2.7 and 2.3 times the amount absorbed from the in-coming solar radiation. While qualitatively this result was not unexpected (see Appendix I), the actual amounts were unknown and are important empirical parameters in the recent model studies by Hubbard and others, referred to in Sec. 1.

f. Participation in NASA Pioneer Missions - Dr. Tom Gehrels is the principal investigator on the NASA Pioneer F (or 10) and G Missions for imagery and polarimetry. These are to operate in two colors at about 3-4 times present earth-based resolutions, for the limited periods of the encounters (Gehrels, Suomi, Krauss, 1972). The polarimetry will extend beyond the earth-based upper bound of 11° phase angle, and will therefore be far more informative than the available polarimetric data. Hopefully, distinct information will be derivable on particle sizes and the refractive index of the cloud material.

g. Laboratory Studies - A comparison program matching the spectral and broadband photometric observations is underway by Fr. Godfrey Sill, a chemist, using laboratory experiments and thermodynamic theory. He is preparing a report on his laboratory data for *LPL Communication No. 184*.

3. Interpretative Remarks

a. Comparisons with the Earth and Levels of Penetration - Since WWII the Earth has been observed as a planet, from above the atmosphere, on an ever increasing scale. What started as efforts to observe extended cloud systems and cyclones from rockets; temperature, pressure, and composition profiles of the atmosphere from rockets; circulation patterns and global weather systems; has developed, with the Tiros and Nimbus series, beginning in 1961, into an increasingly systematic global watch of the Earth. For instance, Nimbus III used (1969-70) five filter bands simultaneously:

(1) 0.2-4.8μ, to observe the integrated reflected sunlight;
(2) 6.3μ, to observe the upper tropospheric H_2O vapor;
(3) 10-12μ, to observe the thermal emission from the Earth's surface, where clear;
(4) 15μ, to observe the atmospheric CO_2; and
(5) 20-23μ, to observe the lower tropospheric H_2O and clouds.

These programs, mostly conducted at the Goddard Space Flight Center for the past decade, have fully succeeded after passing through the expected refinements in instrumentation and communication; and the necessary calibrations, often from specialized airborne equipment.

A simple transfer of these techniques to Jupiter is not feasible, but there are distinct parallels:

(1) color and filter photography 0.3-1μ, as commonly practiced; with vidicon imaging techniques 1-2μ being improved;
(2) the 0.89μ CH_4 photography observes the uppermost cloud layers;
(3) the 5μ window provides the deepest penetration into the Jupiter atmosphere;
(4), (5) filter photography selected to cover intermediate depth and temperatures, e.g. may be selected on the basis of Figure 3.

The penetration into the Jupiter atmosphere may be roughly estimated from Figure 3*d* with the aid of a model atmosphere based on available abundance ratios. The intensities of the IR fundamentals ν_2, ν_3, and ν_4 of CH_4 in mixtures with He, A, and N_2 at pressures up to 3000 atm were derived by Armstrong and Welsh (1960). The IR spectrum of NH_3 from 20-35μ was studied by Walsh (1969), both for pure NH_3 and mixtures with N_2, following the paper by Owen and Walsh (1965) dealing with the Jupiter spectrum and the planetary heat balance. Walsh used path lengths up to 196 meters, examined the pressure effects on the total absorptance, compared his measures with theoretical line models (strong-line, weak-line) and found discrepancies of importance to planetary spectral studies. Unfortunately, similar laboratory data for NH_3 do not appear to exist beyond 35μ which would cover the pure rotation spectrum. For this reason it is difficult to interpret Figure 3*d* beyond 35μ, where, in fact, the temperature measures are only approximate in any case. One would expect a temperature profile somewhat below 150°K, and possibly as low as 135°K, in the region of the rotation spectrum of NH_3. It should be noted that the effective temperature of the planet was found by Aumann *et al.* (1969) to be 134±4°K, which would lead one to assume to be the weighted average for the region of about 8-100μ. The remarkably high temperature observed in the 4.5-5.5μ window averaged over the entire disk indicates that *gas absorptions* (mostly NH_3) rather than clouds are responsible for the low temperatures measured at longer wavelengths. The various windows at $\lambda<6\mu$ should give supplementary information on particle sizes and cloud layers vs. temperature or depth. The relative transparency of the 4.5-5.5μ window suggests that the particles above 220°K are only micron size.

The window 0.74-0.76μ deserves special attention. The Uranus and Neptune spectra show the CH_4 absorptions there to be extremely weak. Owen (1967), who identified as CH_4 the weak lines I had observed here for Uranus and Neptune, derived laboratory data implying that some 100 km atm of CH_4 would be needed to give appreciable CH_4 absorption in this window. Since NH_3 also appears "absent", one could assume that for Jupiter the penetration in this window might be limited by Rayleigh scattering of H_2. Then the required amount of H_2 would be 500-600 km atm, which, however, by Owen's (1969) temperature profile (assumed to be the adiabat) would make T>300°K. Some check on the reality of this deep penetration could be made by setting an upper limit to the CH_4 content seen in this window from high precision high-resolution spectral traces. About 1 km atm of CH_4 is expected if indeed the limit is set by molecular Rayleigh scattering. Alternatively, the penetration limit is set by atmospheric haze. This is probably true except for the blue festoons, discussed later. These areas are probably too small for spectroscopic T determinations (0.82μ H_2, 1.1μ CH_4). Narrow pass-band filter studies up to 1.6μ might assist here.

A filter selected to cover a given band (e.g. CH_4 6190Å or 8900Å) does not show a *single* depth of penetration. A high-resolution spectrum is needed to show the fraction of various degrees of absorption (each with their own penetration) and possibly intervening stretches of continuum. The profiles of the photographic

CH_4 bands are smoother than the NH_3 bands (which show sharper, well-separated lines). The estimate of the effective *mean penetration* of the planetary image in the band must therefore be made with great care. The same problem has arisen for satellite spectral studies of the Earth.

The spectral curve between 0.2-0.3μ has been explained by Stecher, and in more detail by Greenspan and Owen (1967), as due to the scattering of H_2 and mild absorptions due to NH_3. The amount of H_2 so derived is 12 km atm, which is approximately the amount expected for the Jupiter stratosphere. This interpretation is consistent with the small but definite limb brightening at 0.30μ discovered by J. Fountain; and with the fact that the Red Spot and several cloud belts become visible around 3000Å (Fig. 4*b*). The amount of H_2 estimated from the intensity of the Red Spot in Figure 4*b* (assumed to be intrinsically dark) is some 20 km atm of H_2; this deeper penetration is roughly in accord with the lower Rayleigh scattering.

The interpretation of Figure 4*b* is considered by Mr. Fountain in a following *Communication*, in the context of his other narrow-band records of the planet. There is no close resemblance to Figure 1,clearly because of large brightness differences in the UV between the different high-level cloud belts, though all overlain with the common semi-transparent H_2 blanket (these differences cause the large range in color).

Comparison of the atmospheric *models* of Earth and Jupiter can be misleading since *Jupiter has an internally-driven meteorology*. Interesting computations, as have been made for the radiative balance within the Earth atmosphere, resulting from the various gaseous components (e.g. Dopplick, 1972, pp. 1278-1294), are therefore not readily transferable to Jupiter. Goody (1969) pointed out that in the upper atmosphere of Jupiter *the dynamics dominates radiative balance*.

The dynamical parallels between the Earth and Jupiter atmospheres are instructive. These are developed in Sec. 4 on a special topic: the terrestrial Tropical Convergence Zones are compared with the high-level cloud zones on Jupiter at 22° N and S, one of which contains the Red Spot. This leads to an interpretation of the Red Spot in terms of the theory of Organized Cumulus Convection (p. 288 ff).

Two introductory aspects are considered here: (a) the comparison of the Jupiter IR emission spectrum (Figs. 3*b* and 3*d*) with that of the Earth and Mars, all three showing variations in penetration with wavelength due to the gases present; and (b) near-monochromatic images of the Earth, both in the strong water-vapor band at 6.7μ and in a clear window, 10-12μ; to be compared with images of Jupiter taken in the very strong 0.9μ CH_4 band (Fig. 1) and in the clear 5μ window (cf. p. 221), respectively.

Hanel and Conrath (1970) published Earth spectra from 6.7-25μ for selected regions,the Sahara, the Mediterranean, and the Antarctic, which are reproduced in Figure 5*a*. The resolution is 2.8 cm^{-1}; the gases are identified. One notes the 15-20 fold change of intensity in the central atmospheric window, 10-12.5μ, depending on the surface temperature; and the nearly isothermal CO_2 band at 15μ which, because of its high absorptivity, shows the temperature of the atmosphere above 300 mb, which indeed is nearly constant over the Earth. The strong H_2O absorption at 24μ is similarly nearly isothermal over the globe, while the ozone, of medium strength only, shows an admixture with background radiation.

The relation to black-body curves is shown in Figures 5*b* and 5*c* (Hanel *et al.* 1972*a*), and is self-explantory. The effect of clouds in the atmospheric window of 8-14μ is shown in Figure 5*d*. It is seen that the depth of the strong CO_2 band is not affected, because its level is *above* the clouds.

The Mars spectra are not unlike those of the Earth, except that CO_2 is stronger; and H_2O and O_3 very weak or absent. Beautiful data were obtained by Hanel *et al.* (1972*b*) on Mariner 9. The authors have consented to the reproduction here of two of their published spectra. Figure 5*e* shows the spectrum after the atmospheric dust had settled (normal condition). Figure 5*f* shows the spectrum under dusty conditions. Reference is made to the original paper (Hanel *et al.*, 1972*b*, Figs. 7 and 10) for most remarkable spectra of the two Martian polar caps.

The spectra of Mars (Figs. 5*e*, *f*), Earth (Fig. 5*a-d*), and Jupiter (Fig. 3) form a sequence of both increasing gaseous absorptions and interference by clouds. While the Mars continuum (due to its surface) is interrupted only by CO_2 and occasional dust (and locally H_2O ice clouds: Curran *et al.*, 1973); the Earth continuum 8-14μ is the only prominent one in the entire interval 2-1000μ, and even so is for about 50%

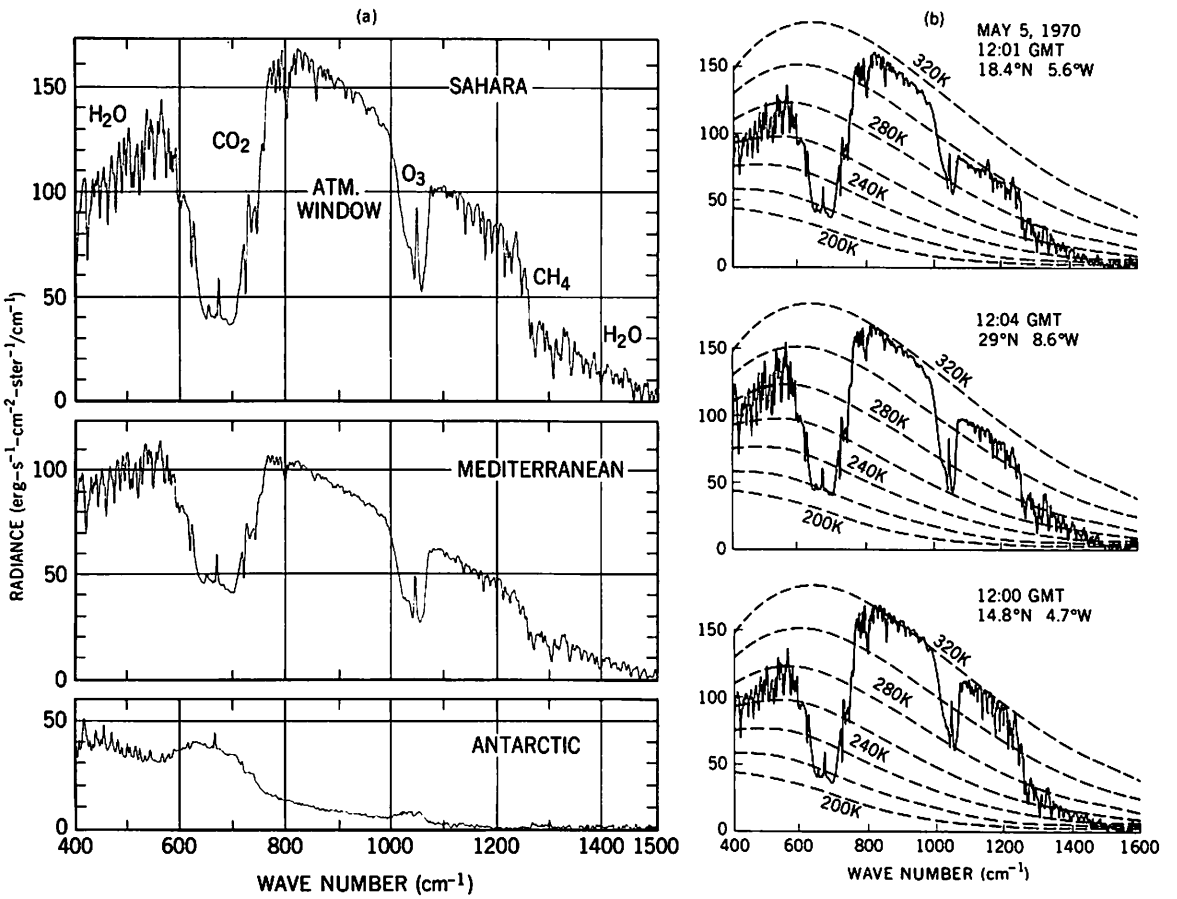

Fig. 5*a*. Thermal emission spectra of Earth, Nimbus IV, Orbit 29, 10 April 1970; 5*b*. Spectra on 5 May 1970, at times and coordinates given (courtesy Dr. Hanel)

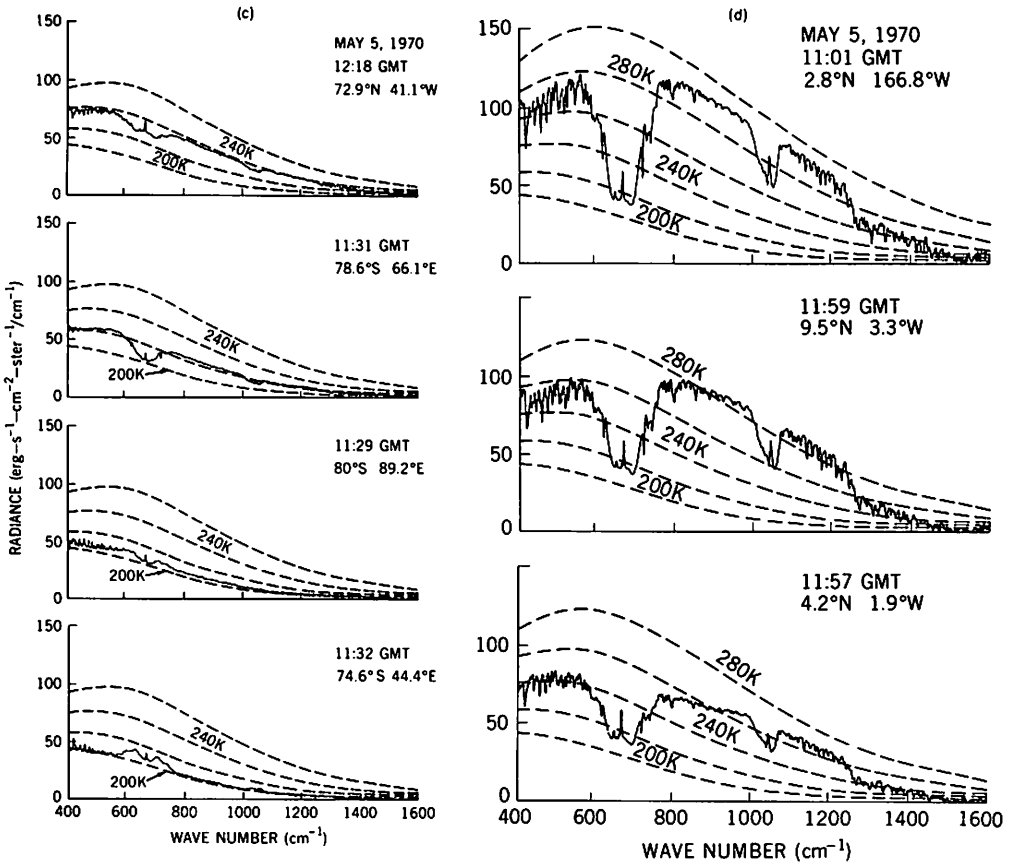

Fig. 5 (cont.) *c*. Spectra of areas of Greenland (upper frame) and Antarctica; *d*. Effects of clouds in atmospheric window, incl. departures from black-body curves (courtesy Dr. Hanel)

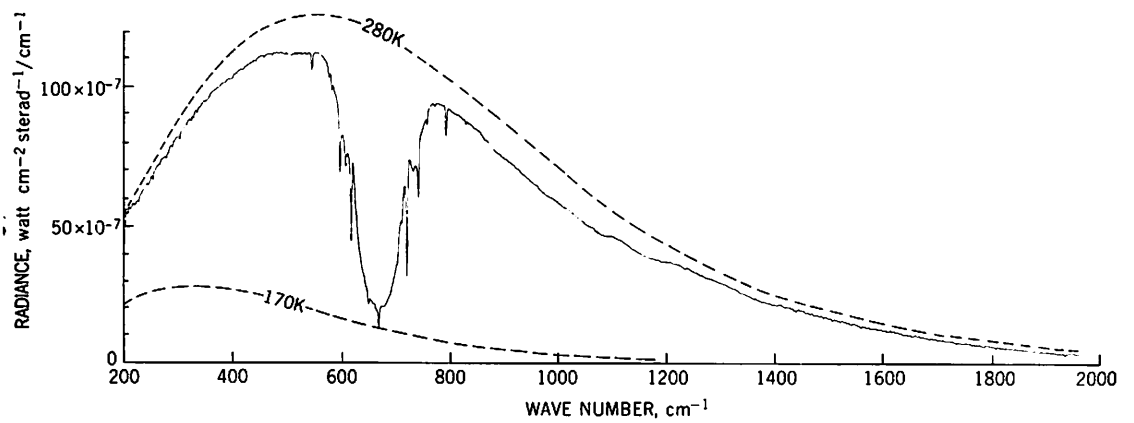

Fig. 5*e* Midlatitude spectrum of Mars, March 1972. Mariner 9 (Hanel *et al*. 1972*b*, Fig. 9), after atmospheric dust had settled

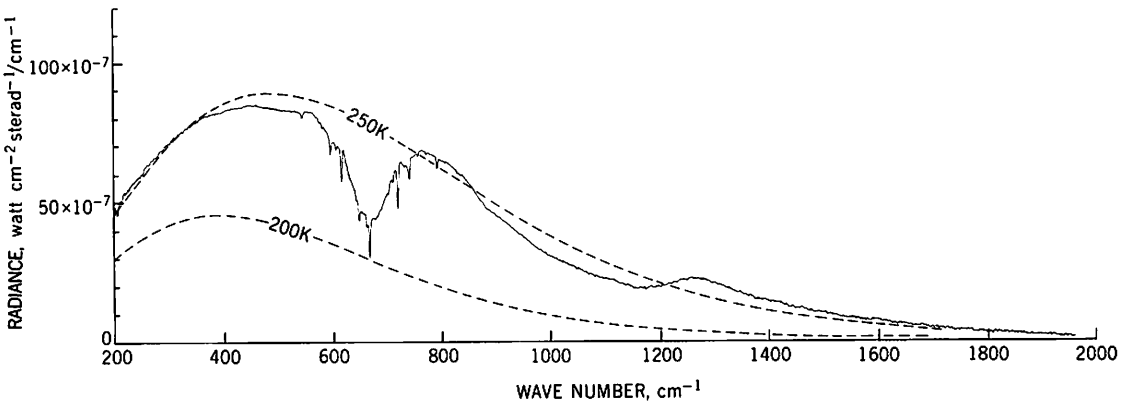

Fig. 5*f* Midlatitude spectrum of Mars, Dec. 1971, under dusty conditions (Hanel *et al.*, 1972*b*, Fig. 8). Reduced atmospheric lapse rate, hence shallow CO_2 band. SiO_2 bearing minerals in evidence from 400-600 cm^{-1} and 850-1300 cm^{-1}

of the Earth's surface interrupted by clouds. Jupiter has only the 4.5-5.5μ major window and its penetration is limited to small equatorial areas without clouds of NH_3 and its compounds; and then stopped entirely by the deeper H_2O cloud zone, at about 300°K.

Through the courtesy of Dr. W. Nordberg, NASA-Goddard, I am able to reproduce in Figures 6*a* and *b* two composite images of the Earth in the 6.7μ H_2O band obtained with the Temperature-Humidity Infrared Radiometer (THIR) aboard Nimbus V. These montages cover most of the globe (with some Central Pacific and North of about 50° missing) and were taken during the daylight orbits on 1 and 8 February 1973. The 11 or 12 strips each cover about 30° in longitude and thus are nearly adjacent near the equator; but N and S of about 40° latitude they show increasing duplication of features. The South Pole has been marked with white dots. Dr. Nordberg advised me that the penetration at 6.7μ is on the average to about 300 mb. Dry, deeper and thus hotter regions than average are shown darker; elevated (and colder) humid regions are shown whiter. The two dry desert zones at ±30° are in evidence (dark) as is the Tropical Convergence Zone (light colored). In the middle latitudes of both hemispheres curious swirling patterns are seen containing several cyclonic vortices. These broad patterns, made up of streamers 100-500 km wide, carry finer-textured clouds (down to 10 km and probably finer) as is seen in the 10-12μ frames taken simultaneously (Figs. 6*c*, *d*). These pictures also show the continents (dark and hot) and thus fix the approximate coordinates.

Figures 6*a-d* are *negatives* of the observed radiation-intensity distribution, printed thus to show the *highest* (coldest) structures as *white*. For this reason they may be compared to Figure 1, though a more direct comparison is made in Figures 7-9, below, which, like Figure 1, were taken in reflected sunlight.

In the 5μ window nearly the entire Jupiter disk is seen to have radiation temperatures above 210°K (Keay *et al.*, 1973; cf. p. 221 of this Volume). This shows that the cloud deck seen visually is composed of small particles, 1μ or less in diameter, a subject already commented on by Owen (1969). Along the central part of the visible equator there is an elongated region, of variable size, above 230°K, often containing one or more hot spots of temperatures 250-300°K. Owen (1969) finds NH_3 in a convective Jupiter atmosphere of solar element-abundance ratios to be saturated above the layer where T = 160°K, and unsaturated below. He thus concludes that the NH_3 ice haze will extend *above* this level, and that the atmosphere should be clear below (until other opacity sources become important). He thus accounts

Fig. 6*a* Montage of 11 consecutive orbital strips of the Earth, each 30° wide at the equator, observed in 6.7μ H_2O band, on Nimbus V; 1 Feb 1973. For identification of longitudes cf. Fig. 6*c*. (Courtesy Dr. W. Nordberg, NASA)

Fig. 6*b* Montage of 12 consecutive strips, 8 Feb 1973; otherwise like Fig. 6*a*. (Courtesy Dr. W. Nordberg, NASA)

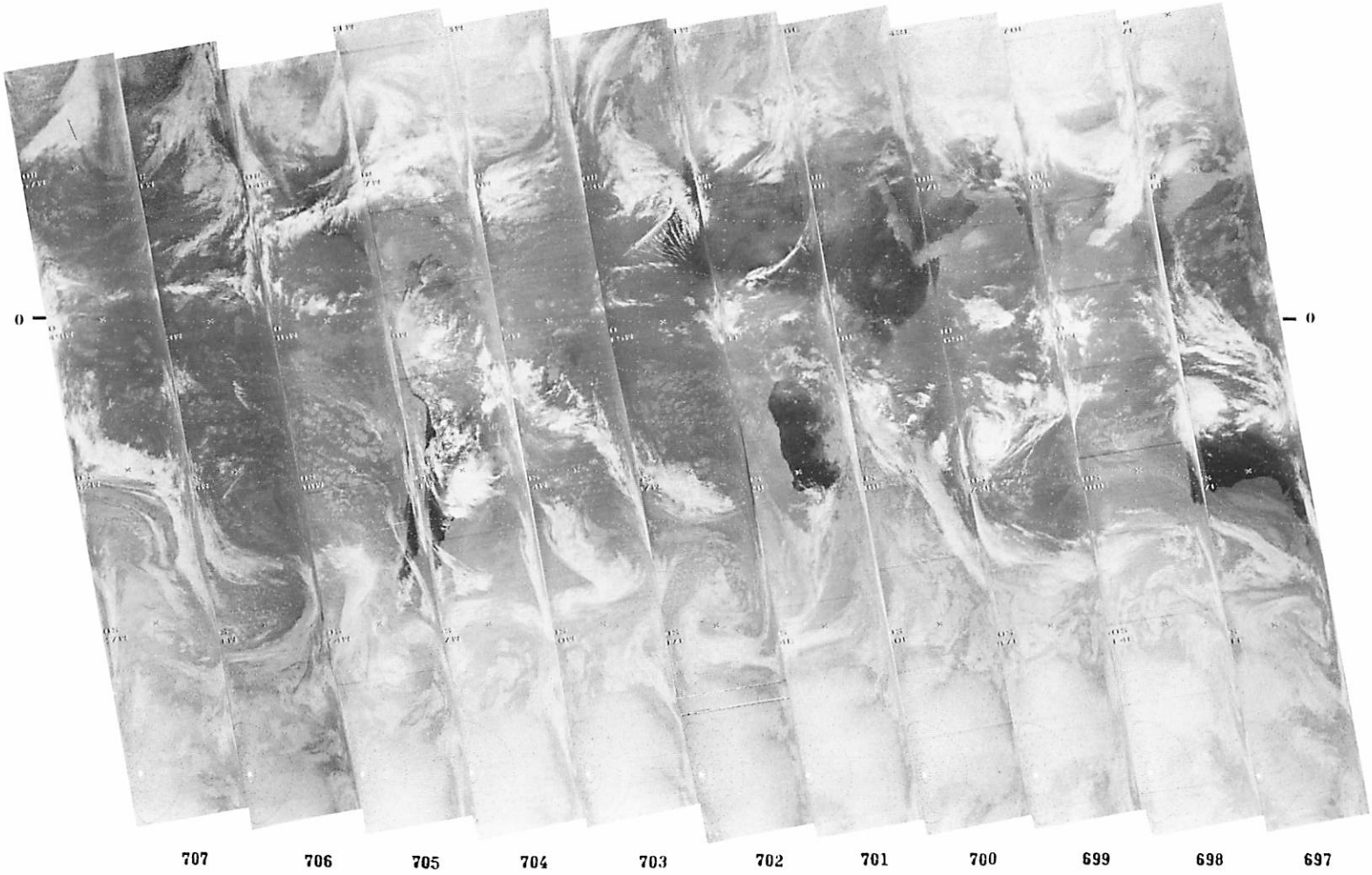

Fig. 6c Montage of 11 consecutive orbital strips taken in window 10-12.5μ on Nimbus V, taken simultaneously with Fig. 6a. South America, Africa, Arabia, India, and Australia well shown, with Pacific coastal outline of North America. (Courtesy Dr. W. Nordberg, NASA)

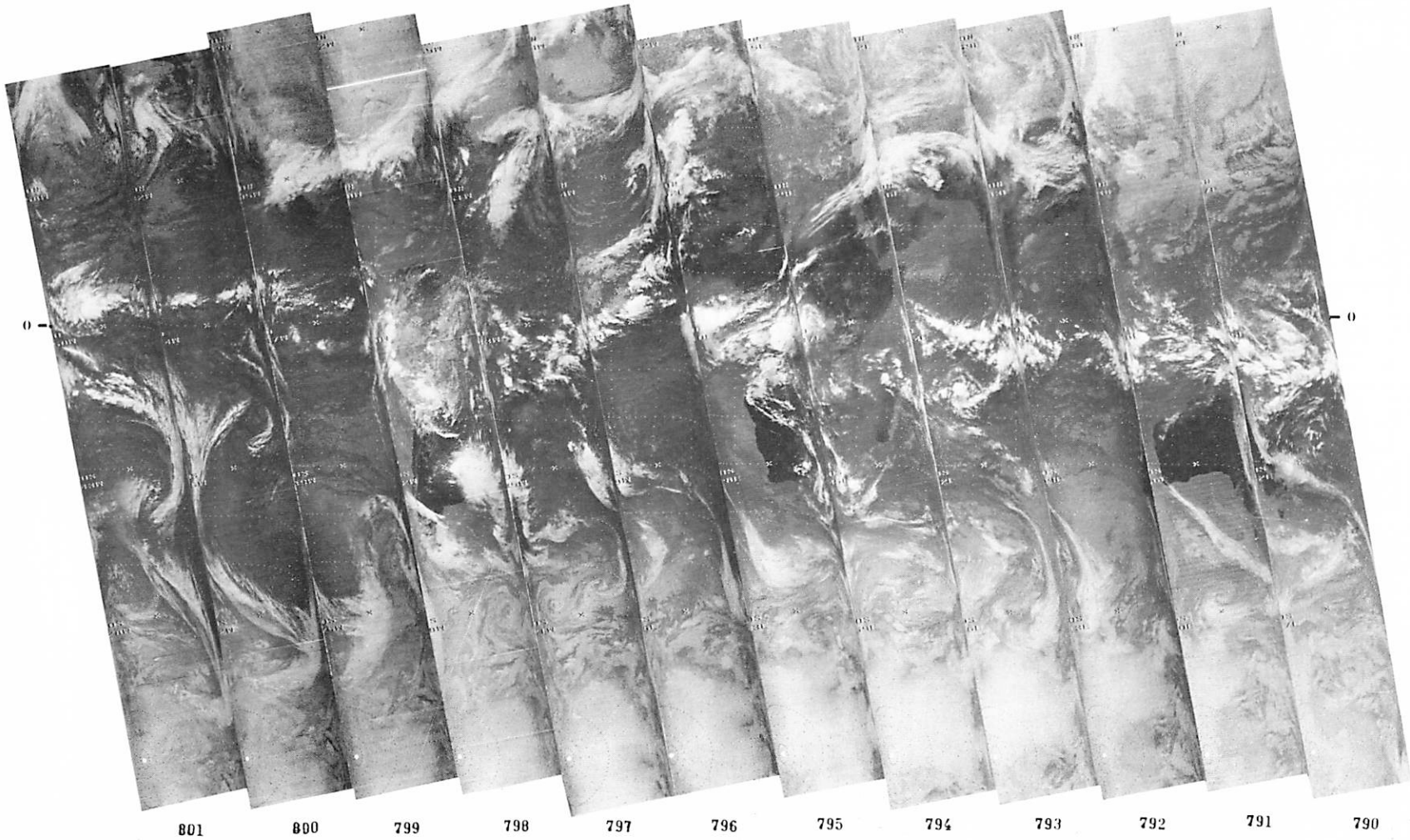

Fig. 6*d* Montage of 12 consecutive orbital strips taken in window 10-12.5μ, Nimbus V, taken simultaneously with Fig. 6*b*. South and Central America, Africa, Arabia, India, and Australia well shown. White dots at bottom indicate position of South Pole. (Courtesy Dr. W. Nordberg, NASA)

for the rotational CH_4 temperature derived (cf. Fig. 3*d*) and possibly for the temperature found for H_2 (0.82μ). This model is essentially consistent with conclusions by Lewis (1969).

Lewis considers two composition models: A and B (differing in He content), with model B probably more closely applicable to Jupiter. He further examines the effects of H_2S interacting with NH_3, and concludes (p. 376) that solid NH_3 would be present above the layer at which T = 160°K (in agreement with Owen); that NH_4SH would become increasingly abundant below the level at which T = 200° up to T = 225°K; that H_2O ice would follow, T = 225°-270°, beneath which an aqueous solution of NH_3 would exist to about 310°K. Lewis concludes "pure water ice cannot be a major component of the clouds and pure liquid NH_3 is found to be absent". Maximum opacities are expected around 160°K (solid NH_3), 225°K (NH_4SH) and 300°K (aqueous NH_3 solution). What is clearly needed is a better definition of the particle sizes and composition (see next section) of the 160°K cloud layer, which can be done readily; and laboratory studies under simulated conditions on the two other layers, both of which are accessible in the 5μ window.

It will be important to derive the precise dimensions and temperature of the Red Spot at 5μ (so far found cooler) and relate the results to the interpretation of the Red Spot proposed in Sec. 4. (If the size is comparable to the visible size of the Red Spot, its T is probably low and the particle size >> 1μ; if the size is much smaller, T is probably higher than its surroundings and refers to the inner system of columns; see Sec. 4). Also, to determine the penetration in the other spectral windows shown in Figure 3*a*, with the purpose of deriving further data on the average cloud particle size.

It is a curious coincidence that the 6.7μ pictures of the Earth (Fig. 6*a*,*b*) should penetrate to nearly the same temperature regions as the 5μ pictures of Jupiter.The differences are important, however; the 5μ pictures of Jupiter show clouds,probably composed of NH_4SH, the 6.7μ pictures of the Earth show the variable elevations of moving air masses containing a given total amount of water vapor, which, when high in the atmosphere, is accompanied by local H_2O cumulus formation.

b. Cloud Colors - The concept of the visible clouds as pure NH_3 ice crystals is contradicted by the vivid colors observed, from white to cream, yellow, brown, dark brown, and bluish-gray. Ammonia ice is white. Owen (1969) comments on the apparent correlation of the colored regions with somewhat increased altitude. Owen and Mason (1969), following the Lewis (1969) discussion, note that $(NH_4)_2S$ is yellow and might be present on Jupiter.

An incisive study was published by Lewis and Prinn (1970). They point out that the yellow color of $(NH_4)_2S$ is due to oxidation in our atmosphere and that the colored substance is in fact the polysulfide $(NH_4)_2S_x$. They add that the oxidation could not occur on Jupiter, but that *photolysis by solar UV* could produce the coloration. They consider the transfer of 2200-2700Å solar radiation (2700Å is the cut-off limit of H_2S absorption) and conclude that in areas of the planet where the NH_3 cirrus cover is thin or absent the 210°-230°K level containing NH_4HS will be reached. The result will be the production of H_2S_x, S_8, and $(NH_4)_2S_x$, all of which are yellow, orange, or brown. No conclusion was reached for areas having a substantial NH_3 ice cloud cover (which would cause absorption of UV); but they do point out that the UV photolysis will act signficantly in periods of about one week, contrary to an earlier suggested explanation of the cloud colors by Sagan through the production of colored organic matter, which would be some 10^5 times slower. The dynamics of the Jupiter cloud masses requires the shorter time scale.

At this Laboratory, a parallel and independent investigation of the cloud colors was started in 1970 by Fr. G. Sill, on which he reported at the San Francisco meeting of the A. G. U., Dec. 8, 1970, Symposium on the Jovian Cloud Layers. Fr. Sill reproduced the processes in the laboratory and at temperatures appropriate for Jupiter, which led to the discovery that *many of these colors are temperature-dependent.* Sulfur is white at the Jupiter temperature; so is NH_4HS. Fr. Sill reports on his experiments in *LPL Communication No. 184.* Plate I shows the Jupiter colors.

Since cosmically S is less abundant than N by 5 or 6x, most of the ammonia will remain and produce clouds composed of ammonia cirrus (whitish). The dynamics of the cloud belts may bring the polysulfides to high altitudes where the photolysis would be enhanced. This would explain the fact that the Red Spot is both very high and orange in color. There is, however, evidence that a few days of solar exposure are needed. A sudden major outburst observed in July 1971 produced a *white* very high-level cloud.

In addition, there are blue areas concentrated in a narrow zone near the equator, often fan-shaped and called "festoons". Wildt's suggestion that the brown and blue colors of Jupiter may be due to alkali metals dissolved in liquid ammonia now appears unlikely because of the laboratory studies of Jolly (1964) and others. These showed the blue color to be due to the red wing of an enormous near-IR absorption strong at 0.6μ, but weaker at 1.0μ. We shall see later that the blue areas are probably essentially cloudless and allow deeper penetration into the atmosphere. The blue-grey festoons are well shown on Plate I.

Miller and Urey, and later Sagan, Ponnamperuma, and Woeller, have considered *non-equilibrium reactions* through electric discharges, and more recently by UV light. They all give rise to hydrogen as a byproduct and run therefore in the opposite sense from purely chemical reactions in the presence of an over-abundance of hydrogen. These reactions appear to depend on the products of interest being continually removed from the reaction site. In some of the experiments the polymers produced are trapped in a cold and colorless condition, with the colors appearing only upon subsequent heating of the product itself. These conditions would clearly not apply to Jupiter. In another experiment the precursors of the polymer are unrealistically concentrated in a small reaction vessel subjected to electric arcs for several days. It is assumed that the colors so produced stem from a conjugated system of bonding, with delocalized electrons. Such a system of multiple double bonds is very liable to attack by hydrogen. Under the comparatively high hydrogen pressure and moderate temperatures in the deeper Jovian atmosphere, it is difficult to see how any polymer could have anything but a fleeting existence. The laboratory reactions also gave rise to various unsaturated carbon compounds: benzene, ethylene, and acetylene. Since the latter two are gaseous, they should be detectable in the Jovian atmosphere, yet have not been found. Not until any carbon compound besides methane is discovered on Jupiter, can Jupiter cloud colors be so explained.

The Fischer-Tropsch synthesis has also been invoked to explain certain hydrocarbons and other more complex reactions in the solar system, particularly in meteorites (Studier *et al.*, 1968). The process involves reacting carbon monoxide and hydrogen:

$$nCO + (2n+1)H_2 \rightarrow C_nH_{2n+2} + nH_2O$$

at temperatures of 450-650°K, over suitable catalysts of iron oxide, cobalt and nickel, to produce aliphatic hydrocarbons and water. Since the reaction will not

occur in the presence of a large abundance of hydrogen (methane is then produced), and since metal and metal oxide catalysts are required, it is impossible to envisage circumstances on Jupiter that would lead to the products of complex hydrocarbons by the Fischer-Tropsch synthesis. The two preceding paragraphs were prepared by Fr. Sill. It may be added that the photolysis of H_2 will favor an effective restoration of CH_4 and NH_3 from more complex compounds (Cadle, 1962).

c. Periods of Rotation - The observations of radio bursts in the 20-Mc frequency range, now available for 20 years (1951-1971), give a *constant period of rotation* for the radio sources, $9^h55^m29^s.75 \pm 0.04^s$ (Carr, 1971; Duncan, 1971), not counting an 11.9 year oscillation attributed to the variation of the Jovicentric declination of the Earth (Carr *et al.*, 1970). We may therefore reasonably assume to know the *period of the solid Jupiter surface* (or stagnant liquid), at the value just quoted; and that this period is *constant*, not wandering, e.g., as the period of the Red Spot. Since the upper molecular layer of the planet cannot, through magnetic forces, be responsible for 20-Mc radio bursts or the general magnetic field (Smoluchowski, 1971),we assume tentatively that they are caused in the Jupiter ionosphere (which explains their frequency range). In order that ionospheric bursts can be caused by events on the solid surface, a propagation mechanism must be postulated. The problem has some similarity with the production of shock waves near the solarphotosphere (Ulmschneider, 1970, 1971), invoked as the heating mechanism of the solar chromosphere and corona. The propagation of acoustic waves over many scale heights presents problems; possibly turbulent energy is involved instead. Gallet (1961) advocated this type of explanation, though he expressed reservation about "volcanic activity" on Jupiter. If the gas vents are few in number, they will not appreciably affect the total heat flux of the planet through the solid surface.* We return to the reality of the gas vents in Sec. 5.

Satellite observations of the Earth (e.g., Cortright, 1968, Sec. I) show its atmospheric circulation system to be very different from that of Jupiter, both judged by the cloud-mass distribution. The enormous weather systems in the middle latitudes are absent on Jupiter. Instead, a rather orderly system of belts and zones is observed. The Earth receives its energy from the Sun; its axis is tilted $23^\circ.5$; and there is a large transportation of heat in latitude by ocean currents. Land, mountains, and water make for complex atmospheric circulation and precipitation. The Jupiter atmosphere receives most of its energy from below; day-to-night changes will be minor. The tilt of its axis on its orbit is 3°. The Jupiter atmosphere is far deeper and denser than that of the Earth. The principal gases producing clouds and "weather" will be water vapor and ammonia (interacting with H_2S). Thus, the entire lower and denser atmosphere is likely to contain no"weather" at all; only the upper 60-80 km or so, with the water condensation in the lower parts, having ammonia in solution; and ammonia condensation in the upper parts. Most likely, the near-adiabatic gradient caused by the weather zone will not continue downward, because radiative transport (through the 4.5-5.5μ window) probably

---

* On the Earth the entire outward heat flow is 10^{13} cal/sec, the heat brought to the surface by volcanism only 2×10^{10} cal/sec, or 0.2% (Coulomb and Jobert, 1963). The rest occurs by conduction at least through the outer layers. The terrestrial flux thus amounts to 10^2 ergs/cm^2 sec, 1% of the Jupiter flux. Since the Earth-like mass within Jupiter is probably about 10x Earth and since the surface area of the planet is more than 10^2 times larger, the terrestrial processes operating on Jupiter (radio-activity, etc.) can contribute only 10^{-3} of the Jupiter heat flux. Thus, this flux is basically gravitational in origin. Cf. also Bishop and de Marcus (1970).

suffices at the higher temperatures. The lower atmosphere may be nearly stagnant. Solidification of hydrogen may then occur at moderate depths. A stagnant lower atmosphere is favored by the periods of rotation of the surface layers, which appear associated with that of the solid surface, $9^h55^m.5$. If a column near the equator could rise vertically 120 km without friction, its period of rotation would increase 60 sec.

Figures 1*a-e* show two high zones at 22°N and 22°S of variable width and intensity, especially prominent in 1970 and 1971; and the Equatorial Zone, of variable height and width. The 22° zones are identified as the *North and South Tropical Zones* (cf. Fig. 2). The South Tropical Zone contains the *Red Spot* which is even more prominent (i.e., higher) than the Zone itself (the high intensity is *not* an albedo anomaly as was verified by photography at nearby wavelengths). The 22° Zones may heuristically be compared with the (double) Tropical Convergence on the Earth, the only cloud belts that are systematically EW, at 6°-10°N. and S., and also the highest. The Trade Winds move toward the Tropical Convergence, from the northeast and southeast in the two hemispheres. The moisture-laden air rises in the Convergence, forms EW series of thunderstorms there, showing tremendous anvils which break off and form cirrus in the upper troposphere, where the flow returns poleward, in the opposite sense to the incoming Trade Winds at low level. (As one who has observed Mars and Venus from the NASA CV-990 aircraft South of Hawaii, I am only too well familiar with this return flow).

4. The Nature of the Red Spot

a. Comparisons with Earth - Among the most informative presentations of the terrestrial Tropical Convergence Zones are the half-monthly and full-monthly photographic averages of the NASA-ATS records composited by the Department of Meteorology at the University of Wisconsin in Prof. V. Suomi's institute. The results for 1967 have been published by Kornfield and Hasler (1969). The Tropical Convergence Zone is prominent over the vast Pacific and the narrower Atlantic. The asymmetry of land vs. water for the Indian Ocean area appears to destroy the regularity of the pattern there, as do the land masses of America and Australasia. Through the courtesy of Dr. Suomi's group, we are able to reproduce in Figure 7*a-d*, the 120° Pacific arcs (90°W to 150°E) of the four *seasonal averages*, typified by January, March, June, and September 1967. In addition, Figures 8*a - b* reproduce six *half-monthly averages*, in Spring and Fall. The North American west coast is recognized, as is the Gulf of California (114°W, 30°N). Hawaii is seen as a small cloud mass (155°W, 20°N). Remarkably "clear" skies appear to prevail near Canton and Jarvis Islands, 172° and 160°W, near the equator. (Canton Island was briefly explored in 1957 by L. Salanave as part of the AURA site survey, included on the basis of favorable weather reports and the assumption that good day-time seeing is to be expected on sites surrounded by water).

The North Tropical Convergence is well-marked and regular in these averages, centered at about 6°N (with little seasonal variation; this appears due to the great thermal inertia of the ocean). The South Tropical Convergence is weaker and broken, with a latitude separation from the North Tropical Convergence of about 12°. More prominent is a broad cloud belt from New Guinea ESE-ward through the Solomon Islands, the New Hebrides, and the Fiji Islands (the two bright masses), constrained by local topography and ocean currents.

On *individual* satellite records the Tropical Convergence Zone is usually broken up into "cloud clusters". Such records are available in large numbers,

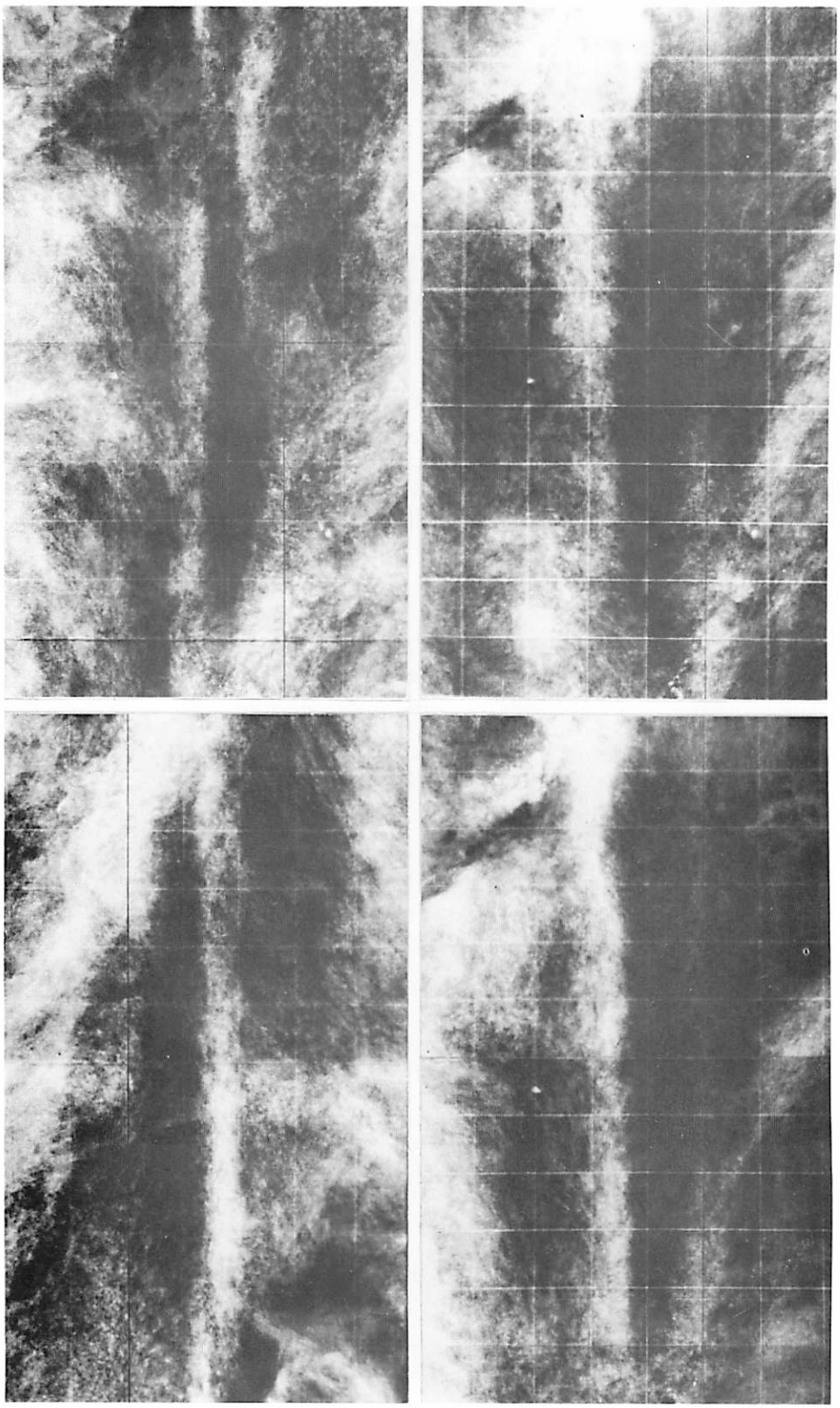

Fig. 7 Monthly averages of cloud cover over tropical Pacific (90°W to 150°E, 30°S to 40°N), Jan, Mar, Jun, Sept 1967 (courtesy Prof. V. Suomi)

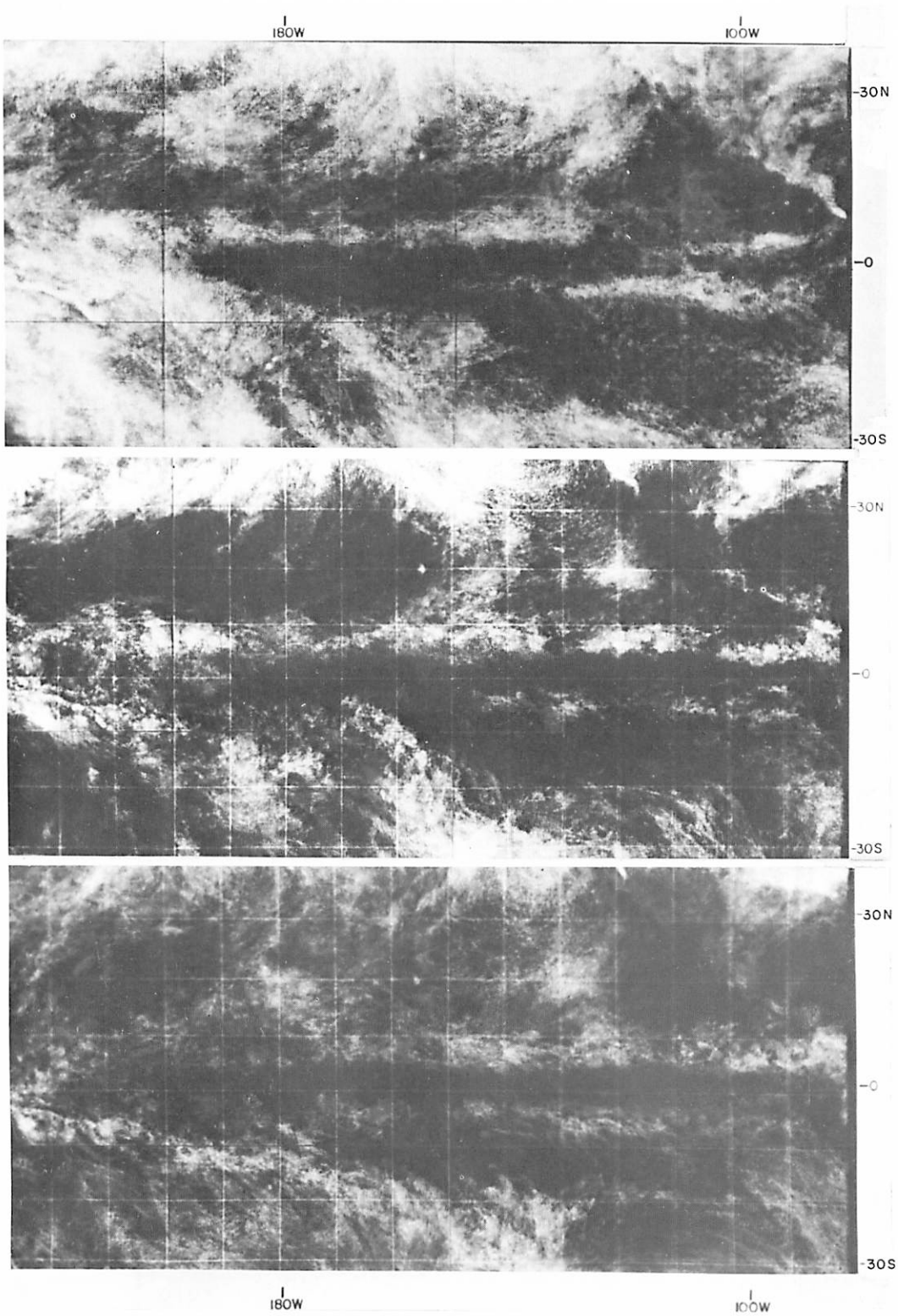

Fig. 8 Half-monthly averages of ATS photographs of tropical Pacific (80°W to 130°E, 30°S to 40°N): *a*. Mar 1 -15; *b*. Apr 16-30; *c*. May 1-15, 1967

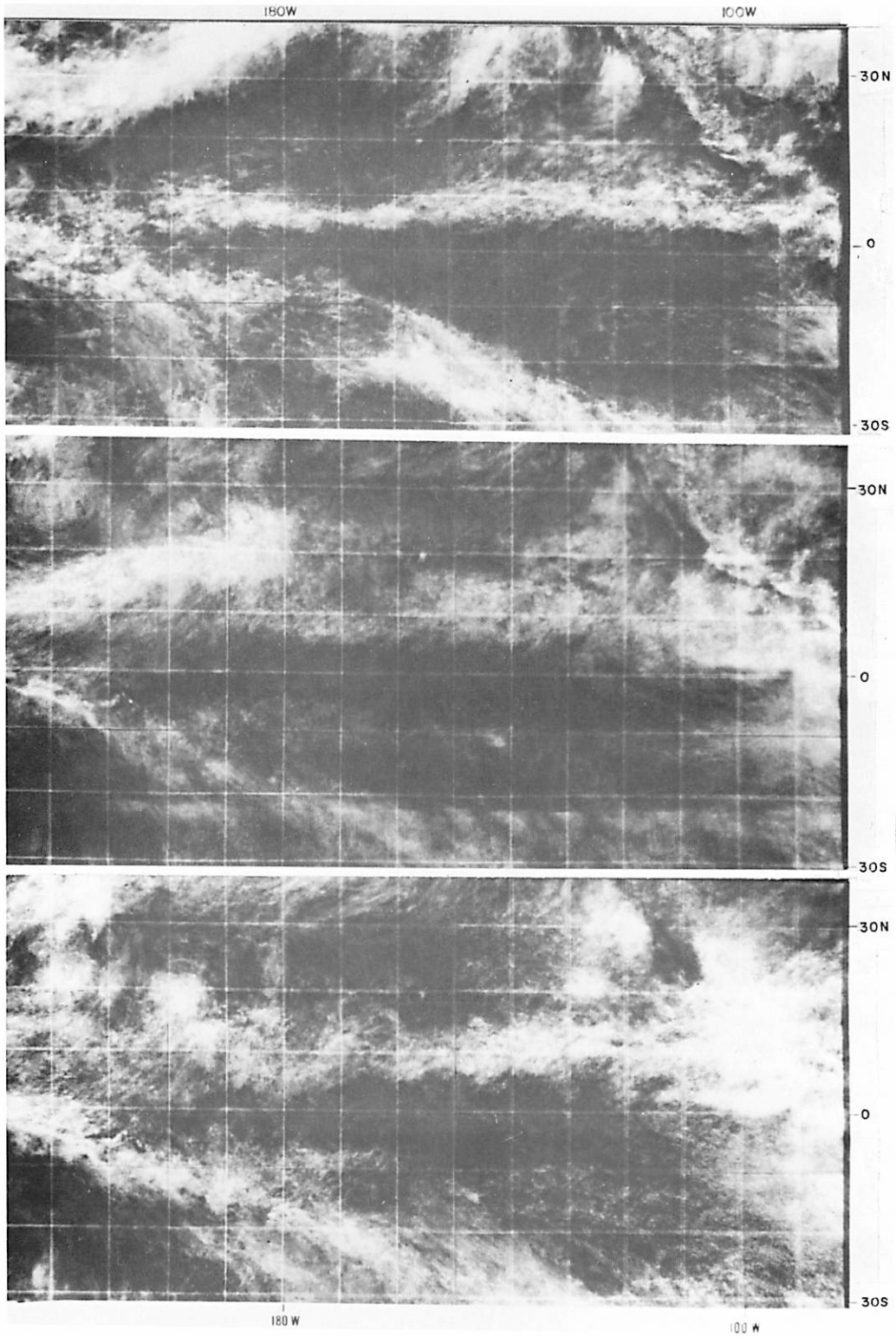

Fig. 8 (cont.) *d*. May 16-31; *e*. Sept 1-15; *f*. Sept 16-30, 1967 (courtesy Prof. V. Suomi)

starting 1967, from the beautiful reproductions in the 5-volume Catalogue of the ATS Meteorological Data. Some are readily available through the article by A. W. Johnson (1969). In Figure 9 we reproduce two representative records, centered on the equatorial Pacific (the Gulf of California is seen at the upper right). These records may be compared with Jupiter photographs. There is a striking contrast especially at the middle and high latitudes where the Earth shows powerful transzonal, often cyclonic, flow patterns.

It is of great interest that the "cloud clusters" in the Tropical Convergence Zones have, on the whole, a systematic Westward motion. Figure 10*a* shows a compilation of ESSA-5 records of the 5°-10°N Pacific zone published by Chang (1970) for 45 consecutive days, July 1-August 14, 1967. The clusters clearly have a tendency to propagate westward (phase velocity 9 m/sec) and often survive as organized masses across the entire Pacific. Chang's composite for the adjacent latitude belt, 10°-15°N, is similar in appearance and yields the same 9 m/sec systematic motion. The cloud centers are marked by heavy precipitation, strong ascent at middle levels, and strong upper-level divergence. The clusters represent concentrations of cyclonic vorticity at low levels and anticyclonic vorticity at 200 mb (Holten *et al.*, 1971). This is due to the strong divergence near the tops of the anvils, causing the upper flow-pattern to resemble that of a barometric high at ground level. Chang's studies were extended to all tropical longitudes and latitudes 20°N-20°S, in 5° strips, by Wallace (1970), for the entire year, Dec. 1966-Nov. 1967. We reproduce in Figure 10*b* one of the many Wallace composites covering the period June 1-Aug. 31, 1967, 0-5°N (thus adjacent to Figure 10*a* but extended for all longitudes). Figure 10*b* shows that some cloud masses may be traced from about 10°E Westward nearly around the globe, to 70° or 80°E or less, with a nearly-constant phase velocity. Wallace (1971, p. 594) published also a time-longitude section of cloud brightness at 10°N based on averages for 5° x 5° squares, for July 1-Oct. 1967, both for unsmoothed and longitudinally-smoothed values. He concludes (p. 595):

> "1. There is a high degree of organization in the brightness pattern at this latitude, the major fluctuations being associated with long-lived synoptic-scale systems that propagate westward.
> "2. Many of these systems retain their identity over a period of weeks, as they pass from one ocean to another.
> "3. The phase speeds of these systems range from 5 to 10° of longitude per day. For a frequency of 0.2 cpd this corresponds to a range of wavelengths between 2500 and 5000 km."

Wallace remained uncertain about the cause of the Westward wave of tropical storms (Wallace, 1971, p. 600, 603 ff).

Holton (1971) states:

> "Several studies indicate beyond reasonable doubt that westward propagating synoptic disturbances do exist in the tropical Pacific and that much of the precipitation in that area is associated with the cloud clusters which are embedded within these waves. At the same time it should be said that the observed average amplitude, period and wavelength of these disturbances vary from year to year, and that the structure of the disturbances also depends on the season and longitude. The range of periods reported in the above spectral studies is ~4-7 days while the reported zonal wavelengths range from 2000-10,000 km.

Fig. 9 The North and South Tropical Convergence zones across the Pacific
a. ATS-1 19 Feb 1969 $21^h21^m44^s$ GMT

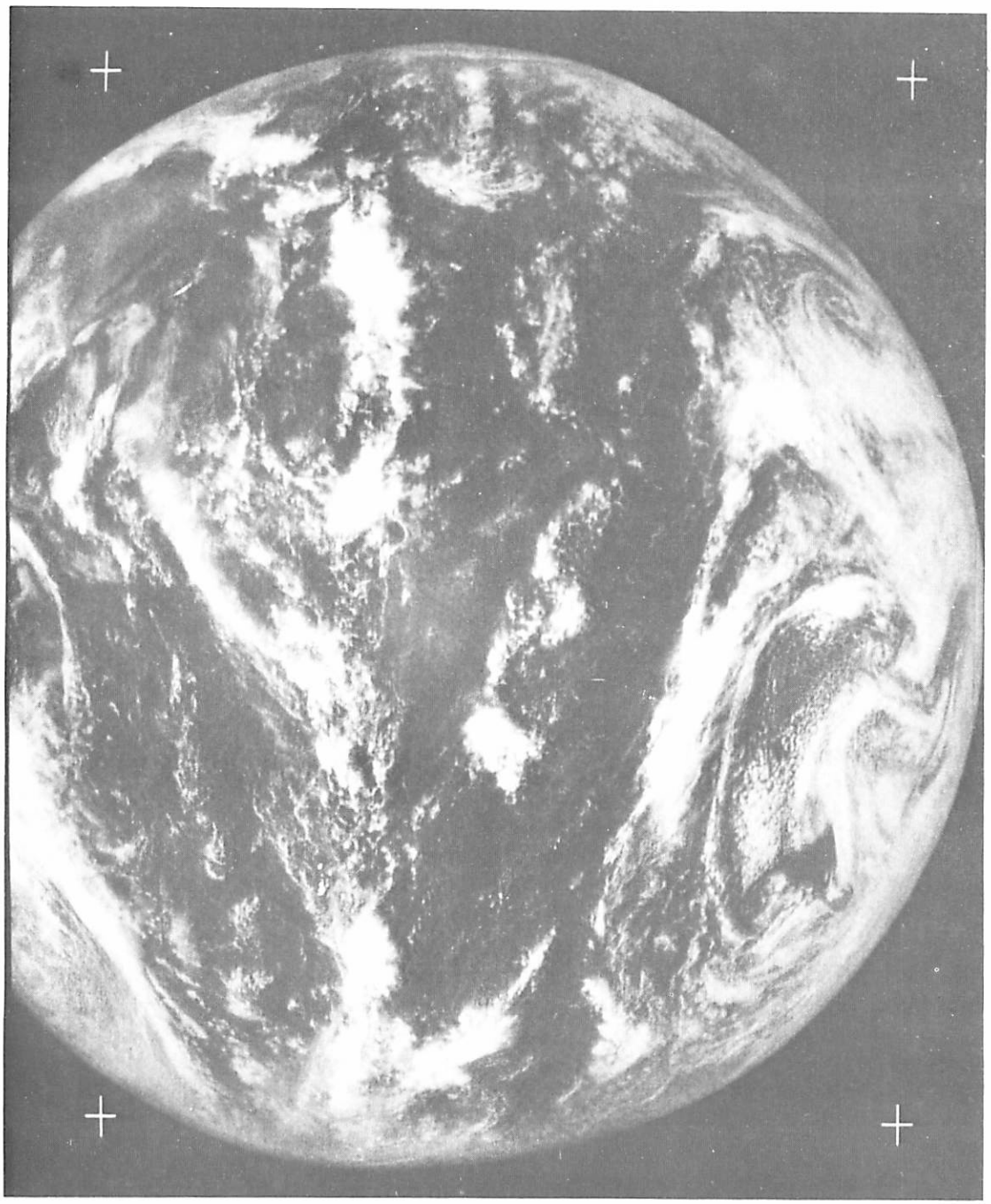

Fig. 9 (cont.) *b*. ATS - 1 18 Mar 1969 $21^{h}45^{m}06^{s}$ GMT

"This wide range in zonal wavelengths is apparently due to the existence of two types of wave modes (Chang *et al.*, 1970). The first type with wavelength range of 6000-10,000 km has its maximum amplitude in the upper troposphere. The axes of waves of this mode generally have substantial tilt with height. Nitta (1970) has suggested that this mode is the mixed Rossby-gravity mode first observed in the stratospheric data by Yanai and Maruyama (1966). This mode has been discussed theoretically by Lindzen and Matsuno (1968). The second type of wave mode with a wavelength range of 2000-5000 km is most prominent in the lower troposphere at the western Pacific stations. Holton (1970) has shown that this latter mode may be theoretically interpreted as a forced equatorial Rossby wave.

"In summary, the observational evidence proves the existence of westward propagating wave disturbances in the equatorial Pacific; however, a number of questions remain concerning their origin, maintenance and structure".

An earlier study by Williams (1970),based on 1257 individual satellite-observed cloud clusters just N. of the equator in the W. Pacific, appears to lead to distinct empirical answers. Williams attributes the Westward drift simply to the Trade Wind; but he does not review the compound wave-like periodicities in longitude. His cloud clusters are mostly located between 4° and 10°N, with some reaching 20°N and a few beyond. Since Williams' observations and deductions have a clear relevance to future studies of the Red Spot and the White Ovals of Jupiter, we quote his statements on the Dynamical Properties of the 1257 observed clusters (note that an Easterly wind or current moves Westward):

"Wind Field at Cloud Center

The typical trade wind cluster is embedded entirely in an easterly current which extends through the depth of the troposphere. The zonal wind is strongest in the lower layers, averaging 10 kts. At 200 mb, the zonal flow is typically easterly but considerably weaker than the low-level flow. This is primarily due to the variability of easterly and westerly winds in the upper troposphere above the lower-level steady trade winds. The meridional wind is observed to be weak, less than 3 kts, at all levels. The horizonal shears of the zonal wind primarily determine the relative vorticity.

"Horizontal Shears and Relative Vorticity

In the low and middle troposphere, the trade flow is revealed to be stronger north of the cloud center than to the south. These clusters exist on the cyclonic shearing side of the trades. Table 1 shows values of 950 mb shear of the zonal wind ($\Delta v/\Delta y$) from 4° north of the cluster to 4° south. For the clusters, this shear averages about 10 kts. The v shear taken east-west ($\Delta v/\Delta x$) is also cyclonic but very much weaker.

"To determine whether clusters are associated with easterly waves, streamline analyses at several low tropospheric levels were made. Upwind from the clusters, the wind direction averages about 110°; downwind, about 85°. There is indeed a weak amplitude wave in the streamline patterns, but there is little contribution by this curvature to the computed values of relative vorticity. Fully 75% of the relative vorticity is contributed by shears in the zonal flow, i.e,, $-\Delta u/\Delta y$. These clusters appear to be associated, therefore, with a weak wave typified not so much by curvature but by cyclonic shear of the trade flow.

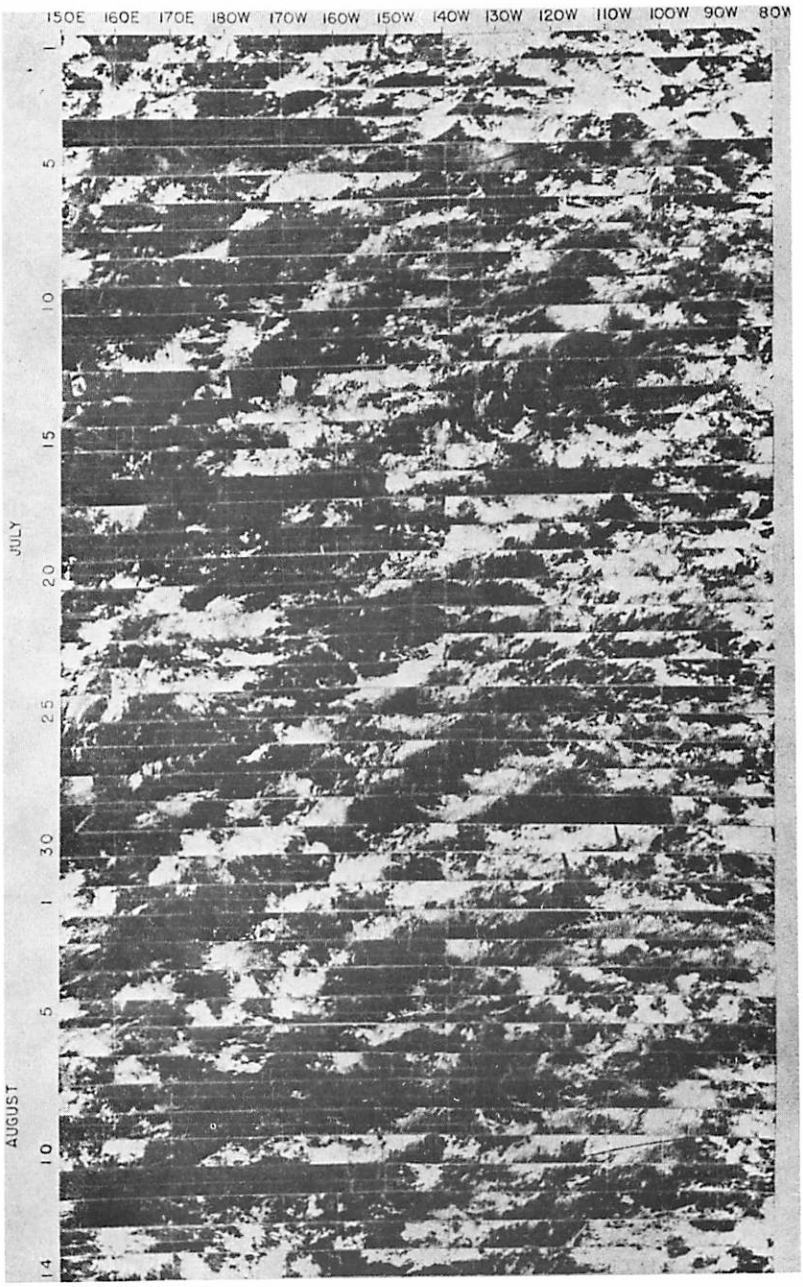

Fig. 10*a* Cloud records for the 5°-10°N Pacific zone for 45 consecutive days, July 1-Aug 14, 1967, based on ESSA-5 data (Chang 1970)

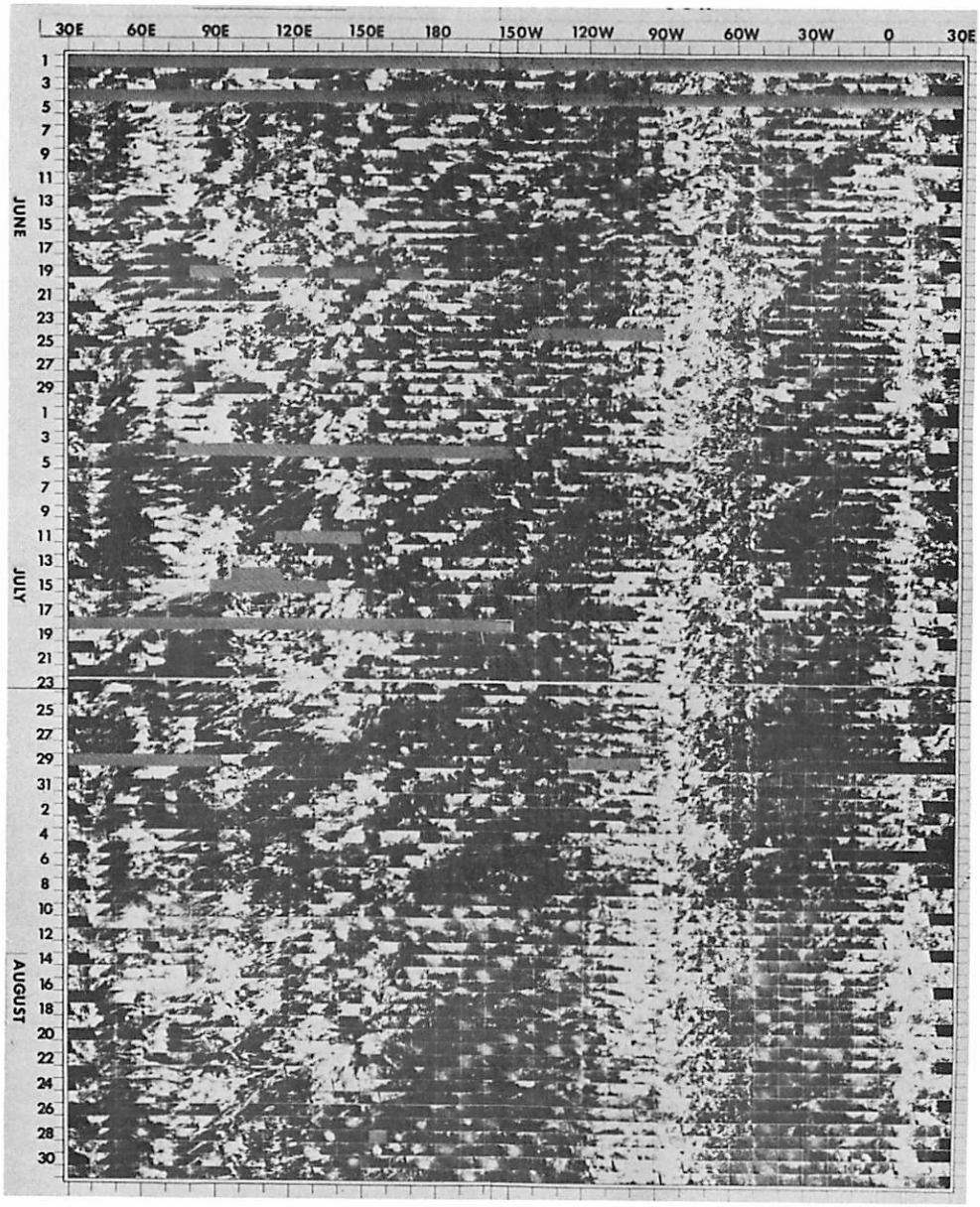

Fig. 10*b* Cloud records for period June 1-Aug 1967, all longitudes, 0-5°N

"The relative vorticity profiles . . . are primarily determined by the horizontal wind shears. For most clusters, the relative vorticity is positive throughout the lower and middle troposphere. The pre-storm clusters possess by far the largest vorticity values; the non-conservative or developing-dying clusters, the smallest.

"It is thought that low-level horizontal shears are critically important to cloud cluster dynamics. Charney and Eliassen have proposed CISK (conditional instability of the second kind) as an instability mechanism by which mesoscale frictionally-forced convergence in the boundary layer in cooperation with the heating potential of cumulus convection combine to initiate development of tropical cyclones. This mechanism is viewed by the author as a plausible means of producing and maintaining tropical cloud clusters, some of which may later develop into tropical storms. Gray has previously shown a strong positive relationship between trade-wind cyclonic wind shear and disturbances which intensify into tropical storms. To maintain the cluster, low-level mass convergence and cumulus convection must be continually active.

"Divergence

Fig. A shows vertical profiles of divergence taken at the center of each cluster type. Convergence is typically maximum at cloud base and gradually decreases with height. A striking maximum of divergence is centered at 200 mb. This agrees very well with previous vertical divergence profiles determined from tropical storms.

"These vertical divergence profiles also show that the mass balance of a cloud cluster is achieved nicely by a two-layer model with inflow below 400 mb and outflow strongly concentrated from 250 to 150 mb (at 250 to 150 mb cumulonimbi updrafts rapidly lose their buoyancy). Because the surface pressure tendencies following a cloud cluster show very little change ($<\pm 2$ mb per day), a rigid balance of the integrated divergence through the troposphere must take place. This requirement is obviously met. It should be noted that the inflow is by no means confined to the lowest layers. Middle-level convergence is probably the result of entrainment into the cumuli, which are developed by boundary-layer frictional convergence.

"These divergence profiles were obtained completely from the computer composites with no 'massaging' of the data. It was indeed surprising that these kinematic-determined divergence and vertical motion profiles should show such a remarkably close mass balance. This lends confidence to the other data computations.

"Moisture Convergence

A computation of moisture convergence for the conservative clusters reveals that although this convergence is a maximum in the lowest 100 mb layer, it is not confined to this layer. More than half the net moisture convergence into the cluster-centered 4°-square box occurs above 900 mb.

"A computation of P-E (where P = precipitation and E = evaporation at the ground) was made from the advective term plus the change in storage over 24 hours. The result is P-E = 2.0 cm/day, with the advective term contributing more than 90%. If E is assumed to be 0.5 cm/day, then the resulting 4°-square area-averaged precipitation from a typical cloud cluster is 2.5 cm/day. Rainfall of this magnitude requires the presence of cumulonimbi, and indeed the bulk of the rainfall in this area comes from cumulonimbi which are maintained by synoptic-scale cyclonic wind shears.

"Vertical Velocity

All cluster categories show maximum vertical motion at 400 to 300 mb. A typical vertical velocity (averaged over an area 4° on a side) at this level is 170 mb/day or 3 cm/sec. The upward motion becomes zero between 200 and 100 mb.

"Table 1. 950 mb horizontal shear in zonal wind (kts) taken over a N-S distance of 8° latitude. A positive value denotes cyclonic shear.

	Pre-Storm	Developing	Conservative	Dying	Dev.-Dying	All Clouds	Clear Areas
$\Delta u/\Delta y$	17.0	10.4	9.4	9.6	3.2	10.4	-6.8

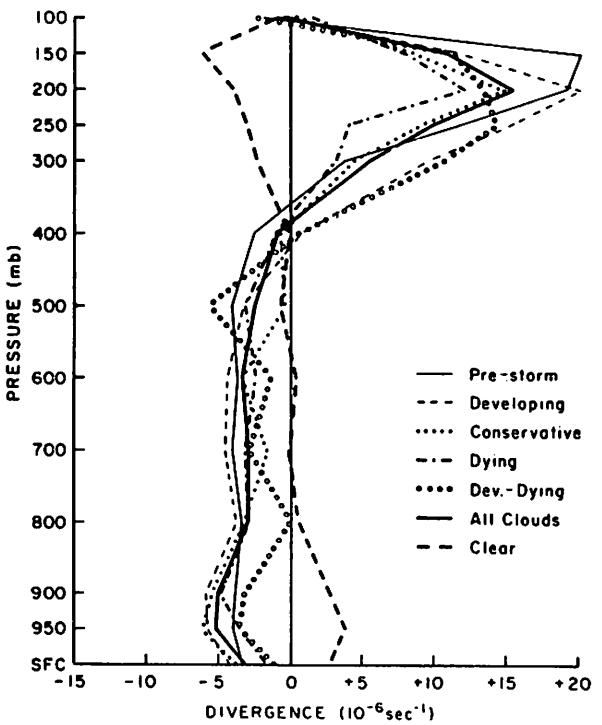

Fig. A. Vertical profiles of 4°-square area-average divergence at cluster centers."

b. Red Spot Motions - The self-rotation of the visible Red Spot of Jupiter is also anticyclonic. This has been particularly well demonstrated by the recent observations of Reese and Smith (1968). *The Red Spot therefore behaves as a giant ascending column, flowing out at the observable level of the top.*

The westward motion within the Earth's North Tropical Convergence is due in part to the Trade Wind Easterlies feeding it but also to a propagation of cumulus column production; individual cumuli usually last only an hour or two. The average rate over the Atlantic is about 10 knots (5 m/sec) or 1% of the rotational velocity (Rosenthal, 1971); compared to the 9 m/sec for the Pacific (Chang, 1970). Chang notes that the Pacific storms (5°-10°N) pass a given longitude every four days or so (12 disturbances in 45 days). The "wavelengths" suggested by Figure 10 are of the order of 3000-6000 km, not unlike figures derived previously by other authors quoted by Chang. On Jupiter the two Tropical Zones rotate with periods that are surprisingly close to that of the solid surface, 1^s faster for the NTropZ, 6^s slower for the STropZ. The Red Spot, whose top is even somewhat higher than the STropZ, is 8^s slower on the average, or 2^s slower than the STropZ The period of the Red Spot has varied from $9^h55^m31^s$ or 32^s in 1831-32, 1872-73, and 1924, to $9^h55^m42^s$-44^sin 1891, 1896-1900, 1907±, 1937-40, 1943-48, etc. On the whole, the period was *short* 1831-1882, *long* 1882-1908, *short* 1908-1937, *long* 1937-1962, shorter thereafter. On the assumption that a longer period would at least in part be due to increased distance from the axis of planetary rotation, a relationship between *period* and *height*, and hence *color*, would be expected. This is indeed the case, as was noted by Peek (*op. cit.* p. 150), who found *maximum visibility* (dark color) associated with abrupt *lengthening* of the period. This important relation could be considered to confirm the concept of the *Red Spot as a rising column of variable activity.*

For a better grasp of the geometry of the Red Spot and the currents in which it is embedded, we show in Figure 11 the planet as seen from different latitudes. These photographs (unretouched) were produced by rephotographing a Jupiter image projected on a white-mat ellipsoid of proper oblateness produced by Mr. R. Turner.

c. Rotation of Jupiter's Belts and Zones - Poleward of each Jupiter Tropical Zone, one expects drops in the periods of rotation, caused by the "peeling off" of cirrus-like material flowing in the opposite sense to the invisible "Trade Winds" below. Movement from 22° to 24°, with conservation of rotational velocity, would shorten the rotational period by 9 min; this is the maximum effect since friction will decrease the amount. Actually, just south of the STropZ on the north edge of the South Temperate Belt, the average period of rotation is 2^m34^s shorter than in the Zone itself, with no major anomalies occurring farther South. The South Temperate Belt at -29° has $P = 9^h55^m20^s$, only a little below the surface value, indicating a slight poleward flow. From -31° to -45°, $P = 9^h55^m7^s$, indicating a slightly larger poleward flow; while South of -45° the period is precisely that of the surface, $9^h55^m30^s$, in accord with the near-absence of zonal structure in the polar region. Figure 12*a* is based on Peek's (1958) compilation. A more recent study, covering the period 1897-1966, is that of Chapman (1969). His composite Figure 3 resembles Figure 12*a* quite well except for S latitudes 15°-20° where a second positive peak occurred in the interval 1917-36. Chapman's composite for the five intervals studied by him (comprising 1, 1, 2, 2, 1 decades) is reproduced in Figure 12*b* for purposes of comparison. Clearly, *there is considerable variation in the Jupiter flow pattern* over the 70 years covered.

In the Northern hemisphere the picture is similar, though not identical. Northward of the North Tropical Zone again a major drop in the period occurs, the south edge of the North Temperate Belt (1°-2°N of the Zone), having an average period

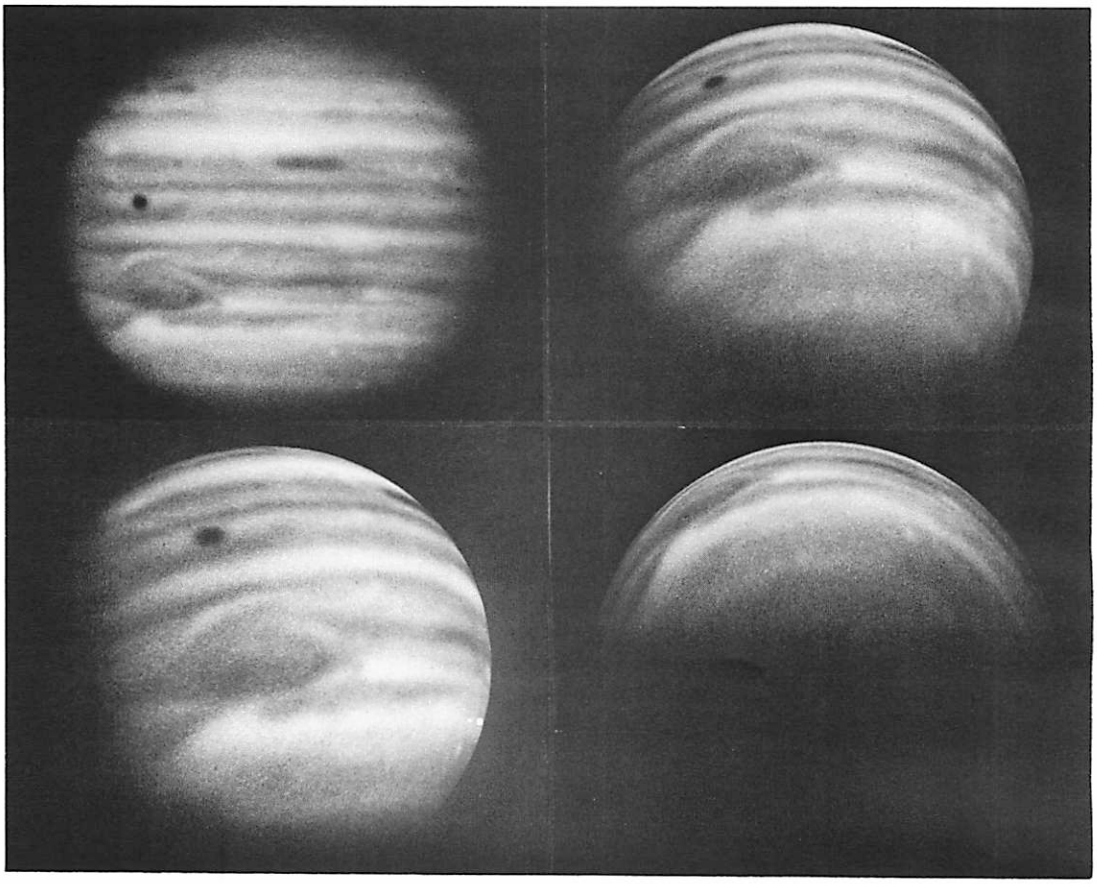

Fig. 11 Planet Jupiter with Red Spot, Zones and Belts, shown from different latitudes

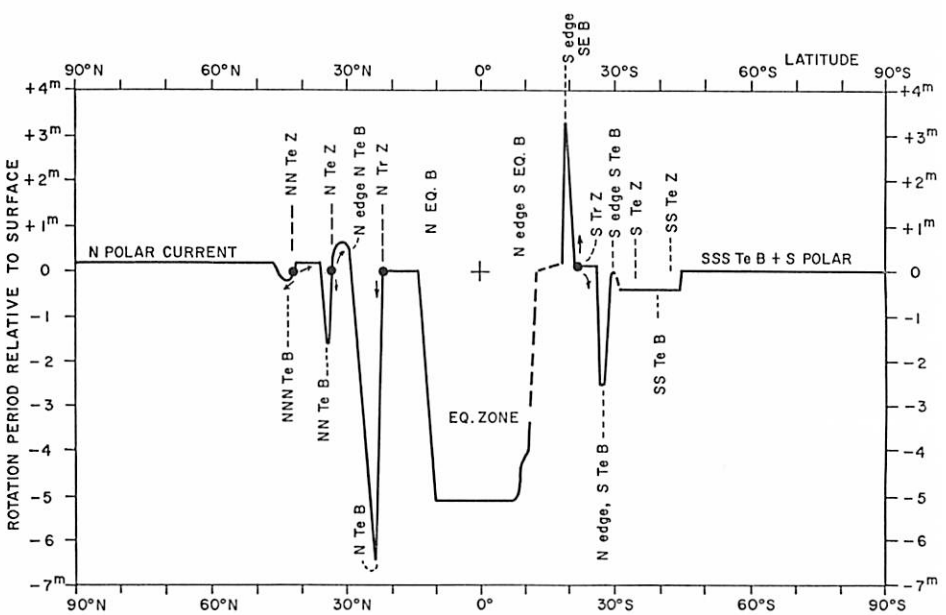

Fig. 12*a* Rotation periods of Jupiter Zones and Belts (after Peek 1958)

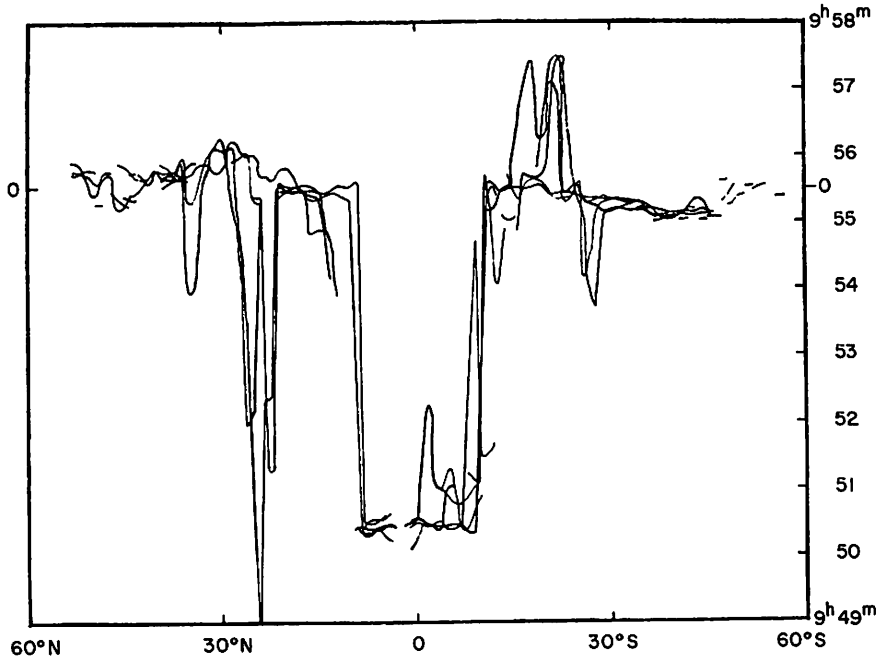

Fig. 12*b* Rotation periods of Jupiter Zones and Belts 1897-1966, during 5 intervals (after Chapman 1969)

6^m22^s (6 apparitions) shorter than the Zone. At +27°, *P* has increased to $9^h53^m17^s$ (N. Temp. Current B); at +29° to +33°, to $9^h56^m5^s$ (N. Temp. Current A, etc.). At +35°, $P = 9^h53^m55^s$; at +36°-40°, $9^h55^m42^s$; at +43°, $9^h55^m20^s$; and at 47°-90°, $9^h55^m42^s$. This pattern calls for a secondary "convergence" around 34°N (between a high *P* value equatorward, a low *P* poleward). At least the 1970 records show such a minor bright zone to exist (just above Io on Fig. 1*c*); it is the North Temperate Zone. Poleward of 35°N no major transzonal currents appear to occur. A minor Zone, the NN Temperature Zone, causes an expected ripple in the rotation periods nearby. The fine structure on Figure 12 is somewhat variable, as shown by Peek and Chapman.

The above description of the flow pattern accounts in a general way for the rotational periods of the planet, with the exception of the Equatorial Zone. The low period of this Zone, $9^h50^m24^s$, includes as well the two adjacent strips of the neighboring Belts: the North Equatorial Belt ($9^h50^m24^s$) and the South Equatorial Belt, North division ($9^h50^m26^s$). The total width of this rapid Zone is about 20°. The higher atmosphere of the Earth presents an analogous phenomenon, though only about half the time, when a 10 meter/sec Eastward current is found in the lower stratosphere, around 50 millibars (20-km altitude). This means a period of rotation 2% faster (12 min if it were Jupiter). Owen (then of LPL) and Staley (1963) first called attention to this parallel; though admittedly the magnitudes of the currents are very different. The significance of divergence above bright zones as affecting the periods of rotation of adjacent strips was first discussed by Hess and Panofsky (1951) based on studies at the Lowell Observatory. As to the Red Spot, they considered it improbable that the variable period was due to variations in solar radiation, though remarkably a correlation coefficient of 0.61 was derived with the terrestrial zonal index.

d. The Red Spot as a Region of Organized Cumulus Convection - Methane photographs show the Red Spot to be the *highest cloud structure on the planet.* This is the *opposite* of what a large suspended ice mass (see Appendix I) would produce; it would impede the heat flow from below and cause the overlying cloud cap to be lower than normal. On the contrary, the Red Spot must contain an *energy source*, responsible for its exceptional height, its rising column, and its outward flow on top (see above). Now, the thunderstorms along the Earth's Tropical Convergence have these properties. The source is the latent heat of the condensed water; they build up to the *full height* of the Tropical troposphere, 16-18 km, and produce enormous outflowing anvils near the tropopause so that, when seen from above, they are about 100 times larger in area than the active column nearer to sea level (cf. Fig. 13). If the height of the terrestrial tropopause were not 2 scale heights, but 5-8, as for Jupiter, the vertical magnification could be much greater.

Our tropical storms are among the long-lasting "severe storms" studied intensively since World War II (*Meteor. Monogr.*, Vol. *5*, No. 27, 1963). They are also called "steady-state storms". The steady-state "giant thunderstorm is a more highly organized phenomenon than its smaller air mass counterpart" (*op.cit.* p. 33). *On Jupiter the steady-state storm is much more probable than on the Earth*: (i) The thunderstorms over the Pacific lose the water they condense to the ocean beneath; only a slow evaporation or transport of new moist air can keep the column active. On Jupiter the water will fall into the hot lower atmosphere and promptly evaporate. The "engine" can therefore go on indefinitely subject only to the limitation of the heat flux; because, if the resulting upward flow of latent heat exceeds that, the column will collapse. (ii) The absence of the day-night *variable* heat supply to the lower atmosphere (which tends to limit the life time of terrestrial thunderstorms). (iii) The stability of thunderstorms *increases with increasing diameter* (Newton, 1963, p. 48).

On a scale larger than the individual cumulus cloud, the Convergence contains "cloud clusters" (Figs. 9, 10). This empirical designation may be replaced by the theoretical concept of *Regions of Organized Cumulus Convection*, signifying the existence of a true physical association, not accidental proximity. This concept, also called *collective, frictionally-controlled dynamics* (Ooyama, 1969, p. 4), was theoretically developed during the last decade (Charney and Eliassen, 1964; Ooyama, 1969) and appears to offer a theoretical framework for an initial interpretation also of the Red Spot and the White Ovals of Jupiter.

"Organized cumulus convection" involves a multitude of cumulus columns some growing to full height and maturity, but each limited in duration (a few hours), with new columns developing and old ones collapsing; all held together by a common circulation system, often for several days. These are the *Tropical Cyclones*, called *Tropical Hurricanes* after winds in excess of 75 mph develop. A typical cyclone system will have a radius of 110-160 km for the array of active columns, while the common cirrus cloud cover has a typical radius of 800 km (Dr. S. L. Rosenthal) or some 6x that of the active array.

Ooyama's (1969) model study of tropical cyclones leads to the prediction of *an upper limit* of the *Region of Organized Convection (op. cit.*, eq. 4.6):

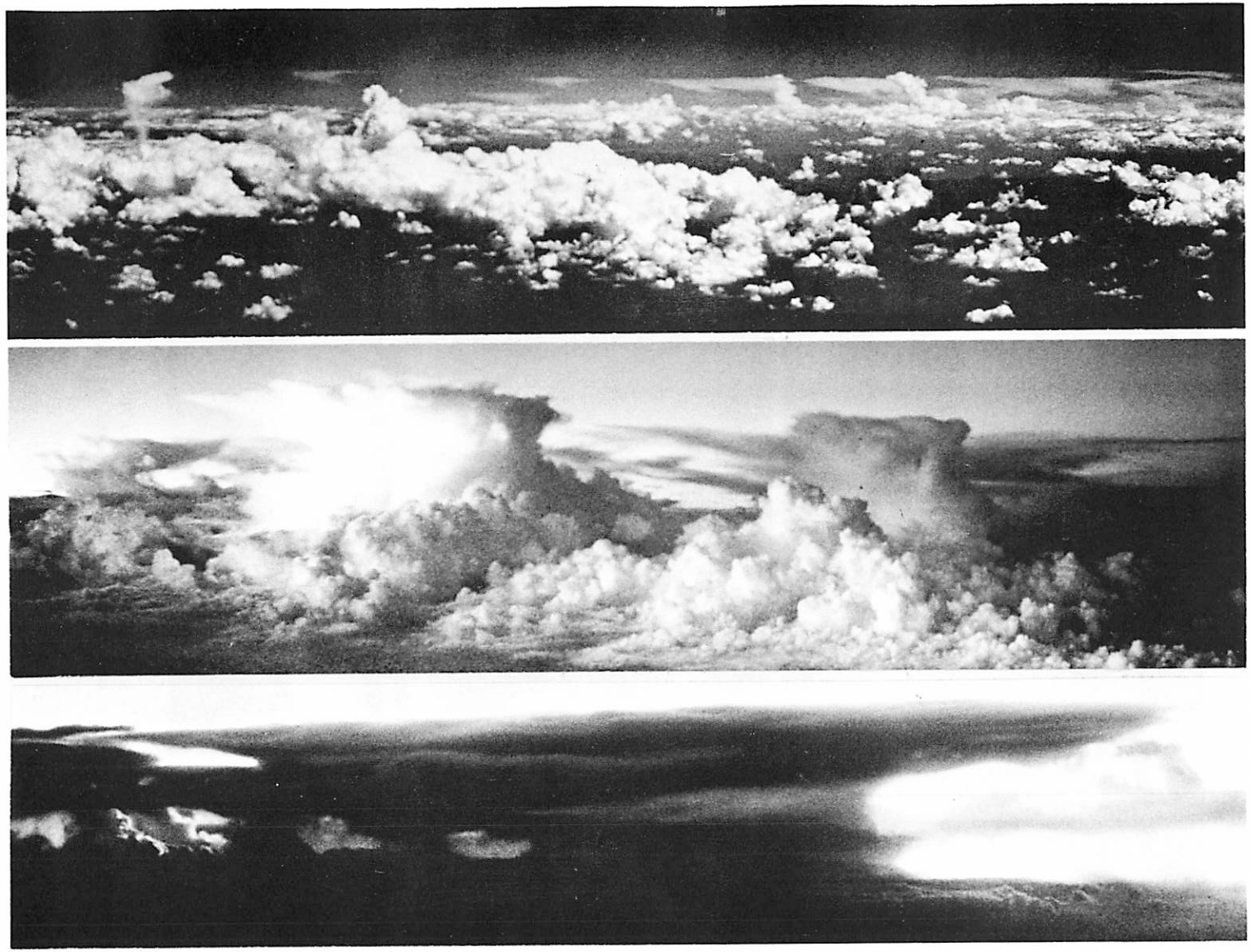

Fig. 13 Cumulus anvils: *a.* (Aug 2, 1968) from 100 miles N of San Francisco, looking toward Sierra Nevada (line of storms with anvils blown to N); *b.* anvils over Mt. Whitney area look- N (Aug 6, 1970); *c.* (Aug 15, 1970) over Atlantic

Fig. 13 (cont'd) *d*. and *e*. (Aug 11, 1968) over Mt. Whitney area, looking N, views beneath large anvil

$$R = (\sigma g h/2)^{\frac{1}{2}} f^{-1}, \qquad \ldots\ldots \qquad (1)$$

in which $\sigma = 1 - \rho_2/\rho_1$, $\rho_{1,2}$ the densities of the two atmospheric model layers; g the acceleration of gravity; h the mean thickness of the two layers; and f the Coriolis parameter ($2\Omega \sin \phi$; Ω is the angular velocity of rotation, ϕ the latitude). We may take $\phi = 22°$ for both Earth and Jupiter; then, with $g_J = 2.6 g_E$, $f_J = 2.4 f_E$; $\sigma_E \sim 1/2$, $\sigma_J \sim 0.9$, $h_J \sim 3 h_E$, $R_J \sim 1.6\ R_E$. Ooyama derives R_E to be about 1000 km; R_J would then be roughly 1600 km, or the diameter of the active column array 3200 km. If the diameter of the cirrus cover were indeed 6x that of active array (see above), it would be about 20,000 km, which is about that of the Red Spot. The White Ovals occur at 33.°5 latitude and should therefore have an upper limit 0.68 of that of the Red Spot at 22°; the actual size ratio is somewhat less (the average Oval dimensions for 1970-71 were 13,400 by 8000 km - Reese). The theoretical framework needs refinement (more layers, etc.) but the Ooyama theory and the observed cirrus cap ratio of about 6, together, appear to account for the observed upper dimensions of the organized Jupiter cloud masses. High-latitude round or oval clouds should be no larger than about half the diameter of the White Ovals, which seems confirmed. Dr. S. L. Rosenthal points out that only order-of-magnitude representations could be expected from the present-day terrestrial models. The absence of long-lived oval clouds *close to the equator* indicates that Coriolis force is an active ingredient of the cloud dynamics elsewhere on the planet. Eq. (1) shows that there is no upper limit ($R = \infty$) to a storm system at the equator. Ooyama's theory also predicts the arresting effects due to friction on the growth of *small* disturbances, somewhat similar to the arresting effects on individual towers noted by Newton (1963).

Terrestrial cyclones or hurricanes usually move about; however, the cyclone motion is essentially that of *the air flow in which it is embedded.* Much meteorological discussion has centered on defining the "steering layer" responsible for the motion of the cyclone; typhoons may be entirely stationary for days, usually near latitudes 25°-30° (Riehl, 1951, p. 912). For Jupiter the zonal motion at the $T \tilde{=} 300°K$ level compared to the subsurface is expected to be small, so that the Red Spot columns would be nearly at rest. Also these columns, or "hot towers", will have *roots* unknown on Earth since the 300°K level is gaseous, not an ocean surface. These roots will further limit the migration of the Red Spot columns.

The terrestrial tropical hurricanes originate above the oceans at temperatures within 1°-2° of 27°C, or 300°K (Bergeron, 1954). The sensitivity of the hurricane life cycle to ocean temperature is explained by Ooyama's model studies (*op. cit.*, Sec. 13). Coincidentally, the $T \tilde{=} 300°K$ level can locally just be observed on Jupiter (Sec. 2*a*). Terrestrial tropical hurricanes produce up to 10^{22} ergs/sec (Dunn and Miller, 1960, p. 123; Dr. S. L. Rosenthal). With the heat flux of 10^4 ergs/cm^2 sec derived below, the heat transport through the Red Spot will be 10^{22}-10^{23} ergs/sec depending on whether the effective diameter of the heat supply area is about 10,000 or 35,000 km. (Cf. Sec. 4*h*).

It is expected that the Red Spot, a region of organized cumulus convection, will have associated with it *gravity waves* and *acoustic-gravity waves* that could possibly lead to observable phenomena. Dr. R. Krauss has informed me that for

the Earth gravity waves are seen emanating (as cloud waves) from storm centers, shown well on time-lapse photography based on ATS frames. If a single layer with depth h, caused, e.g., by a temperature inversion, ΔT, were responsible, the wave velocity would be given by $c^2 = (\Delta T/T)\, gh$; and c might be $\geq$ 10 m/sec. However, a much more complex model may be required (cf. Dickinson, 1969).

e. Confirmation of Red Spot Model - The model of the Red Spot, with a highly-active area some 3000 km in diameter beneath a thick cirrus cover some 6 times that size, makes understandable the remarkable properties of the several encounters of the South Tropical Disturbance with the Red Spot observed from 1902-1939 (Peek, 1958, Ch. 15). Peek describes the first of these as follows: "in June 1902 . . . its preceding end reached the following end of the Red Spot Hollow. . . . During the period of *at least six weeks*, which should have been required for the preceding end of the Disturbance to pass from one end of the Hollow to the other, and indeed during the whole of the conjunction *there was no sign whatever of any encroachment upon the region*; instead, within *a few days* of its arrival at the following end of the Hollow, a facsimile of the p. end of the Disturbance was seen by Molesworth to be forming at the other end of the Hollow, with the result that the Hollow itself, having become completely surrounded by the dusky shading, assumed the now familiar form of a light ellipse on a grey background, within which the Red Spot could be distinctly discerned . . . though it was very much fainter than the dusky region of the Disturbance. The new development at the p. end of the Hollow *proved to be a true p. end of the Disturbance* and it drew away from the Red Spot at approximately the same rate as that which it had shown when approaching it prior to conjunction. *Its rapid leap across the confines of the Red Spot* resulted in the addition of nearly the whole of the length of the Hollow to that of the Disturbance, which then totalled about 90°. The duration of this first conjuction was a little more than three months, the end occurring in 1902 September". Of the second encounter Peek (p. 139) writes: "We are led to the conclusion that its transference across the Hollow was practically instantaneous and similar to that which was observed in the case of the p.end in 1902". Of the third (p. 139): "Thus its passage through the longitudes occupied by the Red Spot region, which would have taken nearly *three months*, at its normal rate of progress, must have been accomplished in a matter of *fourteen days*". Of the ninth (p. 142): "At the beginning of the ninth the p. end of the Disturbance was seen to be appearing at the p.end of the Hollow within a few days of its arrival at the f. end!" - Apparently what is involved here, in the *arrest* before passage, the *leap* through the Red Spot, and the *slow departure* on the other side, are the visible ends of stream lines that would move much more uniformly some 50 km down, projected as shown in Figure 14. (During the nine close passages the Disturbance gradually slowed down and the Red Spot speeded up till the periods of rotation around the planet's axis became essentially equal, whereupon the Disturbance disintegrated). Peek's description may be interpreted as showing *EW asymmetry in the Red Spot*, with its array of towers left of center in Figure 14. (Asymmetric anvils are very common in terrestrial storms; cf. Fig. 13*a*).

As noted above, the proposed model accounts in a general way also for the correlation between Red Spot's variable daily rotation period and its "visibility"; and for the observed anticyclonic surface rotation. The *numerical* aspects merit further study. A local barometric high will cause anticyclonic wind velocities, computed by balancing the outward pressure gradient with the inward Coriolis force (geostrophic approximation); or, one can add as a refinement the centrifugal force (the latter is often very important in cyclonic motion). In the Red

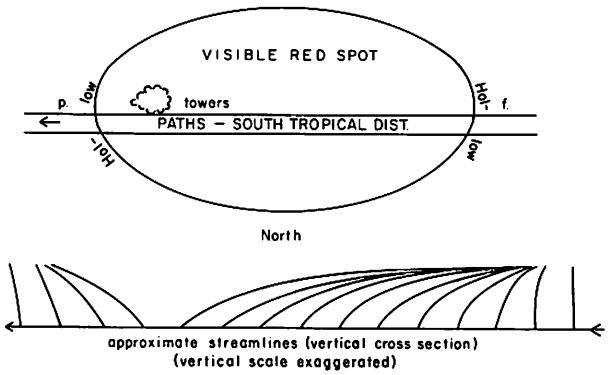

Fig. 14 Map of Red Spot with passing South Tropical Disturbance; and vertical cross section showing typical stream lines at uniform intervals along path of Disturbance

Spot model, however, the rate of ascent in the "hot towers" will set the rate of outflow at the cirrus level. Thus, the horizontal pressure gradient is the result and not the cause of the wind flow. The rate of outflow will also determine the frictional losses in the vorticity of the rising columns. If all vorticity were lost, only the planetary rotational velocity (Coriolis effect) would remain in the outflowing cirrus cover. This would spiral outward with a rotational period $\sim P_J/\sin\phi$. Friction with the lower layers will lengthen this period. The Red Spot model therefore will require an empirically-determined run of its rotational motion with radius to establish both the remaining cyclonic vorticity at the center and the frictional effects throughout. Ideally, this should be done spectrographically along a meridian, with the Red Spot near the planet's limb - a very difficult observation because of the sub-km velocities involved.

To make some estimate of these quantities, we assume that at R = 6000 km the surface rotation period is 5 days. Then v = 87 m/sec; the Coriolis force $F = fv = 2v\Omega \sin\phi$ = 1.15 dynes; the centrifugal force v^2/R = 0.11 dynes, or 10% of the Coriolis force - rather typical of anticyclonic rotation. The radial pressure gradient in the Spot must therefore balance $0.9F$:

$$\frac{dp}{dr} = -0.9\,F\rho; \quad \text{or} \quad \frac{1}{p}\frac{dp}{dr} = -0.9\,\frac{Fm}{RT} \simeq \frac{m}{RT} = 10^{-9.6}, \ldots \quad (2)$$

where the mean molecular weight is assumed to be 2.3, and T = 120°K. This means that the fractional outward pressure drop would be only $10^{-9.6}$ per radial cm, or 1/5 or so for the entire inner half of the Spot. Because of the centrifugal force, the velocity vector would deviate from the circular motion by 0.1 radian, so that the outward velocity would be around 10 m/sec and the outward flow time for the inner half around 8-10 days. For a *shorter period of rotation* v and F will increase proportionally but v^2/R quadratically, so that the outward spiral of motion is more open, and the pressure gradient larger (friction with the lower layers has been neglected in these order-of-magnitude computations; its effect may be small for a model such as shown in Fig. 14).

The available data deal with small spots, blue or dark, seen to enter the Red Spot from the borders of the STropZ, being swept through the Spot, then lost or released. Figure 15 shows a bluish spot observed Jan 25, 1968, recorded dark on red photographs. It will be described by Mr. S. M. Larson together with other structural details observed in the Red Spot. The history of a series of five spots which appeared Dec 1965-Feb 1967 was described by Reese and Smith (1968). Spot *A* overtook the Red Spot, swung with it 1-1/2 periods of 9 days each. Spots *B* and *C* were overtaken by the Red Spot; only a part of each participated in the Red Spot motion for 1/2 period (P = 12 d). Spots *D* and *E* were also overtaken, observed for 5 periods, of 12 days each. All motions were anticyclonic with respect to the Red Spot center. Reese and Smith computed the anticyclonic velocities to be 6100 km/day or 70 m/sec at the Red Spot rims North and South. This means a total relative Doppler shift between the rims of 0.3 km/sec when the Spot is on the limb for solar lines, and half that for the NH_3 and CH_4 lines. Conceivably, the Red Spot itself might move faster (if the spots had roots extending below the Red Spot cirrus cover).

The interaction between the Red Spot and the South Tropical Disturbance, referred to above, was accompanied by period changes of the Red Spot itself, in the sense that the periods of the two storm areas became more nearly equal. This *confirms the concept of both phenomena being atmospheric (meteorological) in nature.* (A mountain or plateau would not be moved by a passing storm!). According to the record compiled by Peek (1958, Chapt. 15), the following stages can

Fig. 15 Photograph of dark spot within confines of Red Spot, 25 Jan 1968, $10^h01^m.3$ UT

be distinguished. The first four encounters occurred from 1901-1909. The Red Spot was moving westward, the STropD moving eastward on the planet, with similar speeds. The two storm areas just met and passed, each keeping its EW motion essentially intact. During the next decade, comprising the 5th, 6th, and 7th encounters, the Red Spot reduced its westward motion, the STropD reduced its eastward motion which by the end of the decade had dropped to zero. During the final two decades, 1920-39, encounters 8 and 9 occurred. The STropD was now moving slowly westward, with its motion reaching equality with the westward motion of the Red Spot toward the end of the period, while the Red Spot itself still moved westward at the reduced speed of the 1910-1920 period. After the 1939 encounter the two storm areas apparently merged, whereupon the Red Spot increased its westward motion on the planet. This timing suggests that *the larger fluctuations in the westward motion of the Red Spot*, referred to in Sec. 4*b*, are also due to *meteorological effects*. These could be interactions with smaller storm centers in the STropZ; or small shifts in latitude. The STropD itself could have entered the Zone from slightly *lower latitudes*, explaining its initial eastward motion and its eventual collision and merging with the Red Spot tower area. Yet another meteorological effect on the Red Spot period would be the *intensity* of the rising towers, as discussed in Sec. 4*b*.

f. EW Asymmetry - The average daily period of rotation (around the planet's axis) of the Red Spot is 8 sec longer than that of the denser layers beneath. This could be viewed as due, at least in part, to the rapid rise of the columns (cf. Sec. 4*b*); but, as in the terrestrial analogue, a true propagation of the Red Spot along the STropZ must be involved as well. The columns will be topped with a very extensive cirrus shield (the visible Red Spot). Since the shield has a finite life time of possibly 40-60 days, as judged by the spots (cf. Sec 4*e*), due to outflow at the center and subsidence or disintegration at the rim, the shield is being continually renewed by the array of columns, and must therefore *appear to move with the array*, though the *center of the Red Spot will be displaced* from the center of the column array, as drawn schematically in Figure 14. A displacement between the two centers is also suggested by Peek's account of the timing of the jump of the STropD across the Red Spot (cf. Sec. 4*e*). Hopefully, other opportunities will occur to observe this type of passage.

If it be assumed that the true daily rotation of the shield material itself is 8 sec longer than that of the center of the Red Spot tower array, the displacement may be computed. If T be the time taken by the Red Spot material to reach the Spot's rim (and then be lost to view or be swept away horizontally), and the 8 sec excess be designated by ΔP, the displacement D will be:

$$D = \frac{\Delta P}{P} \cdot \frac{T}{P} \cdot 2\,\pi R_J \cdot \cos\,\phi \qquad \ldots\ldots \qquad (3)$$

in which the factor following $\Delta P/P$ gives the total path travelled by the rotating sub-surface during T. If $T \simeq 50$ days, $\Delta P \simeq 8$ sec, then $D \simeq 10{,}000$ km, the value used in Figure 14. Clearly, these are merely plausible numbers.

g. Propagation of Red Spot along Zone; Cycloidal Motions - If the Red Spot period is indeed longer than that of the sub-surface in which the column array is rooted (by 8 sec on the average, but by 1^s-14^s through the past century), then the *array itself propagates along the STropZ*. The rate would be on the average of

2.5 meters/sec or 5 knots or 5 years for a complete 360° sweep. Such a motion would be analogous to the movement of the organized cumulus convection centers in the terrestrial Tropical Convergence (Figure 10). This motion along the STropZ,does, however, not trigger the adjacent South Equatorial Belt disturbances occurring every 5-10 years or so; because the longitudes of 10 major and 14 minor disturbances are *not* correlated with the position of the Red Spot (Chapman and Reese, 1968).

The parallel with the terrestrial Tropical Cyclones may be further developed by a comparative study of the *90-day oscillation of the Red Spot*, discovered by Solberg (1968*a*, 1968*b*); and the cycloidal and looping motions of the terrestrial centers. According to Dr. S. L. Rosenthal, the *cycloidal motions* have periods around 12^h-24^h and are probably due to the internal structure of the vortex and its interaction with the prevailing wind of the air mass in which the center is embedded. The *looping motions* have periods of 1/2 day to several days; this effect occurs in *stagnant air masses* and is due to the *vortex being asymmetrical*, providing thereby a steering effect through interactions with the ambient air mass. The 90-day oscillation on Jupiter has been traced back to 1963, and probably to 1946 by Solberg (1969); and carried forward to 1968 by Solberg (1969) and to the present by Reese (1970, 1971*a*). Solberg (1969) found its semi-amplitude to average 0°.8. Figure 16 summarizes the New Mexico data on this important oscillation. (Figs 16*b* and *c*, together with more recent material have been incorporated in a further

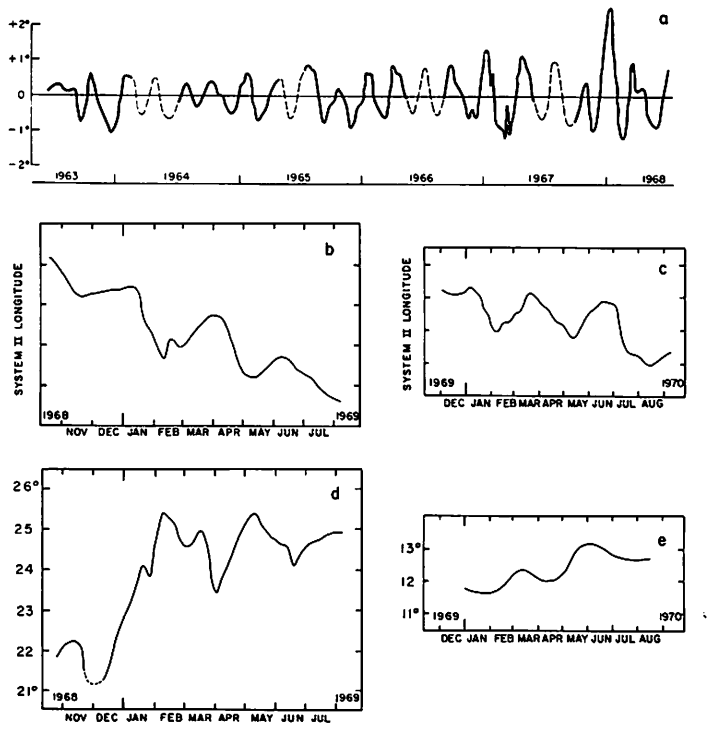

Fig. 16 The 90-day oscillation of Red Spot, based on New Mexico measures: (a) oscillation in longitude after removal of secular drift (Solberg, 1969); (b) same for 1968-1969 apparition, expressed in System II (Reese, 1970); (c) as (b), for 1969-1970 (Reese, 1971*a*); (d) length of Red Spot for 1968-1969 (Reese, 1970); and (e) width of Red Spot, 1969-1970 (Reese, 1971*a*). Vertical markers 1° apart

publication by Reese (1972), drawn on a scale similar to Fig. 16*a*). In addition, Solberg (1968*b*) suspected an 8-year oscillation of 10° amplitude since 1937, but after two cycles of 5-6 years no distinct period of this length has been found (Solberg, personal communication).

A 5-6 year period could be that of the complete sweep of the Red Spot along the STropZ. *The 90-day period is attributed to a rolling action of the asymmetrical vortex and a resultant displacement of the center.* The two periods involved, the hypothetical dimensions of the vortex area (Fig. 14), and the 1° amplitude, are consistent with this model. The trochoidal-type motion of terrestrial vortices was discussed by Yeh (1950, p. 110). Such a motion would probably be more enduring on Jupiter than on the Earth because of the near-absence on Jupiter of major transzonal disturbances; and the absence of oceans, continents, mountains, islands, and other local disturbances in the path. For the same reasons the Red Spot cirrus anvil may be a much more *regular structure* than the cirrus masses above terrestrial cyclones (some rather symmetrical cirrus caps are occasionally seen on photographs from terrestrial satellites). The 90-day oscillation would also be reflected in some measure in the *latitude* of the Red Spot and possibly its *dimensions*. The New Mexico measures indicate that such is the case, though not with complete regularity (Solberg, 1968*a*, Figs. 4-6; 1968*b*, Figs. 4, 6 and 7; Reese, 1970, Fig. 4; 1971*a*, Figs. 3, 4, and 5); and Figure 16.

The cycloidal paths of three terrestrial cyclones are shown in Figure 17. A summary of the first formation or detection of tropical cyclones for the period 1901-1963 and their paths is contained in the publication "Tropical Cyclones of the North Atlantic Ocean", Technical Report No. 55, U. S. Weather Bureau. While these data are of extraordinary interest in the context of this paper, the paths themselves have "been highly smoothed, being best-fit tracks, and hence the cycloidal motions are not discernible" (Rosenthal, personal communication). Case studies of eight cloud clusters of the Tropical Atlantic are presented by Martin and Suomi (1971). Evidently, these case histories are complicated by external factors such as atmospheric shearing or formation over Africa, South America, or the Island chains, with presumably no equivalents on Jupiter.

Comparison between Figures 16 and 17 may be confusing since the time scales in the abscissae in Figure 16 are arbitrary. In Figure 18 a plot of the longitudes is shown with respect to the solid surface (System III) of the same data of Figure 16*c*. The amplitude of the 90-day oscillation is now seen to be small in terms of the displacement of the Red Spot along the STropZ; in fact Figure 18 is not unlike Figure 17*a*.

On Jupiter not only the Red Spot shows *cyclic motions in longitude*.* Peek (1958, Ch. 19) deals with "The oscillating spots of 1940-41 and 1942". The periods are $P = 72^d$ and variable; the semi-amplitudes A both 5°; 24 and 31 observations. Solberg (1969) lists three other such spots, one of 1964-65, $P = 300^d$, $A = 4°$, 51 obs.; one of 1965-66, $P = 67^d$, $A = 1°$, 10 obs.; and 1967-68, $P = 66^d$, $A = 3.°4$, 20 obs. Further details of the last spot are given by Reese and Solberg (1969). Two additional such spots were observed since then (Solberg):

* Often spot positions are measured in longitude only since this is done more easily and since it defines the period of rotation.

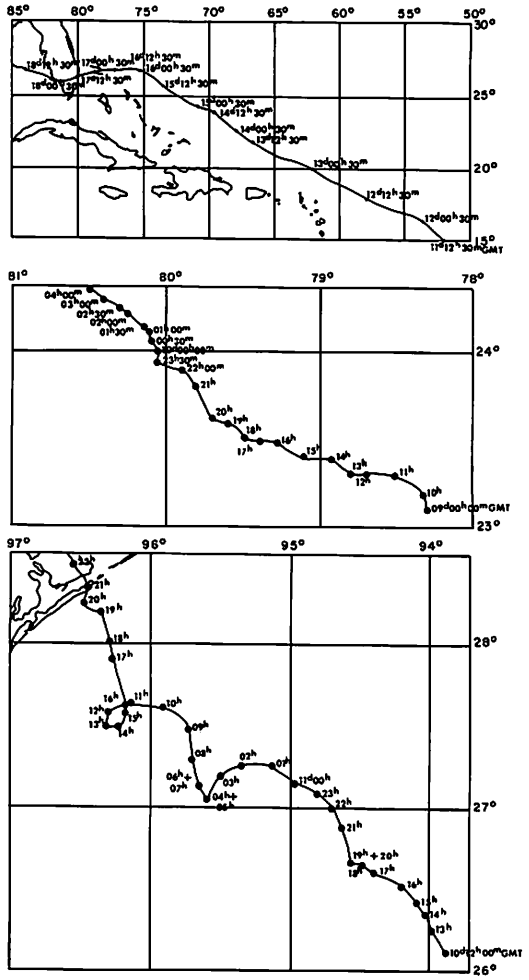

Fig. 17 Paths of three terrestrial cyclones: (a) Sept 11-20, 1957 (Yeh, 1950); (b) Hurricane Donna, Sept 9-10, 1960; and (c) Hurricane Carla, Sept 10-12, 1961 (Neuman and Boyd, 1962)

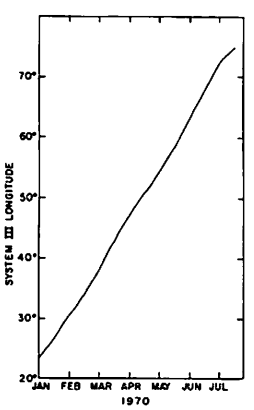

Fig. 18 Longitude vs. time curve for Red Spot, on System III; same data as in Fig. 16c. Shows amplitude of 90-day oscillation to be minor in scale of Red Spot displacement in STropZ

1968-69, $P = 75^d$, $A = 3°$, 18 obs.; 1969-70, $P = 64^d$, $A = 4°$, 9 obs. All but two of these spots were *dark* (the 1965-66, 1969-70 spots were *white*). The preference for cycles near 70 days is noteworthy. Probably numerous oscillating spots exist having still smaller amplitudes.

h. Life of Red Spot; Spin-off Cloud Masses - Another tentative conclusion may be drawn. If the Red Spot propagates along the STropZ in a cycle averaging 5 years (as indicated by the daily period of rotation around the planet's axis), this cycle may be due to the relaxation period discussed in Sec. 5: the *Red Spot triggers on its leading edge* the meteorological instability responsible for *the rapid growth of cumulus towers*. This type of propagation would not be uniform. It would explain why *the Red Spot motion is not precisely constant*; why there is only *one Red Spot in the Zone*; and why its period averages around $9^h55^m38^s$ (corresponding to a 5-year cycle, itself due to the meteorological relaxation period). The Red Spot, once having got into this resonance period, *could then continue to exist almost indefinitely*. Competing instabilities, set off "prematurely" before the next arrival of the Red Spot, may cause a STropD but they would necessarily be less effective in releasing latent heat, and could therefore be destroyed by the Red Spot during slow encounters. (The probability of an enduring large separation in longitude, given the inherent irregularities in motion for both storm centers, appears near zero).

The White Ovals move about $0.^\circ8$/day faster than System II (Peek, p. 124) and thus have a period of about $9^h55^m10^s$, about the same as the STropZ in which they occur (Fig.12; 33°S). Since they have undergone such vast changes during the past 50 years, including a complete merging into a zone, it appears too early to speculate on their separate nature.

The latent heat released by the Red Spot must be less than that of the entire STropZ, since anticyclonic divergence has been observed over the entire zone (Fig. 12). The instability discussed in Sec. 5 must therefore pertain to one atmospheric layer only (perhaps the one between the H_2O and NH_3+H_2S condensation zones). This would require part of the planetary heat flux to continue to pass upward between successive passages of the Red Spot, presumably by radiative transfer. The total energy generated by the Red Spot could therefore be in excess of 10^{23} ergs/sec (cf. Sec. 4*d*). It may also be necessary to reinterpret the observed relationship between the daily period of rotation (around the planetary axis) and visibility or color (Sec. 4*b*). *Strong color* correlated with *long period* would mean: more rapid advance of the Red Spot along the STropZ, thus increased release of latent heat per unit time, hence greater elevation.

At times the Red Spot produces long narrow clouds on its preceding edge (Pl. I*c*), well described by Reese (1970, p. 254). Since the Red Spot falls behind in its daily rotation with respect to the STropZ, the narrow cloud belts really are trailing in the westward motion of the Red Spot. The rate of separation is, however, much faster than corresponds to the 8 sec rotation difference and appears to stem from a slight poleward movement which brings the narrow belts into the S. rim of the STropZ (and the N. edge of the S. Temp. Belt), which tends toward the much more rapid rate of rotation shown in Figure 12*a*. Interestingly, on the best LPL blue photographs a fine line is also seen on the other (f) side of the Red Spot, stretching for 70°+ in longitude (Pl. I). Conceivably, it stretches along the entire 360° arc; or else, it is located slightly closer to the equator (*P* longer, cf. Fig. 12), thus explaining how it also could stem from the Red Spot itself. These spin-off clouds are *brown* as is the envelope of the Red Spot (Pl. I); and dark in blue light.

The NTropZ, itself of variable brightness, has no Red Spot, but shows numerous smaller spots (Pl. I). The N. half of the Zone usually shows only *white* spots, sometimes brilliantly against the Zone. The Southern half shows dark spots and streaks, not unlike the adjacent North Equatorial Belt; the boundary between the Zone and the Belt varies considerably. Peek (pp. 95, 96) lists, for 47 annual apparitions of the planet, mean values of the daily rotation period derived from the measured spots, which numbered from 2 to 28 per year (13 years with 20 or more); the annual means run from $9^h55^m13^s$ to 41^s. Peek (p. 88) felt sure of one cloud mass having been identified for nearly 2 years, though he thought it likely that other such cases existed and he referred to two reported cases (with several spots present, identification across the annual observation gap is uncertain). Daytime observation in the near-infrared is indicated here. A narrow and faint grey line has at times been observed in the middle of the NTropZ (Peek, p. 83), apparently not unlike the line noted in the STropZ following the Red Spot. Nevertheless, some *asymmetry* between the two hemispheres is evident; cf. Sec. 6*c* and Pl. I.

i. Heat Balance in Jupiter Atmosphere - A convenient summary on the heat balance of the Earth's atmosphere is given by Byers (1954). One difference with the Earth will be the greatly increased greenhouse effect (H_2O, NH_3, H_2, as gases, plus condensation products), making for a much-reduced *net* outward thermal flux; but presumably a flux due to the hydrological *cycle* not greatly reduced compared to the Earth (the H_2O content is probably about 0.6%, the NH_3 content 0.2%, both by number (Lewis, 1969, Model B), not unlike our H_2O content). This will cause the transport by the latent heat flux to *dominate* in the Jupiter "weather zone". The latent heat flux will therefore be close to the *total* heat flux, which is readily computed from Dr. Low's effective temperature of the planet (with allowance for its solar radiation component): 10^4 ergs/cm^2 sec. (The predominance of the internal heat source over the absorbed solar flux is the *second* main difference with the heat balance of the Earth). Since 1 cm of precipitation requires a supply of latent heat of about 600 cal (depending on the temperature of the vapor) or $10^{10.4}$ ergs/cm^2, the average precip. rate will be about $10^{-6.4}$ cm/sec or 10^{-3} cm/hr. If the rain columns are 0.001 of the total surface area, the rainfall in the columns could be around 1 cm/hour (or more intense for smaller columns). The planet could therefore be covered with cumulus anvils 10^3 times the area of the precip. columns, on a more or less continuous basis, which appears meteorologically acceptable. The dominant internal heat flux will, of course, encourage a fairly complete *cloud cover*.

j. The Red Spot and Other Persistent Cloud Masses - In some respects the Red Spot is unique: its dimension, color, elevation above the general cloud level, and probably its longevity. Some representative LPL color photographs of the Red Spot and its Hollow are shown in Plate I.* At no time during the past six years was the Red Spot completely covered and white, though this has occurred around 1930 (Slipher, 1964, Plate 45, p. 91).

Among the regular, oval-shaped clouds, the three *White Ovals* follow the Red Spot in dimensions. Two are well shown on Plate I. Since their tops are lower than that of the Red Spot, they are more often obscured.

---

* Additional color reproductions are found on the covers of *Sky and Telescope*, May 1968 and Jan 1972; I*a* is the cover plate on M-30444 Columbia Masterworks, Mozart's Jupiter Symphony.

They appear to have been observed in the 1920's by Phillips (Fox, 1969); they merged as a zone in the 1930's (Peek, p. 123); were partly obscured again in the early 1960's, as reported by Fox; and again in part in 1968. At times the Ovals have dark borders, like the Red Spot, probably an outer edge in subsidence. In summary, there are strong parallels between the Red Spot and the White Ovals, though the latter are smaller, lower, whiter, and presumably have a shorter life time.

Still smaller cloud masses are seen on nearly all good Jupiter photographs, some of them resembling the White Ovals except for scale and life time. See Pl. I. Better definition than this record is obviously most desirable.

5. The SEB Major Eruptions; Atmospheric Instability

The year 1971 marked another major eruption in the South Equatorial Belt. This type of eruption was first observed in 1919-20, then 1928-29, and in great detail in 1943. The 1971 outbreak was spotted by Mr. Fox observing visually with our 61-inch telescope on June 21, 1971, as a small white cloud, and he at once recognized its significance. The outbreak was reported by Reese (1971*b*) and was found to have been first photographed by the NASA Planetary Patrol on June 18, 1971 (*Sky and Telescope*, Sept, 1971). A description of the LPL observations of the 1971 outbreak is given by Messrs. R. B. Minton and S. L. Larson in *LPL Comms. Nos. 178* and *179*).

In view of the absence of a correlation found by Chapman and Reese (1968) between the rotational periods of the SEB outbreaks and that of the Red Spot or the System III (solid-surface) rotation period, we examined whether purely meteorological processes could lead to a cyclic eruption process. Condensation in the water-vapor zone is expected to lead to a *temperature inversion* between the water and the NH_3, H_2S condensation layers, which, when gradually overcome by the heat flux build-up, could lead to almost explosive cumulus growth below the ammonia layer. Such an almost explosive growth following a period of stagnation is well-known in the terrestrial cumulus-formation process. Cf. Figure 13*a*, cloud in left margin, which is the first to break through the barrier layer.

Assume that the atmosphere on Jupiter *above* the level at which p = 5 atm -- at which the temperature is expected to be 290°K (Owen, 1969, Fig. 1)-- must on the average heat up 10°C to cause incipient instability. The atmospheric *mass* then corresponds to one that would cause p = 2 atm on the Earth, a mass equivalent of 20 meters of water. To heat this 10°C would take 2.10^4 cal/cm^2 or $10^{11.9}$ ergs/cm^2. If hydrogen gas of the same mass is substituted for water, the needed energy will be $10^{12.45}$ ergs/cm^2; if the mean molecular weight is assumed to be 2.3, as deduced, the value becomes $10^{12.4}$. With the internal heat flux of Jupiter, this would take $10^{8.4}$ sec or 8 years to produce. Cyclic phenomena could therefore be produced by this process.

Since the above was written, Reese (1972) has re-examined the SEB outbreaks in a plot of time vs. the System III longitudes (based on the decametric radio rotation period of $9^h55^m30^s$). He now found that the outbreaks arranged themselves on *three* parallel lines, a possibility not examined by Chapman and Reese: (a) the three greatest disturbances ever observed, 1919, 1928, and 1971A; (b) five great disturbances (1943A, 1949, 1952, 1958, 1964), four of them with very active SEBZ branches; and (c) four secondary or less active disturbances (1943B, 1955, 1962,

1971B). Thus, *three discrete sources* appear to exist, defining the same rotation Period, $9^h55^m30^s.11 \pm 0.03$. This is only $0^s.36$ longer than Carr's (1971) mean value for the decametric rotation period. In 1966.0 the longitudes in System III of the three SEB sources were about 50°, 225°, and 120°, respectively. By comparison, the much-more-frequently active 18 Mc radio sources A and B had λIII (reduced to $D_E = 0°$) of A ≃ 256° and B ≃ 145° (Carr *et al.*, 1970), some 25°-30° larger than SEB sources *b* and *c*. Clearly, the Reese (1972) results are of extraordinary importance; they suggest that *three vents exist in the Jupiter sub-surface* erupting with intervals of several years, with differing, but roughly repetitive, powers, *which trigger the enormous SEB outbreaks*. These eruptions will interact with the cyclic meteorological instabilities, described above, and together shape the intensity and extent of the observed disturbance. Another vent or at least a deep-seated storm center, nearly stationary in System III, is described by G. Solberg in *LPL Communication No. 180* and by R. B. Minton in *No. 182*.

The constant and equal rotation times derived from these vents indicate the presence of a *genuinely-solid crust* beneath the atmosphere. A supercritical fluid would not possess *fissures in fixed positions*, erupting every decade or so, with cycles not unlike, e.g., Mauna Loa. It further shows that the Red Spot, with all its motions described in Sec. 4, *could not possibly be related to any crustal feature*, which would have a constant rotation of $9^h55^m30^s$. Cf. also Appendix I, Sec. 2.

6. Other Topics

a. Planetary Cloud Patterns - The Earth's Tropical Convergence has a planetary cause and appearance (Figs. 6-9) in spite of the rather short life cycles of its component members - the cloud clusters or regions of Organized Cumulus Convection.

Likewise, the Jupiter Belts and Zones have persisted over at least a century, in spite of frequent major upheavals, which has made it appropriate to give them *names*. A separate discussion will be published on the Belts and Zones based on the LPL color photography and spectrophotometry.

b. Limb Brightening in the UV - Mr. J. Fountain photographed Jupiter with 37 narrow-band filters ($\lambda/\Delta\lambda = 30$) from 3000-9100Å. The 3000 and 3100Å images show the planet with *limb brightening*, evidently due to the increased molecular scattering near the limbs. Both polar caps are slightly enhanced on these pictures. Mr. Fountain is preparing a report (*LPL Comm. No. 175*).This limb brightening does not conflict with the near-absence of the secant effect reported above in the methane and ammonia distributions; because the 3000Å images see little more than the stratosphere which will contain no ammonia haze.

c. Asymmetry Between the Hemispheres - The marked asymmetry between the two Jupiter hemispheres has long been known, with the Red Spot and the White Ovals in the southern hemisphere, and no corresponding northern-hemisphere structures. The sources of the blue festoons are just North of the equator, with no corresponding sources South. The heat flux measurements at 5μ have shown hotter regions, around 300°K, than observed at the same southern latitudes, indicating a local absence of a high cloud cover just North of the equator. The polarization measures by Gehrels and his group (Fig. 4) also show a distinct asymmetry, as does the rotation curve of Figure 12. The asymmetry in the polarization has been observed also photographically, by J. Fountain, through polaroid filters, composited to show variations over the disk. The cloud belts on the planet are never strictly symmetrical.

The asymmetry between the two hemispheres may well be due to uneven energy release through the solid hydrogen surface; with presumably an above-average flux conducive to increased average storm activity. Indeed, *all three major gas vents* (Sec. 5)*appear to occur between 13° and 14° S* with their major eruptions every 3-6 years developing typically into three cloud masses, centered at 8°, 14°, and 19° S, respectively (Reese, 1972). Possibly the same latitude (14°S) is responsible for the additional two or three sources causing the 18-20 Mc radio bursts. Direct observation of the latitudes of these sources has not yet succeeded in spite of some remarkable interferometer tests with baselines up to nearly 1/2 million by Dulk (1970) and Carr *et al.* (1970) (summarized in the JPL report referred to), which indicate these sources to have *diameters* less than 400 km to 4000 km.

d. Radio Frequency Emission by the Electrical Discharges - On the Earth they cause a very broad spectrum peaked at about 10 Kc but extending upward to 100 Mc. On Jupiter, because of the higher density of the water condensation zone, the discharges will be correspondingly shorter and the expected frequencies correspondingly higher, by about 1 decade.

e. Concluding Remarks - Past discussions of Jupiter have often been confused by the fact that we observe only the uppermost layers of the Jupiter clouds, from *above*, while our familiar concepts are based on observations from the *ground*, on Earth. Figure 13*e* shows what this may mean. Similar problems exist in the interpretation of planetary polarization results; in fact, Dr. D. Coffeen has participated in using the NASA CV-990 for an infrared polarimetric study of terrestrial clouds below the aircraft. The circulation of the Jupiter atmosphere appears more confined than the Earth. In spite of enormous upheavals every 5-10 years or so, which temporarily destroy much of the familiar Belts and Zones near the equator, the planet returns to a pattern quite familiar from earlier years, so that the nomenclature system of the past still applies. This stability appears related to the low obliquity of Jupiter's equator, its high rate of rotation, the correspondingly-large Coriolis force, and thus the strict confinement to narrow belts in latitude, and long and narrow brown clouds. This paper focuses on the nature of the Red Spot, deferring a discussion of the wealth of information now available on the cloud belts, the bright zones, and numerous smaller features. Fortunately, ammonia makes more colorful compounds than water and makes wonderful tracers for cloud origins!

Acknowledgments. Much of the work described in this article, including the 61-inch telescope and the photographic programs carried out with it, have been supported by the National Aeronautics and Space Administration since the inception of this Laboratory, most recently through Grant NGL 03-002-002. I am indebted to several meteorologists for advice and assistance, particularly Drs. V. Suomi and S. L. Rosenthal. Helpful comments were also made by Drs. E. Roemer and T. Owen, and especially Messrs. R. B. Minton, H. G. Solberg, and E. J. Reese. Messrs. S. M. Larson, R. B. Minton, and J. Fountain assisted in the selection of the illustrations; and Mr. W. E. Fox, Director of the Jupiter Section of the B. A. A., supplied valuable early references. I am indebted to Mrs. I. Edwards for her assistance with the earlier drafts of this paper and the references; to Mrs. M. Wilson for preparing the press copy.

REFERENCES

Anderson, R. C., Pipes, J. G., Broadfoot, A. L., and Wallace, L. 1969, *J. Atm. Sci., 26*, 874.

Armstrong, R. L. and Welsh, H. L. 1960, *Spectrochimica Acta, 16*, 840-852.

Armstrong, K. R., Harper, D. A., and Low, F. J. 1972, "Far-Infrared Brightness Temperatures of the Planets", *Ap. J., 178*, L89-L92.

Aumann, H. H., Gillespie, C. M., and Low, F. J. 1969, "The Internal Powers and Effective Temperatures of Jupiter and Saturn", *Ap. J., 157*, L69-L72.

Bergeron, T. 1954, "The Problem of Tropical Hurricanes", *Quart. J. Roy. Meteorol. Soc., 80*, 131-164.

Bishop, E. V. and de Marcus, W. 1970, "Thermal Histories of Jupiter Models", *Icarus, 12*, 317-330.

Byers, H. R. 1954, "The Atmosphere up to 30 Kilometers", THE EARTH AS A PLANET, Vol. II of THE SOLAR SYSTEM (ed. G. P. Kuiper), Chapt. 7, 306-307 (Chicago: U. of Chicago Press).

Cadle, R. D. 1962, "The Photochemistry of the Upper Atmosphere of Jupiter", *J. Atm. Sc., 19*, No. 4, 281-285.

Carr, T. D. , Lunch, M. A., Paul, M. P., Brown, G. W., May, J., Six, N. F., Robinson, V. M., and Block, W. F. 1970, "Very Long Baseline Interferometry of Jupiter at 18 MHz", *Radio Sci., 5*, 1223.

Carr, T. D., Smith, A. G., Donivan, F. F., and Register, H. I. 1970, "The Twelve-year Periodicities of the Decametric Radiation of Jupiter", *Radio Sci., 5*, 495-503.

Carr, T. D. 1971, "Jupiter's Magnetospheric Rotation Period", *Astrophysical Letters, 7*, 157-162.

Chang, C. P. 1970, "Westward Propagating Cloud Patterns in the Tropical Pacific as seen from Time-Composite Satellite Photographs", *J. Atm. Sci., 27*, 133-138.

Chapman, C. R. and Reese, E. J. 1968, "A test of the Uniformly Rotating Source Hypothesis for the South Equatorial Belt Disturbances on Jupiter", *Icarus, 9*, 326-335.

Chapman, C. R. 1969, "Jupiter's Zonal Winds: Variation with Latitude", *J. Atm. Sci., 26*, 986-990.

Connes, J., Connes, P., and Maillard, J. P. 1969, NEAR INFRARED SPECTRA OF VENUS, MARS, JUPITER AND SATURN, Centre National de la Recherche Scientifique.

Cortright, E. M. 1968, EXPLORING SPACE WITH A CAMERA, Office of Technology Utilization, NASA, Washington, D. C., NASA SP-168.

Coulomb, J. and Jobert, G. 1963, THE PHYSICAL CONSTITUTION OF THE EARTH (New York: Hafner Publish. Co.), 244.

Curran, R. J., Conrath, B. J., Hanel, R. A., Kunde, V. G., Pearl, J. C. 1973, "Mars: Mariner 9 Spectroscopic Evidence for H_2O Ice Clouds", Goddard Space Flight Center Preprint X-651-73-156.

de Marcus, W. 1958, "The Constitution of Jupiter and Saturn", *A. J., 63*, 2-28.

Dickinson, R. E. 1969, "Propagators of Atmospheric Motions", *Rev. of Geophs., 7*, No. 3, 483-537.

Dopplick, T. G. 1972, "Radiative Heating of the Global Atmosphere", *J. Atm. Sci., 29*, 1278-1294.

Dulk, G. A. 1970, "Characteristics of Jupiter's Decametric Radio Source Measured with Arc-Second Resolution", *Ap. J., 159*, 671-684.

Duncan, R. A. 1971, "Jupiter's Rotation", *Planet. Space Sci., 19*, 391-398.

Dunham, T. 1952, "Spectroscopic Observations of the Planets at Mt. Wilson", THE ATMOSPHERES OF THE EARTH AND PLANETS, Chapt. XI, ed. G. P. Kuiper (Chicago: U. of Chicago Press), 286-303.

Dunn, G. E. and Miller, B. I. 1960, ATLANTIC HURRICANES (Louisiana State Univ. Press).

Fink, U., Dekkers, N. H., and Larson, H. P. 1973, "Infrared Spectra of the Galilean Satellites of Jupiter", *Ap. J., 179*, L155-L159.

Fox, W. E. 1969, "Report on the apparitions of 1966-67 and 1967-68", *Journ. British Astron. Assoc., 79*, 310-312.

Gallet, R. M. 1961, "Radio Observations of Jupiter II", PLANETS AND SATELLITES, Vol. III of THE SOLAR SYSTEM (eds. G. P. Kuiper and B. Middlehurst), Chapt. 14, 500-533, (Chicago, U. of Chicago Press).

Gehrels, T., Herman, B. M., and Owen, T. 1969, "Wavelength Dependence of Polarization XIV. Atmosphere of Jupiter", *A. J., 74*, 190-199.

Gehrels, T.,Suomi, V. E., and Krauss, R. J. 1972, in SPACE RESEARCH XII, ed. A. C. Stickland, (Berlin, Akad. Verlag).

Gillett, F. C., Low, F. J., and Stein, W. A. 1969, "The 2.8-14 Micron Spectrum of Jupiter", *Ap. J., 157*, 925-934.

Goody, R. 1969, "The Atmospheres of the Major Planets", *J. Atm. Sci., 26*, 997-1001.

Greenspan, J. and Owen, T. C. 1967, "Jupiter's Atmosphere: Its Structure and Composition", *Science, 156*, 1489-1493.

Hanel, R. A. and Conrath, B. J. 1970, "Thermal Emission Spectra of the Earth and Atmosphere from the Nimbus 4 Michelson Interferometer Experiment", *Nature, 228*, 143-145.

Hanel, R. A., Conrath, B. J., Kinde, V. G., Prabhakara, C., Revah, I., Salomonson, V. V., and Wolford, G. 1972*a*,"The Nimbus 4 Infrared Spectroscopy Experiment. I. Calibrated Thermal Emission Spectra", *J. of Geophysical Research, 77*, 2629-2641.

Hanel, R. A., Schlachman, B., Breihan, E., Bywaters, R., Chapman, F., Rhodes, M., Rodger, D., and Vanous, D. 1972*b*,"Mariner 9 Michelson Interferometer", *Ap. Opt., 11*, 2625-2634.

Harper, D. A., Low, F. J., Rieke, G. H., and Armstrong, K. R. 1972, "Observations of Planets, Nebulae, and Galaxies at 350 Microns", *Ap. J., 177*, L21-L25.

Hess, S. L. and Panofsky, H. A. 1951, "The Atmospheres of the Outer Planets", *Compendium of Meteorology*, Amer. Meteor. Soc., Boston, Mass., 391-398.

Holton, J. R. 1971, "A Diagnostic Model for Equatorial Wave Disturbances: The Role of Vertical Shear of the Mean Zonal Wind", *J. Atm. Sci., 28*, 55-64.

Holton, J. R., Wallace, J. M., and Young, J. A. 1971, "A Note on Boundary Layer Dynamics and the ITCZ", *J. Atm. Sci., 28*, 275-280.

Hubbard, W. B. 1970, "Structure of Jupiter: Chemical Composition, Contraction, and Rotation", *Ap. J., 162*, 687-697.

Irvine, W. M., Simon, T., Menzel, D. H., Pikos, C., and Young, A. T. 1968, "Multicolor Photoelectric Photometry of the Brighter Planets. III Observations from Boyden Observatory", *A. J. 73*, 826, Table XIV.

Johnson, A. W. 1969, "Weather Satellites", *Scientific American, 220*, 52-68.

Johnson, H. L. 1970, "The Infrared Spectra of Jupiter and Saturn at 1.2-4.2 Microns", *Ap. J. 159*, L1-L5.

Jolly, W. L. 1964, THE INORGANIC CHEMISTRY OF NITROGEN (New York: W. A. Benjamin).

Keay, C. S. L., Low, F. J., Rieke, G. H., and Minton, R. B.,"High-Resolution Maps of Jupiter at Five Microns", (in press).

Kornfield, J. and Hasler, A. F. 1969, "A Photographic Summary of the Earth's Cloud Cover for the Year 1967", *J. of Applied Meteorology, 8*, No. 1, 687-700.

Kuiper, G. P. 1952, THE ATMOSPHERES OF THE EARTH AND PLANETS (Chicago: U. of Chicago Press).

Kuiper, G. P. 1957, "Infrared Observations of Planets and Satellites", abstract, *A. J., 62*, 245.

Kuiper, G. P. 1963, "Infrared Spectra of Planets and Cool Stars: Introductory Report", *Mémoires Soc. R. Sc. Liège, Vol. IX*, 365-391.

Lewis, J. S. 1969, "The Clouds of Jupiter and the NH_3-H_2O and NH_3-H_2S System", *Icarus, 10*, 365-378; 393-409.

Lewis, J. S. and Prinn, R. G. 1970, "Jupiter's Clouds: Structure and Composition", *Science, 169*, 472-473.

Low, F. J. and Davidson, S. W. 1965, "Lunar Observations at a Wavelength of 1 Millimeter", *Ap. J., 142*, 1278-1282.

Low, F. J. 1966, "Observations of Venus, Jupiter, and Saturn at λ20μ", *A. J.*, *71*, 391.

Low, F. J., Rieke, G. H., and Armstrong, K. R. 1973, "Ground-Based Observations at 34μ", *Ap. J. Letters*, (in press).

Martin, D. W. and Suomi, V. E. 1971, "A Satellite Study of Cloud Clusters Over the Tropical North Atlantic Ocean", Final Report on Contract E-127-69-(N), Space Science and Engineering Center, U. of Wisconsin, Madison.

Moroz, V. I. and Cruikshank, D. P. 1969, "Distribution of Ammonia on Jupiter", *J. Atm. Sci.*, *26*, 865-869.

Neuman, S. and Boyd, J. G. 1962, "Hurricane Movement and Variable Location of High Intensity Spot in Wall Cloud Radar Echo", *Monthly Weather Review*, *90*, 371-374.

Newburn, R. L. and Gulkis, S. 1971, "A Brief Survey of the Outer Planets, Jupiter, Saturn, Uranus, Neptune, Pluto, and their Satellites", JPL Tech. Report 32-1529.

Newton, C. W. 1963, "Dynamics of Severe Convective Storms", *Meteorological Monographs*, *5*, Amer. Meteor. Soc., 33-58.

Newton, C. W. 1967, "Severe Convective Storms", ADVANCES IN GEOPHYSICS, *12*, (Academic Press, New York).

Ooyama, K. 1969, "Numerical Simulation of the Life Cycle of Tropical Cyclones", *J. Atm. Sci.*, *26*, 3-40.

Owen, T. C. and Staley, D. O. 1963, "A Possible Jovian Analogy to the Terrestrial Equatorial Stratospheric Wind Reversal", *J. Atm. Sci.*, *20*, No. 4, 347-350.

Owen, T. C. 1965, "Comparison of Laboratory and Planetary Spectra. II. The Spectrum of Jupiter from 9700 to 11200A", *Ap. J.*, *141*, 444-456; and "III. The Spectrum of Jupiter from 7750 to 8800A", *Ap. J.*, *142*, 782-786.

Owen, T. C. and Walsh, T. E. 1965, "Radiation of Jupiter and Saturn", *Nature*, *208*, 477.

Owen T. C. 1967, "Comparisons of Laboratory and Planetary Spectra: IV. The Identification of the 7500Å Bands in the Spectra of Uranus and Neptune", *Icarus*, *6*, 108-113.

Owen, T. C. 1969, "The Spectra of Jupiter and Saturn in the Photographic Infrared", *Icarus*, *10*, 355-364.

Owen, T. C. 1970, "The Atmosphere of Jupiter", *Science*, *167*, 1675-1681.

Palmén, E. and Newton, C. W. 1969, "Tropical Cyclones, Hurricanes and Typhoons", ATMOSPHERIC CIRCULATION SYSTEMS (New York: Academic Press).

Peek, B. M. 1958, THE PLANET JUPITER (London: Faber and Faber).

Reese, E. J. and Smith, B. A. 1968, "Evidence of Vorticity in the Great Red Spot of Jupiter", *Icarus*, *9*, 474-486.

Reese, E. J. and Solberg, H. G. 1969, "Latitude and Longitude Measurements of Jovian Features in 1967-68", Rpt. TN-701-69-28, NASA grants, New Mexico State University.

Reese, E. J. 1970, "Jupiter's Red Spot in 1968-1969", *Icarus*, *12*, 249-257.

Reese, E. J. 1971*a*, "Jupiter: Its Red Spot and Other Features in 1969-1970", *Icarus*, *14*, 343-354.

Reese, E. J. 1971*b*, I. A. U. Circular 2338, July 2, 1971.

Reese, E. J. 1972, "Jupiter: Its Red Spot and Disturbances in 1970-1971", Rpt. TN-72-40, NASA grant, New Mexico State University.

Riehl, H. 1951, "Aerology of Tropical Storms", *Compendium of Meteorology*, Amer. Meteor. Soc., Boston, Mass., 902-913.

Rosenthal, S. L. 1971, National Hurricane Research Lab., Miami, Fla., personal communication.

Slipher, E. C. 1964, THE BRIGHTER PLANETS, Lowell Observatory.

Slipher, E. C., Shapiro, R., Giclas, H. L., Lorenz, E. N., and Hess, S. L. 1951, "The Project for the Study of Planetary Atmospheres", Rpt.No. 9, Lowell Observatory, Flagstaff, Arizona.

Smith, B. and Tombaugh, C. 1963, "Observations of the Red Spot on Jupiter", Rpt. TN-557-63-2, New Mexico State University.
Smoluchowski, R. 1971, "Metallic Interiors and Magnetic Fields of Jupiter and Saturn", *Ap. J., 166*, 435-439, and references given there.
Solberg, H. G. and Reese, E. J. 1966, "Recent Measures of the Latitude and Longitude of Jupiter's Red Spot, *Icarus, 5*, 266-273.
Solberg, H. G. 1968*a*, "Jupiter's Red Spot in 1965-1966", *Icarus, 8*, 82-89.
Solberg, H. G. 1968*b*, "Jupiter's Red Spot in 1966-1967", *Icarus, 9*, 212-216.
Solberg, H. G. 1969, "A 3-Month Oscillation in the Longitude of Jupiter's Red Spot", *Planet. Space Sci., 17*, 1573-1580.
Studier, M. H., Hayatsu, R., and Anders, E. 1968, "Origin of Organic Matter in Early Solar System - I. Hydrocarbons", *Geochim. et Cosmochim. Acta, 32*, 151-174.
Trafton, L. M. 1967, "Model Atmospheres of the Major Planets", *Ap. J., 147*, 765.
Ulmschneider, P. 1970, "On Frequency and Strength of Shock Waves in the Solar Atmosphere", SOLAR PHYSICS, (Dordrecht-Holland: Reidel Publish. Co.), pp. 403-415.
Ulmschneider, P. 1971, "On the Propagation of the Spectrum of Acoustic Waves in the Solar Atmosphere", *Astron. and Astrophys., 14*, 275-282.
Wallace, J. M. 1970, "Time-Longitude Sections of Tropical Cloudiness (Dec. 1966-Nov. 1967)", ESSA TECH. REPORT NESC 56, Washington, D. C., 37 pp.
Wallace, J. M. 1971, "Spectral Studies of the Tropospheric Wave Disturbances in the Tropical Western Pacific", *Rev. of Geophy. and Space Physics, 9*, 557-612.
Walsh, T. E. 1969, "Infrared Absorptance of Ammonia - 20 to 35 Microns", *J. Opt. Soc. Amer., 59*, 261-267.
Westphal, J. A. 1969, "Observations of Localized 5-Micron Radiation from Jupiter", *Ap. J., 157*, L63-L64.
Williams, K. 1970, "Characteristics of the Wind, Thermal, and Moisture Fields Surrounding the Satellite-Observed Mesoscale Trade Wind Cloud Clusters of the Western North Pacific", PROCEEDINGS SYMPOSIUM TROPICAL METEOROLOGY, American Geophysical Society, pp. D IV-1 to 7.
Yeh, T. C. 1950, "The Motion of Tropical Storms Under the Influence of a Superimposed Southerly Current", *J. of Meteorology, 7*, 108-113.

APPENDIX I

1. Planetary Energy Flux; Contraction Time Scale - During the second Lowell Observatory Conference on Planets, August 1951, much discussion ensued on the nature of the Jupiter and Saturn cloud covers. The spontaneous major eruptions and related phenomena indicated that the meterologies of these two planets differed greatly from that of the Earth and Mars; they appeared *internally driven* instead of *sundriven*.

In other words, the effects of the internal heat fluxes of Jupiter and Saturn appeared to exceed the effects of the absorbed solar radiation. Since for equal fluxes the effects on cloud formation of an internal source would be larger, the conclusion could *not* be reached that the fluxes of planetary origin were necessarily larger than the absorbed solar fluxes.

In THE ATMOSPHERES OF THE EARTH AND PLANETS (1952) I computed the total release of gravitational energy *after* the protoplanet stage, starting with $1.5R_J$. The result was that the average Jupiter emission will have been some 40 times the absorbed solar flux and the average surface temperature 250°K (*op. cit.* pp. 326-327). Since the present value was clearly much below that figure, "during Jupiter's early history, its surface temperature must have greatly exceeded 250°K and may well have corresponded to red heat". It was pointed out that the 8-14μ window did not

allow the measurement of the *present* flux ratio, planet/solar contribution, because of the double NH_3 band centered at 10-11μ which automatically gave T ≃ 130°K; but that this ratio might possibly be estimated from the observed cloud phenomena (*op. cit.* pp. 327, 376).

Öpik (1962) pursued the matter further, and derived from the cloud phenomena a provisional ratio of 1.6 ± 0.4.

As to the *time scale of the Jupiter contraction*, this was presented in the 1940's in my lectures at the University of Chicago along the following lines:

The empirical mass-luminosity relation for solar-type and smaller stars is $L \sim M^3$; the released gravitational energy for homologous stellar models, $E \sim M^2/R$; the Helmholtz-Kelvin contraction time scale therefore $E/L \sim M^{-1} R^{-1}$; or $\sim M^{-4/3}$ if ρ = constant. An extrapolation of the stellar data to Jupiter ($M_M = 10^{-3} M_\odot$) and Saturn would therefore make their time scales somewhat longer than the age of the solar system. Jupiter and Saturn in that sense, were considered small stars as well as planets. The planetary observations were considered a confirmation of this conclusion: "The Jovian atmospheres, at least those showing visible clouds (Jupiter and Saturn), are probably heated primarily from below. The spectacular cloud phenomena, sometimes altering the entire aspect of these giant planets, the motions of the clouds and their colors, do not appear to be governed by solar heating. It is quite likely that continued cooling and gravitational energy of contraction are still important in the heat budget of these bodies" (THE ATMOSPHERES, p. 376).

The first direct measures of Jupiter that indicated an excess of planetary radiation were made by Low (1966) who found that the energy emitted by the planet shortward of 25μ was already in excess of the absorbed solar radiation. He and his associates added data for the longer wavelength soon thereafter as described in the main text and illustrated in Figure 3*d*.

2. *Earlier Red Spot Hypotheses* - In the recent summary by Newburn and Gulkis (1971) the Red Spot is called "truly one of the great solar system puzzles". The Spot has been seen for 305 years since Cassini first described it (cf. *Sky and Telescope*, May 1968) but it may have existed before the telescope was invented. Its irregular motions had suggested that it was not attached to a large mountain; and its long life, that it was not a fluid-dynamic feature (a large eddy), but possibly instead a cloud cap about a large island floating in a highly compressed gaseous medium, as proposed by Wildt in 1939. Other authors have assumed that the solid surface might rotate irregularly after all, since the Earth exhibits minor fluctuations in its rotation, caused by variable interactions with the liquid core. They held that a "Taylor column" above a large plateau would fit the case.

Taylor (1923) used a fluid of very low viscosity; his "column" (being a quasi-cylindrical upward deflection of the flow) was produced by moving a strictly cylindrical box in a rotating liquid at right angles to the axis of rotation; and the "column" was observed only above the cylinder at a height comparable to that of the cylindrical box itself. While the application to the Jupiter Red Spot has been widely quoted, there are insurmountable difficulties with the application to the Red Spot of the phenomena observed by Taylor:

(a) The deeper atmosphere of Jupiter is *nearly stagnant* with respect to the solid surface; this was discussed on the basis of Figure 12.

(b) The solid surface has a constant period of rotation, at $9^h55^m30^s$ (Sec. 5), not the *near-periodic motion*, both in longitude and latitude, with P ≅ 90 days, as shown in Figure 16; other *period changes* every 25-30 years causing overall departures from uniform motion by 1200° during the past 140 years; or even the departure of the average rotation period from that of the radio sources by 8 sec, indicating *a complete revolution* of the Red Spot with respect to the solid surface every 5 years or so.

(c) Even if a current of *unexplained origin* in the dense, viscous H_2-He-H_2O-NH_3-CH_4 mixture ($p > 10^5$ atm) existed relative to the solid surface, the hypothesis further assumes that a protruding box-like cylindrical mesa of solid H_2 exists, some 11,000 km wide and 25,000 km long, with sharp vertical walls, as required for the upward flow to retain the cylindrical shape of the column. The *formation* of such a cylindrical box has no counterpart in geophysics and is inconceivable; nevertheless, if it once existed it would quickly *erode* by the hypothetical current itself, be rounded off on the upper rim, and thereupon cause the current to pass as a simple overflow.

(d) The cylindrical mesa postulated under (c) would have to undergo *semi-periodic changes in length and width* with amplitudes 1000-4000 km over a period around 90 days (Fig. 16); and undergo *total changes in length* well in excess of 10,000 km. (The induced flow observed by Taylor (1923) had the diameter and shape of the moving cylinder below and was co-axial with it; the vertical dimensions of the Jupiter "atmosphere" are presumably below 1000 km).

(e) The concept of a Taylor column of height some two orders of magnitude or more greater than that of the cylindrical mesa does not appear to have any *empirical* basis. Nor does the column as reported by Taylor just over the cylindrical box constitute a complete cylinder; it spans only some 300° of the periphery.

(f) Such phenomena as the 9 passages of the South Tropical Disturbance between 1902 and 1939, first halting and then jumping beneath the Red Spot, would have no explanation on the basis of the Taylor column hypothesis, nor would it explain the anticyclonic surface rotation, the great altitude of the Red Spot, and other structural features cited in this paper; nor *the lasting changes in the daily rotation period of the Red Spot*, caused by passing meteorological structures (South Tropical Disturbance).

These problems and contradictions are all avoided by assuming that the Red Spot, the largest of the numerous oval-shaped clouds, has a *meteorological* explanation like the others. *The central location of the Red Spot within the South Tropical Zone* (one of the two symmetrical 22°-latitude high-level zones shown in Fig. 1) *re-enforces this conclusion.*- I am indebted to Mr. F. de Wiess for assistance with this summary.

After the above was written, Dr. R. Hide kindly called my attention to a joint quantitative experimental investigation by him and Dr. A. Ibbetson (Hide and Ibbetson, 1965; Hide and Ibbetson, 1966) designed to repeat and extend the original Taylor experiment. The result was that *already at a height of twice the cylinder thickness, the observed "column" was reduced to a minor disturbance in the flow pattern sweeping across the area above the cylinder.* This confirms the critique of the hypothesis made above as being entirely inapplicable to the Red Spot.

Further, Dr. A. Ibbetson has called our attention to a recent study, "Rotating Flow Over Shallow Topographies" by A. Vaziri and D. L. Boyer (1971). The authors state: "Since the time of Taylor's (1923) experiments, a great deal of effort has been expended in investigating the effects of bottom topography on flows in rotating frames of reference. Unfortunately, most of the theoretical studies are so restrictive as to make experimentation difficult, if not impossible, while for many of the experimental studies the theory is intractable. The present investigation is one for which both the range of applicability of the theory and the capabilities of the laboratory experiment coincide". They find the flow pattern over both conical and $\cos^2$ topographic features for height-to-width ratios of 0.0625, 0.125, 0.250, and 0.375. No "Taylor column" is present, only a perturbation in the flow pattern across the obstruction which at one point becomes a small (rotating) eddy.

De Marcus and Wildt (1966) showed that conceivably a "thermodynamic Cartesian diver" could exist in a "region where phase separation occurs under the condition that two distinct phases have the same density". Streett *et al.* (1971) examined this question further and found that some oscillations in the diver's rotation period, as observed for the Red Spot, would not be inconsistent with the model. In a second paper Streett (1971) estimates the "diver" to be about 800 km deep and the solid surface about 1600 km. Sagan (1963) objected to the floating-island concept on the grounds that it will tend to shift its latitude by the "pole-flight" force introduced into geophysics by Eötvös. If the island is truly floating, however, the density of the hydrogen ice must *equal* that of the hydrogen-helium compressed gas, with no "pole-flight" force acting on the island. In Sec. 4*d* a strong objection is given to the floating ice mass.

REFERENCES

De Marcus, W. C. and Wildt, R. 1966, "Jupiter's Great Red Spot", *Nature, 209*, 62.

Hide, R. 1963, "On the Hydrodynamics of Jupiter's Atmosphere", *Mémoires Soc. R. Sc. Liège, Vol. VII*, 481-505.

Hide, R. 1971*a*, "Motions in Planetary Atmospheres: A Review", *Meteor. Magazine, 100*, 268-276.

Hide, R. 1971*b*, "On Geostrophic Motion of a Non-homogeneous Fluid", *J. Fluid Mech., 49*, 745-751.

Hide, R. and Ibbetson, A. 1965, "Taylor Columns", MAGNETISM AND THE COSMOS, 343-347.

Hide, R. and Ibbetson, A. 1966, "An Experimental Study of 'Taylor Column'", *Icarus, 5*, 279-290.

Kuiper, G. P. 1952, THE ATMOSPHERES OF THE EARTH AND PLANETS (Chicago: U. of Chicago Press).

Newburn, R. L. and Gulkis, S. 1971, "A Brief Survey of the Outer Planets, Jupiter, Saturn, Uranus, Neptune, Pluto, and their Satellites", JPL Tech. Rpt. 32-1529.

Öpik, E. J. 1962, "Jupiter: Chemical Composition, Structure, and Origin of a Giant Planet", *Icarus, 1*, 200.

Sagan, C. 1963, "On the Nature of the Jovian Red Spot", *Mémoires Soc. R. Sc. Liège, Vol. VII*, 506-515.

Streett, W. B. 1971, "Phase Behavior of Light Gas Mixtures at High Pressures", PLANETARY ATMOSPHERES (ed. Sagan), 363-370.

Streett, W. B., Ringermacher, H. I., and Veronis, G. 1971, "On the Structure and Motions of Jupiter's Red Spot", *Icarus, 14*, 319-342.

Taylor, G. I. 1923, *Proc. Roy. Soc. A., 104*, 213.

Vaziri, A. and Boyer, D. L. 1971, "Rotating Flow over Shallow Topographies", *J. Fluid Mech., 50*, Part 1, 79-95.

APPENDIX II

by S. M. Larson

Much discussion on cloud heights is based on the appearance of Jupiter on photographs taken with the "methane filter", an interference filter with pass-band 8850-9050Å (Fig. 19). (Actually, its pass-band is slightly displaced with respect to the CH_4 band which would optimally require 8820-9000Å). It will be shown that the gross features thus recorded are due to differential methane gas absorptions and not to intrinsic albedo differences. We here use photographs taken through three available interference filters, A, B, and C, around the λ8900Å methane band, whose transmission curves are also shown in Figure 19.

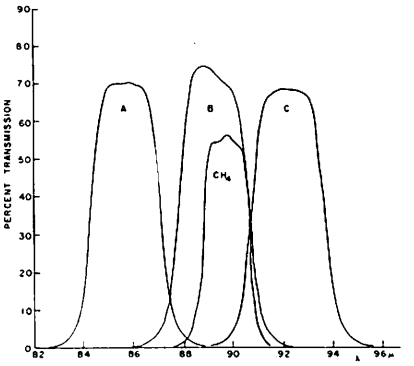

Fig. 19 Transmission curves for filters A, B, C, and the "methane filter" used in the Jupiter photography, Figure 1

The method used was that of photographic subtraction and is illustrated in Figure 20. To this end, gamma-one contrast positives were made from the original negatives taken on Kodak High-Speed Infrared film. We used a film whose response is nearly linear over a large range of densities (DuPont Commercial-S). While the originals and copies will not be entirely linear, the effects will not interfere with the detection of the strong contrasts produced by the methane absorption. The images were exposed on the straight-line portion of the characteristic curves, and the density difference between the planet's limb and the sky averaged 0.7; therefore, the largest departures from linearity are caused by "adjacency effects". These effects will be less serious on most methane-filter images because on them the differences between sky and limb are small. Since the λ8950 methane band is deep and the film sensitivity there already low, the methane images require long exposures and inevitably are often on the toe of the characteristic curve. This non-linearity causes a lowering of contrast of images A+C' in Figure 20.

The features shown on the methane images result from differences in path lengths to the reflecting cloud layers. Since methane will not condense on Jupiter and is therefore representative of the equilibrium atmosphere, regions of less absorption must be higher. The features recorded since 1968 are consistent with those described by Owen (1969).

We find no clear correlation between cloud heights and brightness measured in the near-IR. In some frames of unusually high resolution, the bluish festoons can be recognized, and it is assumed that this is an albedo effect, caused by contamination due to the slight mismatch of the CH_4 filter.

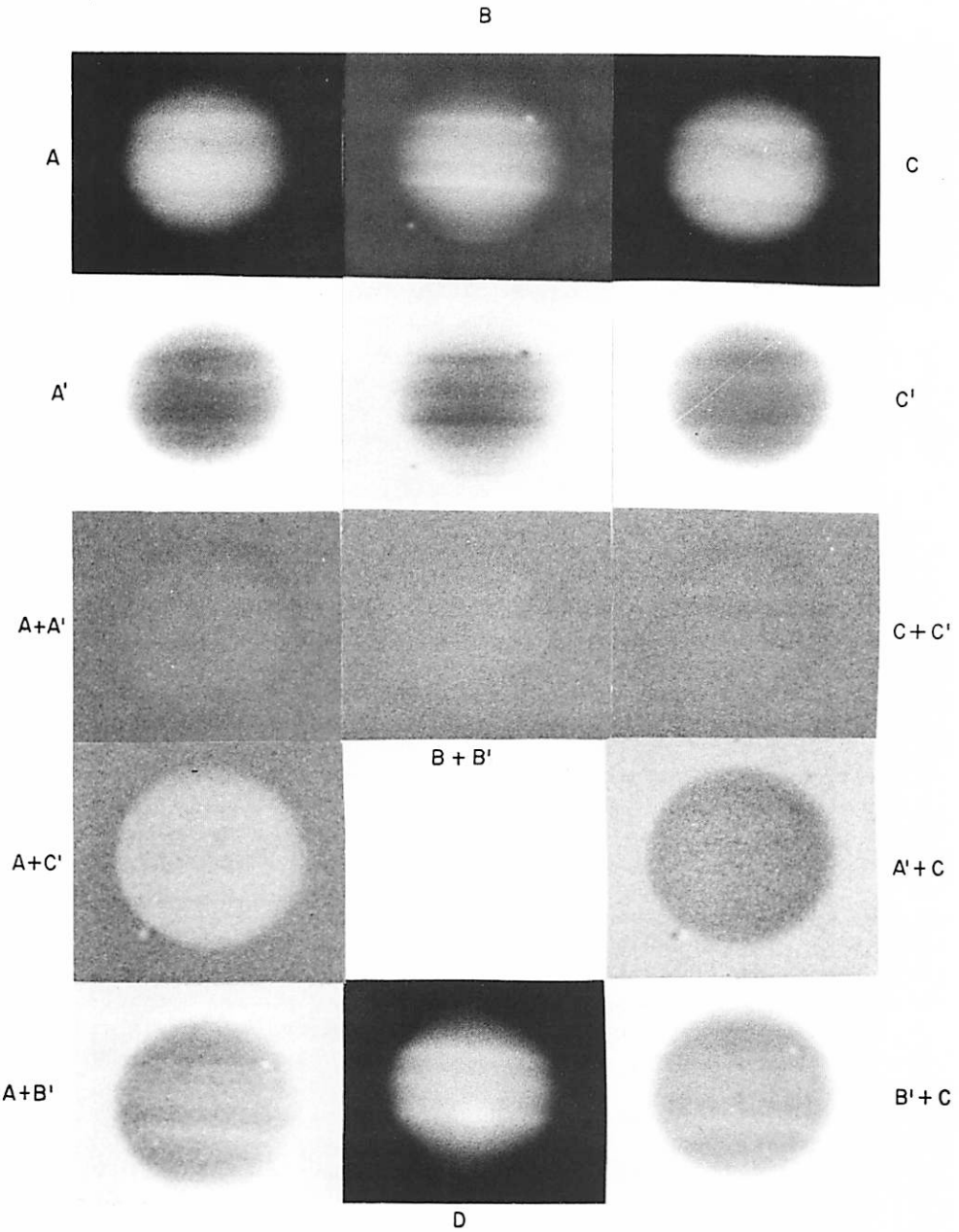

Fig. 20 - A, B, C,- Photographs taken on April 8, 1971, by J. Fountain with filters shown in Fig. 19. Exposure times 2 sec, 8 sec, and 120 sec.
A', B', C' - Gamma-one contrast copies of A, B, and C.
A+A', B+B', C+C' - Combinations showing that A', B', C' are actually very close to having a contrast of one, and that registration errors and photographic edge effects are minor.
A+C', C+A' - Combinations showing that intrinsic albedo differences between wavelengths A and B are negligibly small.
A+B', C+B' - Showing the distribution of CH_4 absorption by subtracting true albedo differences. Note that these two frames agree.
D - Taken about $2^h.5$ later (Red Spot has rotated into view), with regular CH_4 interference filter used. Exposure 90 sec, seeing poorer.

Reference is made to a more extensive discussion of Jupiter filter photography by J. W. Fountain and S. M. Larson in *LPL Communications Nos. 174* and *175*.

Sensitometric and spectral regions data can be found in Kodak's PLATES AND FILM FOR SCIENCE AND INDUSTRY, p. 9, 1967, along with a good summary of photographic edge effects. See also Dupont's GRAPHIC ARTS FILMS TECHNICAL DATA on the Commercial-S film A-30238, referred to above.